COMPOUNDS FOR DEACTIVATING PHOSPHOLAMBAN FUNCTION ON CA-ATPASE (PHOSPHOLAMBAN INHIBITORS)

Field of the invention

The present invention relates to determining the three-dimensional structure of phospholamban (PLB) using NMR data of sufficiently high resolution for three dimensional structure determination. The invention also relates to methods for rational drug design enabling the design of compounds for deactivating phospholamban based on using the three-dimensional structure data provided on computer readable media, as analyzed on a computer system having suitable computer algorithms. The invention also relates to phospholamban deactivating compounds with structural, physicochemical and spacial characteristics that allow for the interaction of said compounds with specific residues of phospholamban. The interaction prevents the inhibiting effect of phospholamban on Ca-ATPase, making these compounds useful for treating diseases where the Ca-pumping activity of the Ca-ATPase may be diminished, such as congestive heart disease.

Background of the invention

Phospholamban (PLB) is a low molecular weight protein (52 amino acids), present in cardiac, slow-twitch and smooth muscle, which can be phosphorylated by both cAMP- and Ca^{2+}/calmodulin-dependent phosphokinases. The amino acid sequences of phospholamban from different species are shown in Figure 1. The phosphorylation/ dephosphorylation of phospholamban has been shown to regulate the Ca^{2+}-ATPase of the sarco/endoplasmic reticulum in myocytes (SERCA_2). It has been shown that phospholamban, in its non-phosphorylated form, binds to a specific region of the large loop in the cytoplasmic domain of SERCA_2 and inhibits this pump by lowering its affinity for Ca^{2+}, while the phosphorylated form does not inhibit SERCA_2.

It has been proposed that a region essential for functional association of phospholamban with Ca^{2+}-ATPase lies in the cytoplasmic domain of phospholamban, while the transmembrane region anchors PLB to the sarcoplasmic membrane.

During the last decade, efforts have been made to elucidate, at least partially, the secondary structure of PLB either by means of cross-linking experiments or by reconstitution of SERCA_2 with point-mutated PLB, or, finally, by obtaining direct structural information by circular dichroism, laser light scattering photometry - FTIR

spectroscopy and NMR spectroscopy). Molecular modelling has been used to formulate hypotheses on the quaternary structure of the transmembrane region in the PLB pentamer. The structural information obtained has been recently reviewed (Arkin, I. T. et al. (1997) Annu. Rev. Biophys. Biomol. Struct., 26, 157-179).

Since PLB i) is an amphiphatic oligopeptide, ii) contains three cysteins, and iii) is prone to pentamerization also *in vitro* , it is not straightforward to find good conditions to study its structure and, in particular, an appropriate solvent system which prevents unspecific aggregation. Therefore, until now NMR studies have been carried out either on short PLB fragments or in organic solvents. In no cases has evidence of a tertiary structure for the cytosolic domain of PLB been found.

Inhibition of CaATPases may play a causative role in cardiac disorders where the calcium levels of myocytes are high. As phospholamban inhibits SR CaATPase this inhibition may be harmful in such disorders. A compound capable of relieving the inhibitory effects of phospholamban on cardiac SR Ca^{2+}-ATPase, e.g. by interrupting phospholamban-Ca^{2+}-ATPase interaction, would be potentially useful in the treatment of such disorders. There have been very few examples on compounds which can prevent the inhibition of CaATPase by phospholamban in the literature. Such compounds include anti-phospholamban antibodies, some large polyanionic oligopeptides and tannins. No small molecules with specific interactions with phospholamban has been reported.

In the present invention it has been found that phospholamban can assume a well characterized conformation in which it can bind a broad series of small compounds with common structural, physicochemical and spacial characteristics that allow an interaction of the said compounds with specific residues of phospholamban in the defined conformation. This interaction deactivates phospholamban and prevents its inhibiting effect on Ca-ATPase. The phospholamban deactivating compounds are potentially useful in the treatment of cardiac disorders, where the activation of the SR CaATPase is beneficial.

SUMMARY OF THE INVENTION

The present invention is based on our complete resolution of the three-dimensional structure of the entire cytosolic domain of phospholamban and the ligand binding site therein.

In one aspect the present invention provides compounds capable of relieving the inhibitory effects of phospholamban on cardiac SR Ca^{2+}-ATPase, such compounds thus acting as phospholamban deactivators through direct binding to the phospholamban

protein. These componds have common structural, physicochemical and spacial characteristics that allow for the interaction of said compounds with specific residues of the ligand binding site of phospholamban.

In another aspect the present invention provides a method of deactivating phospholamban which comprises administering to a mammal in need thereof a compound of the invention, as well as a pharmaceutical preparation comprising a compound of the invention together with a pharmaceutically acceptable carrier.

In another aspect, the present invention provides methods for rational drug design enabling the design of phospholamban deactivators based on using the three-dimensional structure data of phospholamban cytosolic domain provided on computer readable media, as analyzed on a computer system having suitable computer algorithms.

In still another aspect, the present invention provides the three-dimensional structure of phospholamban cytosolic domain provided on computer readable media.

Other aspects of the present invention will be apparent to one of ordinary skill in the art from the following detailed description and examples relating to the present invention.

BRIEF DESCRIPTION OF THE FIGURES

Fig. 1 shows the amino acid sequences of phospholamban from different species (human, pig, dog, rabbit, rat, mouse, chicken).

Fig. 2 is an illustration of the NMR structure of the cyclic peptide cP226.

Fig. 3 is an illustration of the NMR structure of PLB(1-36).

Fig. 4 is an illustration of the model structure of the complex between PLB(1-36) and cyclic peptide cP226.

Fig. 5 is an illustration of the main interactions of cP226 with PLB(1-36) in the model of the binary complex. The distances between the heavy atoms capable for electrostatic binding, H-bonding, or hydrophobic interactions are shown.

Fig. 6 is an illustration showing the PLB amino acid side chains which form the binding site for ligands, divided to four interactions sites denoted as S1-S4.

Fig. 7 is the summary of the observed sequential and medium-range NOE connectivities for PLB(1-36).

Fig. 8 is an illustration of the superposition of compound of Example 1c onto the PLB structure.

Fig. 9 shows the quality of the structure of PLB(1-36) obtained by NOE data. RMSD per residue and the number of restraints per residue is shown.

Fig. 10 is the summary of the observed sequential and medium-range NOE connectivities for cP226.

Fig. 11 is an illustration of the family of 12 structures of cP226 deduced from NMR data.

Fig. 12A and 12B show the effect of the compound of Example 1c (50 and 100 μM) on the Ca^{2+} uptake rate into the cardiac (A) and fast skeletal muscle (B) SR vesicles.

DETAILED DESCRIPTION OF THE INVENTION

Structure of phospholamban (1-36)

The present invention is based on our complete resolution of the three-dimensional structure of the entire cytosolic domain of phospholamban (PLB) and the ligand binding site therein. It was possible to determine the structure of the phospholamban cytosolic domain using a method of NMR spectroscopy wherein the NMR data is of sufficiently high resolution for the three-dimensional structure determination. The method comprises providing the 1-36 a.a. fragment of phospholamban, which comprises the cytosolic domain and 6 amino acids of the transmembrane domain, for the NMR analysis in aqueous solution containing 30% trifluoroethanol. The three-dimensional structure can then be determined from the NMR data by distance geometry followed by simulated annealing. The method is described in detail in EXAMPLE 1.

It was found that phospholamban (1-36) fragment assumes a conformation characteristic of a helix-turn-helix motif. The residues of the turn are Ile18, Glu19, Met20, and Pro21, which are adjacent to the two phosphorylation sites Ser16 and Thr17. The proline is in a *trans* conformation. Both helices have predominantly charged and polar residues on one side, whereas the other is lipophilic. The hydrophilic side of the N-terminal helix faces always the lipophilic side of the C-terminal helix defining a pocket which could be described as an amfiphatic armpit. This may mean that in order to interact with SERCA_2, PLB should assume a prolonged position (i.e. the axes of two α-helices should be nearly parallel), while in the bent conformation those charges would not be exposed to the ATPase but eventually to the surface charges of the phospholipid bilayer. The loose relative positioning of the two helices around the mobile central hinge domain is thus a functional feature of PLB. This flexibility may explain also why, in organic solvent, PLB can assume a prolonged structure.

The structure also reveal that the pocket between the hydrophilic side of the N-terminal helix and the lipophilic side of the C-terminal (defined as an amfiphatic armpit) is an ideal target for small amfiphatic drug molecules designed with the purpose of deactivating PLB by stabilizing its bent conformation. Such molecules would relieve the inhibitory effect of phospholamban on cardiac SR Ca^{2+}-ATPase, and therefore act as a PLB deactivator through direct binding to the active site of PLB.

Structure of cP226

In order to find a lead molecule which would interact with PLB a series of peptides were screened. It was found that a cyclic peptide of formula (pI) was able to bind to PLB and activate the calcium intake in liposomes containing both SERCA_2 and PLB while being inactive in liposomes lacking PLB. It was concluded that the cyclic peptide of formula (pI) binds to unphosphorylated PLB and prevents the inhibition exerted by PLB on SERCA_2 thus acting as a PLB deactivator. The cyclic peptide (pI) has the structure:

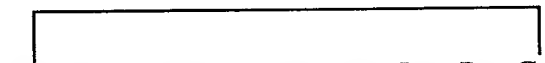

(pI)

X is preferably Tyr or Ala.

The cyclic peptide of formula (pI) wherein X is Tyr was named cP226. In order to determine the ligand binding site of PLB, the tertiary structure of the cP226 was resolved by NMR spectroscopy. The method used is described in detail in EXAMPLE 2. The three-dimensional structure of cP226 show bend-coil-bend motif. The lipophilic side chains of Trp-3, Leu-5, Trp-7 and Leu-8 are clustered on one side of the cyclic peptide, leaving the most of the polar carbonyl and amine groups of the backbone on the other side. The three dimensional coordinates of the cyclic peptide cP226 are provided in Table I annexed to the present application.

Structure of the complex cP226•PLB(1-36)

On the basis of the resolved tertiary structures of PLB(1-36) and its ligand cP226 it was possible to prepare a model of the complex cP226•PLB(1-36) by molecular modelling. The three-dimensional model describes the interactions between PLB(1-36) and its ligand which are important in binding of ligands to the cytosolic domain of PLB.

The NMR-solved structures of PLB[1-36] and cP226 were used as templates for the building of the complex. cP226 was docked interactively with help of molecular graphics and guided by possible interactions between the two peptides. The structure of cP226 shows that the peptide has two negative side chains (Glu-4 and Glu-6) on one side while the other side is hydrophobic (Trp-7, Leu-8, Pro-9) (Figure 2). In PLB(1-36) there is a cluster of three positive side chains (Arg-9, Arg-13, Arg-14) opposed by a mainly hydrophobic surface of the C-terminal helix (e.g. Leu-28, Leu-31, Phe-32, Phe-35) (Figure 3). cP226 was manually docked onto PLB(1-36) so that Glu-4 and Glu-6 come to contact with Arg-9, Arg-13 and Arg-14, while at the same time Trp-7, Leu-8 and Pro-9 are near the hydrophobic surface of PLB C-terminal helix. This gave the starting point for an energy refinement of the complex.

The energy of the obtained complex was minimized by InsightII using the general valence force field (gvff93). Rough minimization was made by the steepest descents method, followed by conjugate gradients and the Newton method.

The structure of the energy minimized complex cP226•PLB(1-36) is shown in Figure 4. The final total energy of the complex was 113 kcal/mol (non-bond dispersion energy -1574 kcal/mol, coulomb energy -690 kcal/mol).

A schematic sketch of the binding mode of cP226 to PLB is shown in Figure 5. The binding can be described by four binding sites (S1-S4) which bind Glu-4, Glu-6, Trp-7 and Pro-9, respectively (Table II, Figure 6). Glu-4 has electrostatic/H-bonding interactions with Tyr-6, Arg-9 and Arg-13 (S1), Glu-6 binds to Arg-14 (S2), Trp-7 is buried in a hydrophobic pocket (S3) formed mainly by Met-20, Lys-27 and Leu-28 and Pro-9 binds to a hydrophobic cleft (S4) formed mainly by Phe-32 and Phe-35. Besides, Leu-5 is lined by the hydrophobic part of the side chain of Arg-13 and NH of the indole of Trp-7 can form an H-bond to the carbonyl of Arg-13. The positive N-terminal amino group (NH3+) is near the hydrophobic binding site S4.

Table II: Binding of cP226 to PLB

Site	PLB	cP226
S1	Tyr-6, Arg-9, Arg-13	Glu-4
S2	Arg-14	Glu-6
S3	Met-20, Lys-27, Leu-28	Trp-7
S4	Phe-32, Phe-35	Pro-9

Thus, the term "binding site S1" is defined as the space surrounded by amino acid residues Tyr-6, Arg-9 and/or Arg-13, particularly -OH group of Tyr-6, guanidinium group of Arg-9 and/or guanidinium group of Arg-13.

The term "binding site S2" is defined as the space surrounded by amino acid residue Arg-14, particularly guanidinium group of Arg-14.

The term "binding site S3" is defined as the space surrounded by amino acid residues Met-20, Lys-27 and/or Leu 28, particularly the side chains thereof.

The term "binding site S4" is defined as the space surrounded by amino acid residues Phe-32 and/or Phe-35, particularly the phenyl groups thereof.

The three dimensional atom coordinates of phospholamban (1-36) in a conformation which allows binding of cyclic peptide cP226 are disclosed in Table III annexed to the present application. The three dimensional atom coordinates of the complex between phospholamban (1-36) and the cyclic peptide cP226 are disclosed in Table IV annexed to the present application. Figure 8 is an illustration of the superposition of one compound of the invention (compound of Example 1c) onto the PLB structure.

Rational drug design

Structure determination methods are also provided by the present invention for rational drug design (RDD) of PLB ligands. Such drug design uses computer modeling programs that calculate different molecules expected to interact with the determined binding sites or other structural or functional domains of PLB. These molecules can then be produced and screened for activity in deactivating PLB according to methods of the present invention.

The present invention reveals the ligand binding site of PLB cytosolic domain heretofor unknown and comprises a distinct three dimensional arrangement of atoms. The atom coordinates of PLB (1-36) in a conformation which allows binding of a PLB deactivator of the invention to the PLB cytosolic domain are disclosed in Table III. This structure for the first time enables the structure-based design of highly active PLB deactivators. The structure of PLB cytosolic domain provided herein permits the screening of known molecules or designing of new molecules which bind to the ligand binding site of PLB cytosolic domain, via the use of computerized evaluation systems. For example, computer modeling systems are available in which the atomic coordinates of PLB cytosolic domain and the ligand binding site thereof as provided in Table III can be used

as input. Thus, a computer readable medium may be encoded with data representing the coordinates of Table III in this process.

The present invention provides a method for identifying a PLB deactivator comprising the steps of:

i) providing atom coordinates of the structure of PLB cytosolic domain or portion thereof in a computerized modeling system, ii) identifying compounds which are capable of interacting with said structure, and iii) testing the compounds identified or analogs derived therefrom for the activation of CaATPase in the presence of phospholamban.

In particular, the present invention provides a method for identifying a PLB deactivator comprising the steps of:

i) providing the atom coordinates of the structure of PLB cytosolic domain or portion thereof in a computerized modeling system, ii) identifying compounds which are capable of interacting with at least three of the binding sites S1, S2, S3 and S4 of the PLB cytosolic domain, and iii) testing the compounds identified or analogs derived therefrom for the activation of CaATPase in the presence of phospholamban.

In particular, the present invention provides a method for identifying a PLB deactivator comprising the steps of:

i) providing atom coordinates of the structure of PLB cytosolic domain or portion thereof in a conformation which allows binding of a PLB deactivator to PLB cytosolic domain, in a computerized modeling system, ii) identifying compounds which are capable of said interaction iii) testing the compounds identified or analogs derived therefrom for the activation of CaATPase in the presence of phospholamban.

In the method of the invention candidate molecules may be obtained by carrying out computer-aided molecular design using the three-dimensional structure of the PLB cytosolic domain particularly when complexed with a PLB inhibitor, and in particular the three-dimensional structure at and/or aroud the binding sites S1 to S4, and synthesising the molecules so-designed.

In the method of the invention candidate molecules can be tested for their ability to deactivate phospholamban, for example, using assays which are described in detail in EXAMPLE 3 or modification thereof.

The invention also provides a computer readable medium having stored therein atom coordinates of the structure of the PLB cytosolic domain or portion thereof in a conformation which allows binding of a PLB deactivator to the PLB cytosolic domain.

As used herein, "computer readable media" refers to any medium which can be read and accessed directly by a computer. Such media include, but are not limited to: magnetic storage media, such as floppy discs, hard disc storage medium, and magnetic tape; optical storage mediasuch as optical discs or CD-ROM; electrical storage media such as RAM and ROM; and hybrids of these categories such as magnetic/optical storage media. A skilled artisan can readily appreciate how any of the presently known computer readible media can be used to create a manufacture comprising computer readable medium having stored therein atom coordinates of the structure of the PLB. The choice of the data storage structure will generally be based on the means chosen to access the stored information. Variety of data processor programs and formats can be used to store the atom coordinate data of the present invention on the computer readable medium.

By providing computer readable media having stored therein atom coordinate data of the structure of the PLB, a skilled artisan can routinely access the atom cordinate data of the structure of the PLB cytosolic domain or portion thereof. Computer algorithms are publicly and commercially available which allow a skilled artisan to access this data provided on a computer readable medium and analyze it for structure determination and/or rational drug design. See, e.g. Biotechnology Software Directory, Mary Ann Liebert Publ., New York (1995).

Structural atom coordinates of the PLB (1-36) presented in Table III may be stored in a computer readable form on a computer readable storage medium for display as a three-dimensional shape or for other uses involving computer-assisted manipulation of the structural coordinates they define. For example, data defining the three dimensional structure of a PLB cytosolic domain or portions thereof may be stored in a computer readable storage medium, and may be displayed as a graphical three-dimensional representation of the protein structure, typically using a computer capable of reading data from said storage medium and programmed with instructions for creating the representation from such data. The invention thus encompasses a machine, such as a computer, having memory which contains data representing the structural coordinates of the PLB protein of the invention, e.g. coordinates presented in Table III, together additional optonal data and instructions for manipulating such data. Such data can be used for a variety of purposes, such as the rational drug design. The invention

encompasses the coordinates of Table III as well as any translation or rotation or the like thereof which maintains the internal coordinates, i.e. which maintains their intrinsic, internal relationship. Those skilled in the art will appreciate that the coordinates may be subjected to other transformations including, e.g. molecular mechanics calculations such as dynamic simulation, minimization, etc.

For example, a first set of computer readable data defining the three-dimensional structure of PLB cytosolic domain or a portion thereof is combined with a second set of computer readable data defining the structure of a candidate molecule using a computer programmed with instructions for evaluating the ability of the candidate molecule to associate PLB cytosolic domain protein and/or the location and/or orientation of such association.

The protein structure encoded by the data may be displayed in a graphical format permitting visual inspection of the structure, as well as visual inspection of the structures association with candidate molecules. Alternatively, more quantitative of computational methods may be used. For example, one method of this invention for evaluating the ability of a candidate molecule to associate with PLB cytosolic domain comprises the steps of i) employing computational means to perform a fitting operation between the candidate molecule and the binding sites of PLB, and ii) analyzing the results of said fitting operation to quantify the association between the candidate molecule and the binding sites of PLB.

One method of this invention provides for selecting from a database of chemical structures a compound capable of binding to PLB cytosolic domain. The method starts with structural coordinates defining the three dimensional structure of PLB cytosolic domain or portion thereof. Binding sites of that three dimensional structure are characterized with respect of the favorability of interactions with one or more functional groups. A database of chemical structures is then searched for candidate compounds containing functional groups disposed for favorable interaction with the PLB based on the prior characterization. Compounds having structures which best fit the points of favorable interaction with three dimensional structure are thus identified.

Computer programs for viewing three dimensional structures or manipulating atom coordinates are available and well known for one skilled in the art.

Phospholamban deactivating compounds

The invention provides phospholamban deactivating compounds being capable of associating with any three of the binding sites S1, S2, S3 and S4 of the PLB cytosolic domain. In particular, the invention provides a phospholamban deactivating compound comprising at least any three of the following:

(a) a first electronegative moiety being capable of associating with the S1 binding site of the PL cytosolic domain when the deactivator is bound thereto said binding site comprising Tyr-6, Arg-9 and/or Arg-13,

(b) a second electronegative moiety being capable of associating with the S2 binding site of the PL cytosolic domain when the deactivator is bound thereto said binding site comprising Arg-14, and

(c) a first hydrophobic moiety being capable of associating with the S3 binding site of the PL cytosolic domain when the deactivator is bound thereto said binding site comprising Met-20, Lys-27 and/or Leu-28.

(d) a second hydrophobic moiety being capable of associating with the S4 binding site of the PL cytosolic domain when the deactivator is bound thereto said binding site comprising Phe-32 and/or Phe-35.

In particular, the invention provides a phospholamban deactivating compound comprising at least any three of the following:

(a) a first electronegative moiety being capable of forming a hydrogen bond with the -OH group of Tyr-6, a salt bridge with the guanidinium group of Arg-9 and/or a salt bridge with the guanidinium group of Arg-13, of the PL cytosolic domain when the deactivator is bound thereto,

(b) a second electronegative moiety being capable of forming a salt bridge with the guanidinium group of Arg-13, of the PL cytosolic domain when the deactivator is bound thereto,

(c) a first hydrophobic moiety being capable of associating with a hydrophobic pocket created by Met-20, Lys-27 and/or Leu-28, of the PL cytosolic domain when the deactivator is bound thereto and.

(d) a second hydrophobic moiety being capable of associating with a hydrophobic pocket created by Phe-32 and/or Phe-35, of the PL cytosolic domain when the deactivator is bound thereto.

In particular, the invention provides a phospholamban deactivating compound comprising:

(a) a first electronegative moiety being capable of forming a hydrogen bond with the -OH group of Tyr-6, a salt bridge with the guanidinium group of Arg-9 and/or a salt bridge with the guanidinium group of Arg-13, of the PL cytosolic domain when the deactivator is bound thereto,

(b) a second electronegative moiety being capable of forming a salt bridge with the guanidinium group of Arg-13, of the PL cytosolic domain when the deactivator is bound thereto and

(c) a first hydrophobic moiety being capable of associating with a hydrophobic pocket created by Met-20, Lys-27 and/or Leu-28, of the PL cytosolic domain when the deactivator is bound thereto and.

Therefore, for a phospholamban deactivator of to the invention, at least three of the first electronegative moiety of (a), the second electronegative moiety of (b), the first hydrophobic moiety of (c) and the second hydrophobic moiety of (d) are capable of forming said hydrogen bond and/or salt bridges of (a), said salt bridge of (b), said associations with the hydrophobic pocket of (c), and said associations with the hydrophobic pocket of (d), respectively, with said groups or hydrophobic pockets of PLB, at the same time.

Phospholamban deactivating compounds of the invention include, but are not limited to, compounds of formula (I) or (II):

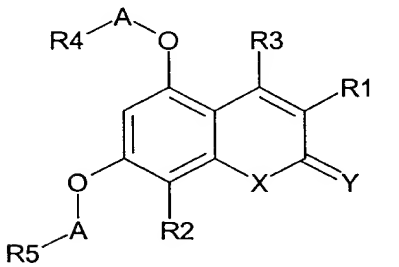

(I)

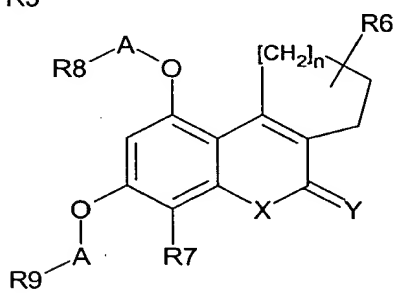

(II)

in which

R_1 is hydrogen, alkyl, alkenyl, aryl, arylalkyl, hydroxyalkyl, halogenalkyl, alkoxy, COR_{10}, $CONR_{10}R_{11}$, OR_{10}, $S(O)_mR_{10}$, $NR_{10}COR_{11}$ or $NR_{10}R_{11}$, where R_{10} is hydrogen, alkyl, alkenyl, aryl, arylalkyl, hydroxyalkyl, halogenalkyl, alkoxy or hydroxy and R_{11} is hydrogen, alkyl, aryl, arylalkyl, alkoxy, aryloxy, hydroxy or acyl, or in case where X is NR_{11}, can R_1 also be carboxylalkyl,

R_6 is hydrogen, alkyl, alkenyl, aryl, arylalkyl,

R_2 and R_7 mean hydrogen, alkyl, aryl, arylalkyl, alkenyl, COR_{10}, $CONR_{10}R_{11}$, halogen, trifluoromethyl, nitro or cyano, where R_{10} and R_{11} are defined as above,

R3 is hydrogen, alkyl, aryl or arylalkyl,

A means alkyl or substituted alkyl,

m is 0-2 and n is 1-3,

Y means O, NR11 or S, where R11 is the same as above,

X means O, NR11 or S, where R11 is the same as above,

R_4, R_5, R_8 and R_9 mean independently one of the following groups:

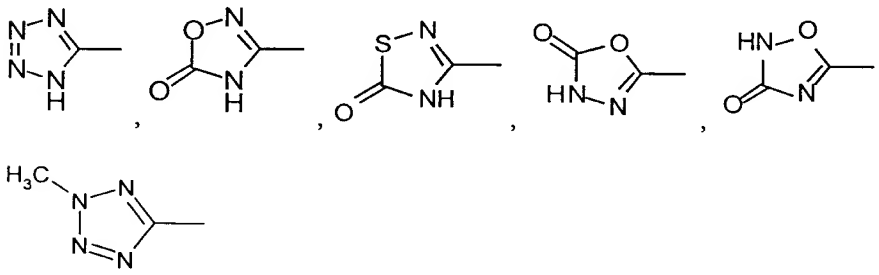

or in case where X is NR_{11}, can R_4, R_5, R_8 and R_9 also independently mean HOOC-, $R_{12}OOC$-, H_2NCO- or HOHNCO- wherein R_{12} means alkyl, arylalkyl or aryl,

and wherein each aryl residue defined above by itself or as part of another group may be substituted,

and pharmaceutically acceptable salts and esters thereof.

The compounds of formula (I) or (II) share the structural features which allow them to associate with the ligand binding site of PLB cytosolic domain thereby relieving the the inhibitory effects of PLB on cardiac SR Ca^{2+}-ATPase.

Compounds of formula (I) or (II) can be prepared from the 1,3-dihydroxy substituted heteroaromatics by alkylation of the dihydroxy compounds by suitable

alkylating agents, for example by chloroacetonitrile or bromoacetic ester according to the following Scheme 1, wherein R_1,R_2, R_3, X and Y are the same as defined above, R' is a protecting group for the hydroxyl, e.g. methyl, benzyl or tetrahydropyranyl.

SCHEME 1

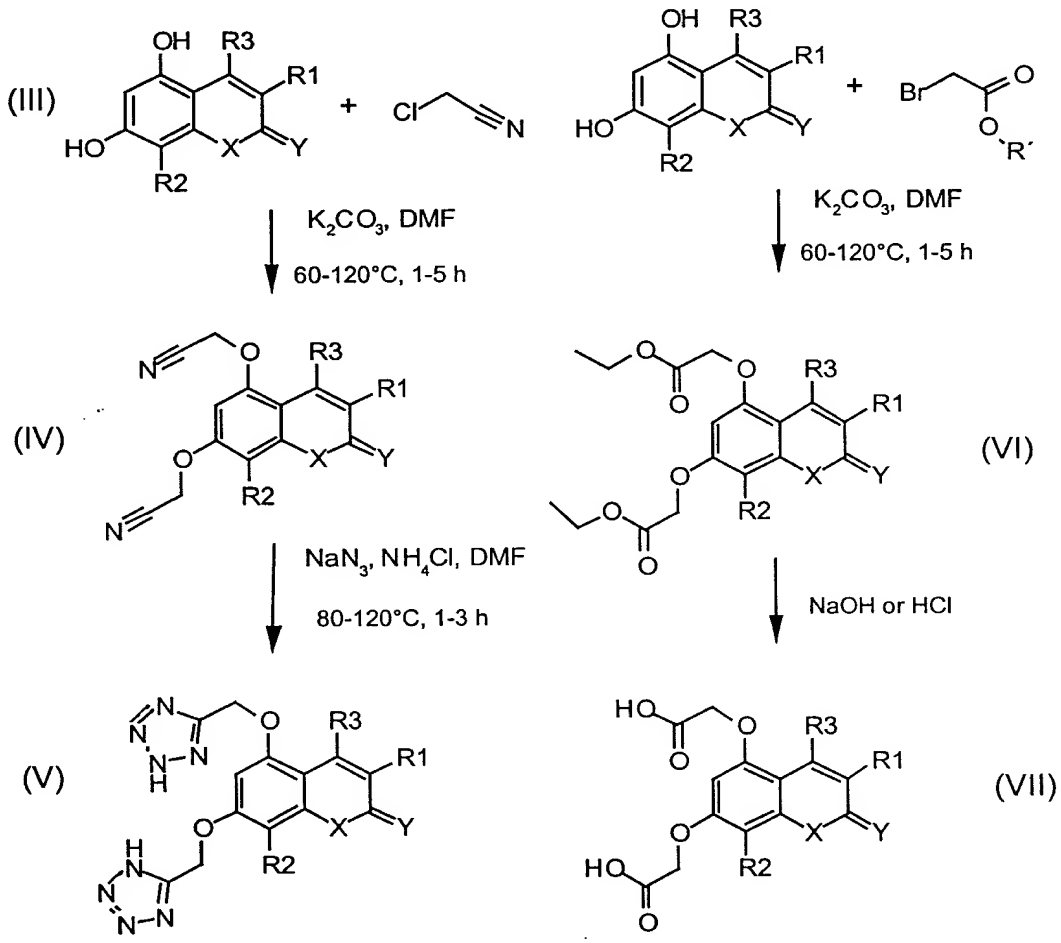

The cyano compound (IV) described above is used to prepare the 1,2,4-oxadiazole and 1,2,4-thiadiazole derivatives using the methods described in J. Med. Chem. 1996, 39, 5228-5235.

The syntheses are shown in Scheme 2 , wherein R_1, R_2, R_3, X and Y are the same as defined above.

SCHEME 2

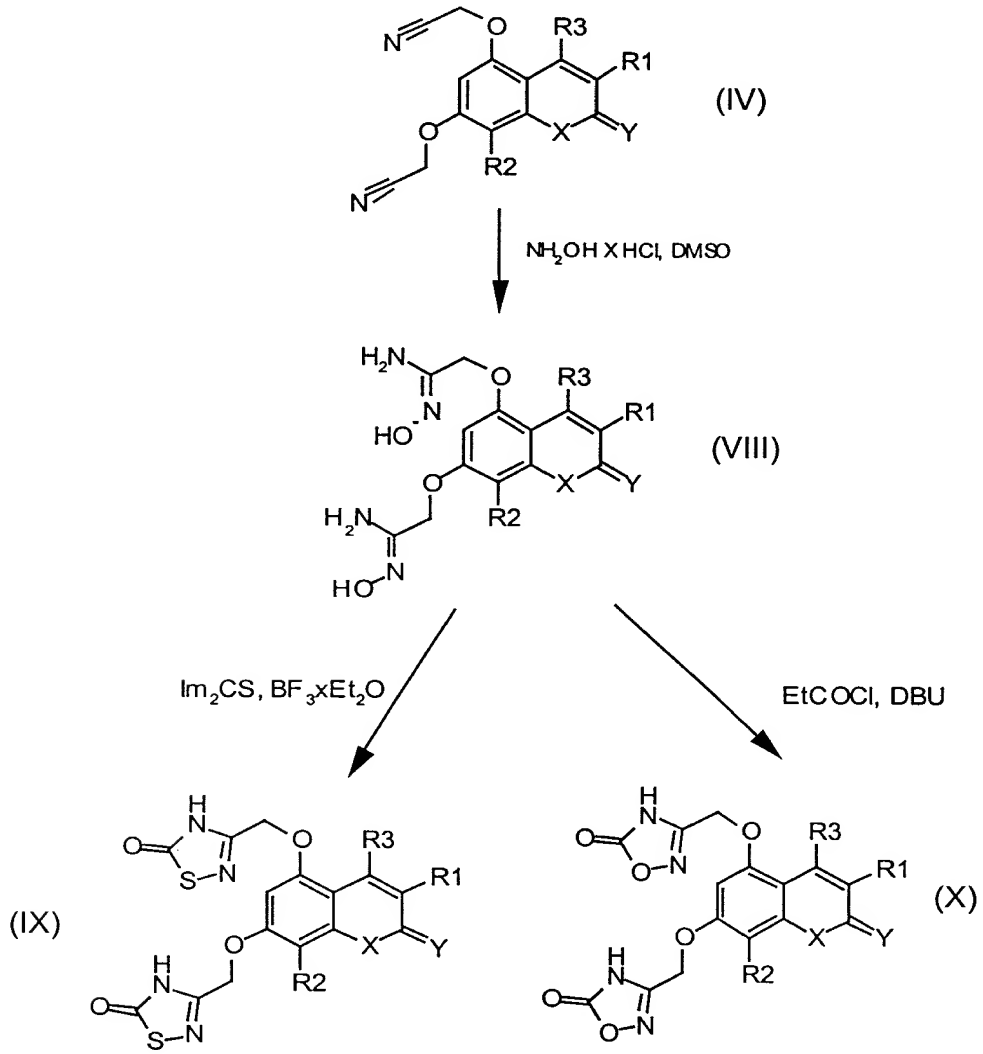

The other heterocyclics as groups R4, R5, R8 and R9 are prepared as described in Bioorg. Med. Chem. Lett., 1994, 4, 45-50.

The dihydroxyaromatics (III) are made by use of the literature methods. The coumarins (XIV), (XVI) and (XX) are made by the use of the Knoevenagel condensation or von Pechmann reaction as presented in Scheme 3 and 4, where R_1,R_2 and R_3, are the same as defined above, Z is alkyl, aryl, arylalkyl or alkenyl and R´is a protecting group for the hydroxyls e.g. methyl, benzyl or tetrahydropyranyl.

SCHEME 3.

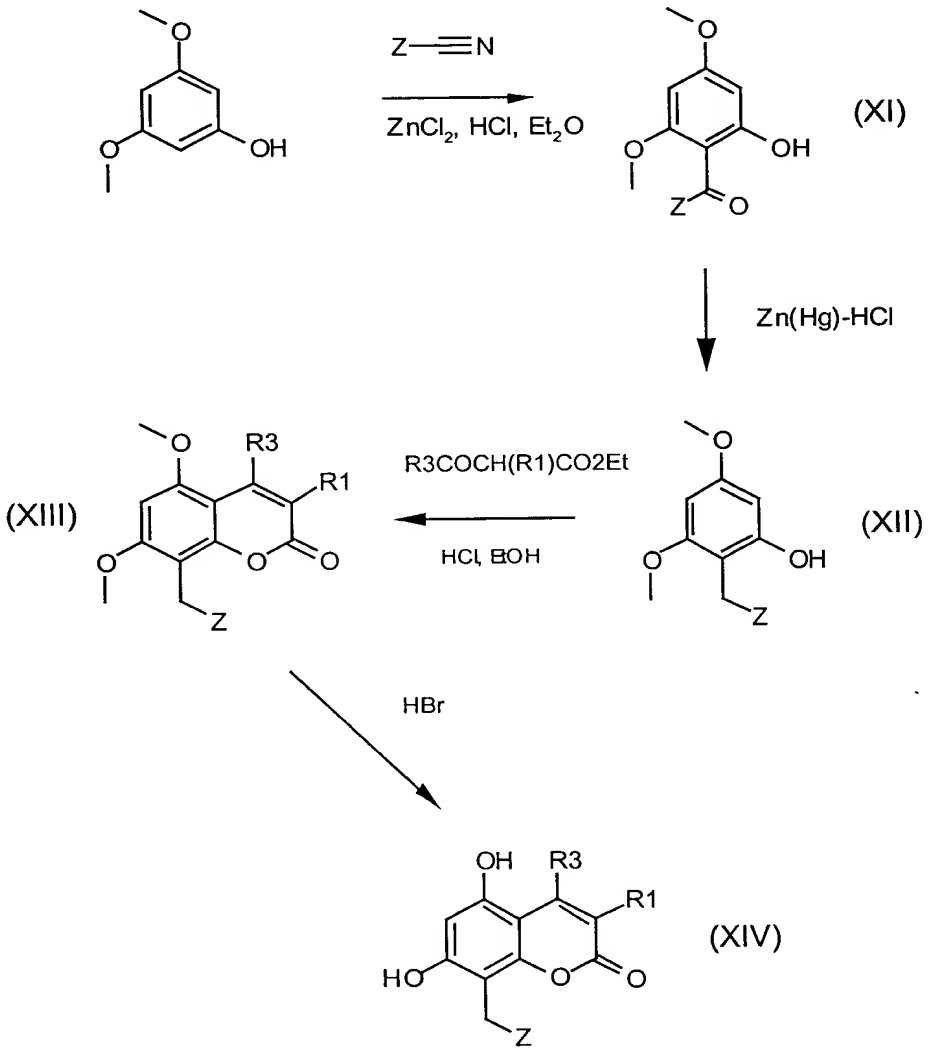
Z—≡N
ZnCl2, HCl, Et2O
(XI)
Zn(Hg)-HCl
R3COCH(R1)CO2Et
HCl, EtOH
(XII)
(XIII)
HBr
(XIV)

SCHEME 4.

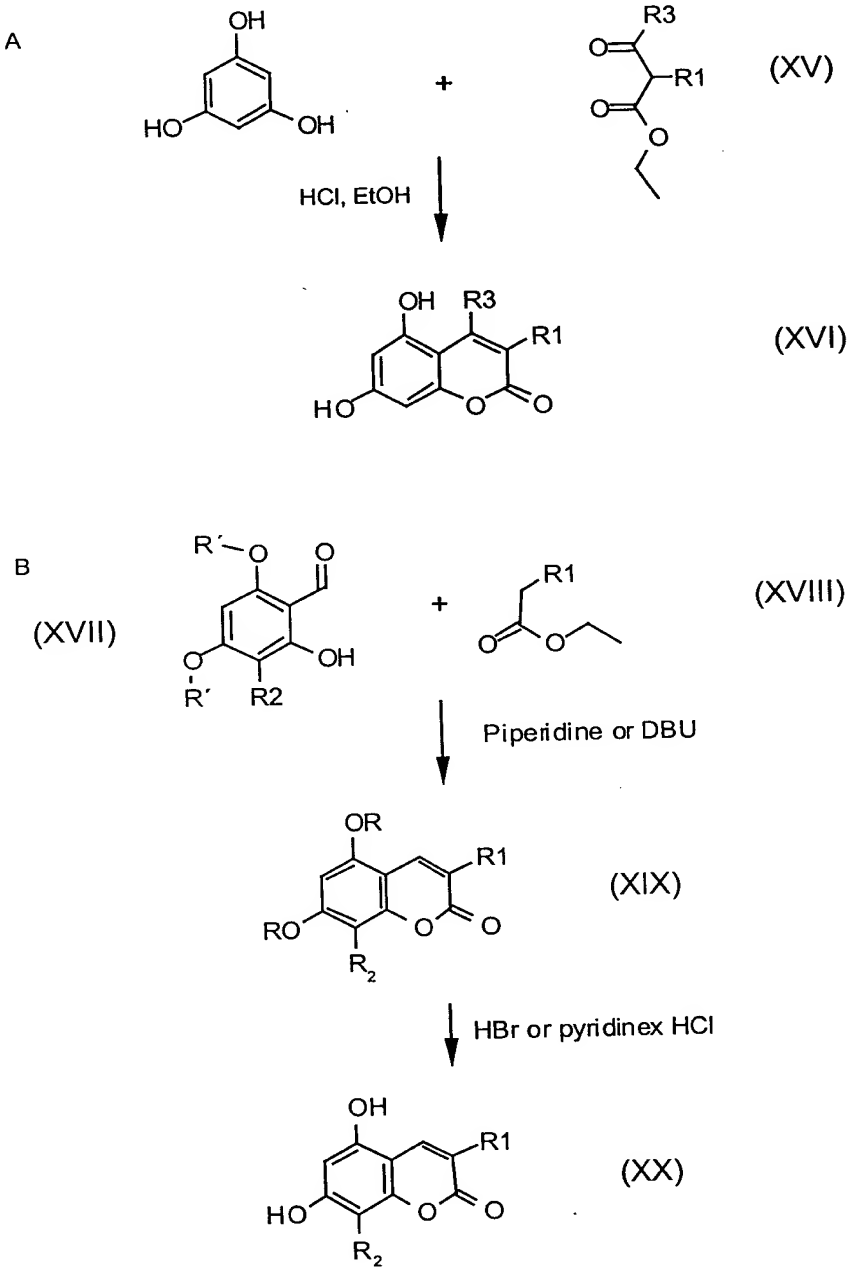

The quinolinones are prepared by the Knorr reaction as described in Scheme 5, wherein R_1,R_{11} and R_3 are the same as defined above, X is a halogen.

SCHEME 5.

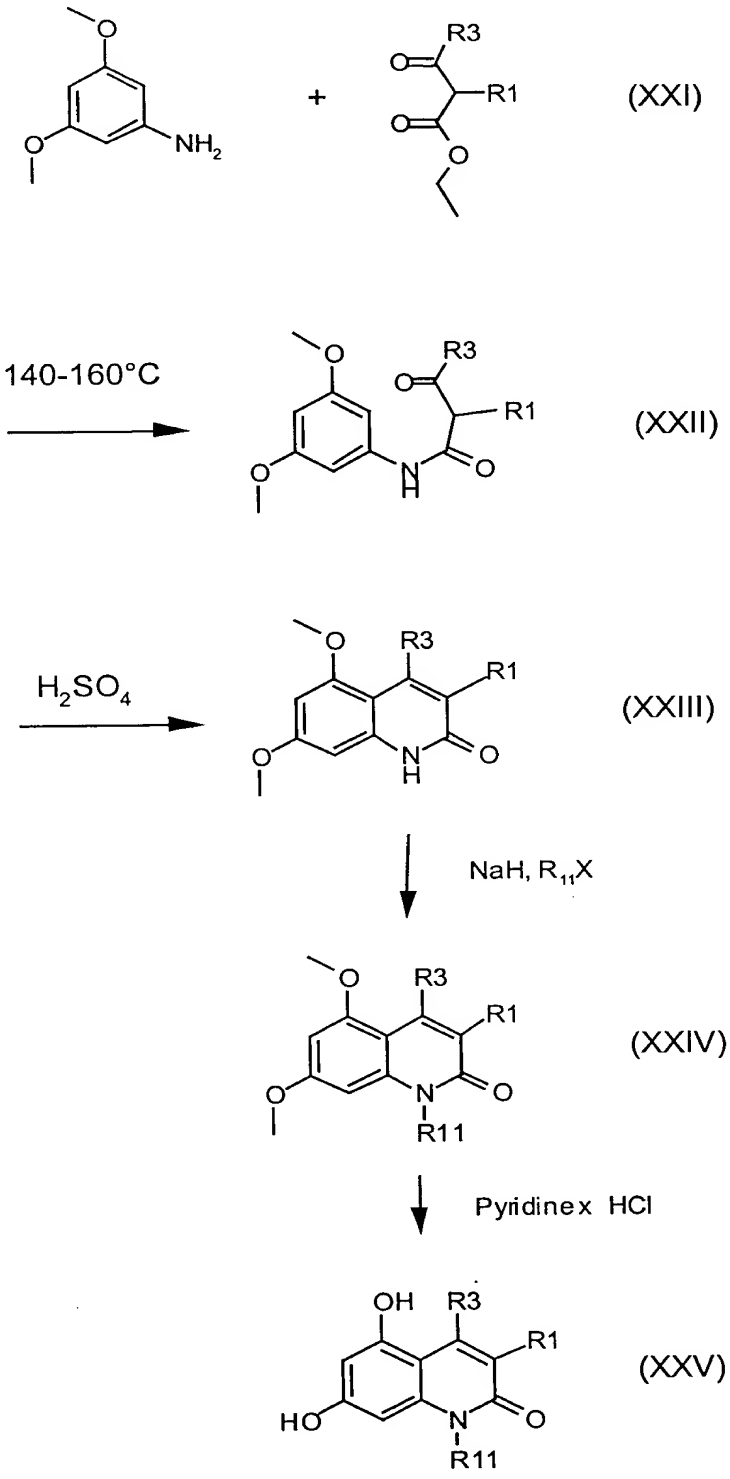

The cyclic compounds (II) can be prepared correspondingly from compound (XXXI) which can be prepared according to the Scheme 6, wherein R_2 and R_6 are the

same as defined above, R´is a protecting group for the hydroxyls e.g. methyl, benzyl or tetrahydropyranyl.

SCHEME 6.

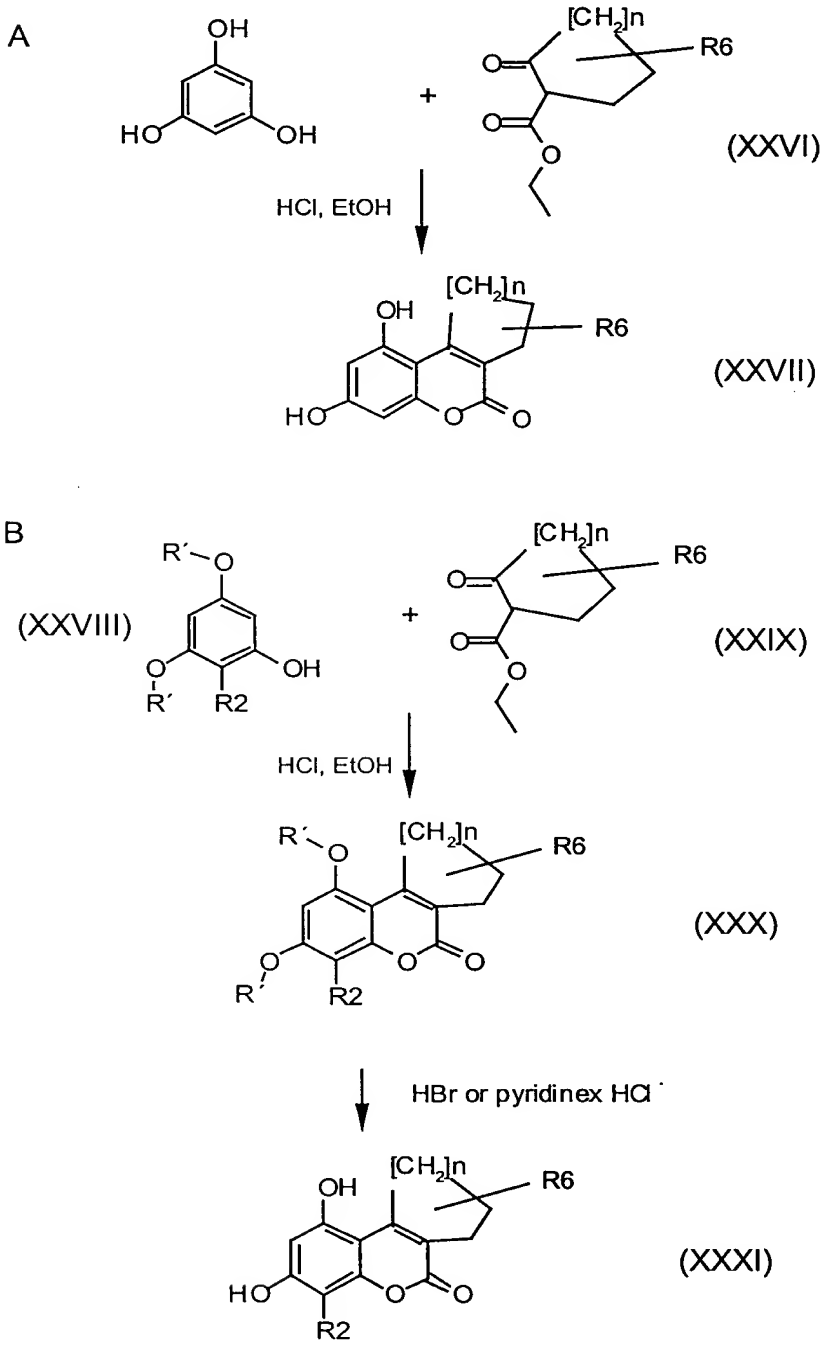

Cyclic quinolinone compounds (II) can be prepared correspondingly from (XXVI) using Scheme 5.

Salts and esters of the compounds, when applicable, may be prepared by known methods. Physiologically acceptable salts are useful as active medicaments, however, preferred are the salts with alkali or alkaline earth metals. Physiologically acceptable esters are also useful as active medicaments. Examples are the esters with aliphatic or aromatic alcohols.

The term "alkyl" as employed herein by itself or as part of another group includes both straight and branched chain radicals of up to 18 carbon atoms, preferably 1 to 8 carbon atoms, most preferably 1 to 4 carbon atoms. The term "lower alkyl" as employed herein by itself or as part of another group includes both straight and branched chain radicals of 1 to 7, preferably 1 to 4, most preferably 1 or 2 carbon atoms. Specific examples for the alkyl and lower alkyl residues, respectively, are methyl, ethyl, propyl, isopropyl, butyl, tert. butyl, pentyl, hexyl, octyl, decyl and dodecyl including the various branched chain isomers thereof.

The term "acyl" as employed herein by itself or as part of another group refers to an alkylcarbonyl or alkenylcarbonyl group, the alkyl and alkenyl groups being defined above.

The term "aryl" as used herein by itself or as part of another group refers to a monocyclic or bicyclic group containing from 6 to 10 carbon atoms in the ring portion. Specific examples for aryl groups are phenyl, naphtyl and the like. "Aroyl" means in a corresponding way an arylcarbonyl group.

The term "alkoxy" as employed herein by itself or as part of another group includes an alkyl group as defined above linked to an oxygen atom. "Aryloxy" means in a corresponding way an aryl group linked to an oxygen atom.

The term "substituted" as used herein in connection with various residues refers to halogen substituents, such as fluorine, chlorine, bromine, iodine or trifluoromethyl group, amino, alkyl, alkoxy, aryl, alkyl-aryl, halogen-aryl, cycloalkyl, alkylcycloalkyl, hydroxy, alkylamino, alkanoylamino, arylcarbonylamino, nitro, cyano, thiol, or alkylthio substituents.

The "substituted" groups may contain 1 to 3, preferably 1 or 2, most preferably 1 of the above mentioned substituents.

Compound of the invention may be administered to a patient in therapeutically effective amounts which range usually from about 0.1 to 500 mg per day depending on the age, weight, condition of the patient, administration route and the phospholamban deactivator used. The compounds of the invention can be formulated into dosage forms using the principles known in the art. It can be given to a patient as such or in combination with suitable pharmaceutical excipients in the form of tablets, dragees, capsules, suppositories, emulsions, suspensions or solutions. Choosing suitable ingredients for the composition is a routine for those of ordinary skill in the art. It is evident that suitable carriers, solvents, gel forming ingredients, dispersion forming ingredients, antioxidants, colours, sweeteners, wetting compounds and other ingredients normally used in this field of technology may be also used. The compositions containing the active compound can be given enterally or parenterally, the oral route being the preferred way. The contents of the active compound in the composition is from about 0.5 to 100 %, preferably from about 0.5 to about 20 %, per weight of the total composition.

The following Examples serve purely as an illustration of the various aspects of this invention, and is not intended to be limiting the present invention.

EXAMPLE 1. Structure Of The Cytosolic Domain of Phospholamban

Phospholamban (1-36) synthesis, purification and characterization

The cytosolic part of phospholamban peptide having the amino acid sequence MEKVQYLTRSAIRRASTIEMPQQARQKLQNLFINFC was synthesized with an automated peptide synthesizer (Perkin-Elmer, Applied Biosystems 431A) using the fluorenylmethoxycarbonyl strategy. The synthesis was started from the hydrophobic C-terminal end. The side chain protecting groups employed during the synthesis were: Trityl (Trt) for Asn, Gln, and Cys, tert-Butoxy (OtBu) for Glu, tert-Butyl (tBu) for Ser, Thr and Tyr, tert-Butoxycarbonyl (Boc) for Lys and 2,2,5,7,8-Pentamethyl chroman-6-sulphonyl (Pmc) for Arg.

The amount of the preloaded resin was 100 μmol and the quantity of the amino acids at each step of the synthesis was 1 mmol. This is a 10 times excess as compared to the amount of the resin loaded.

The peptide cleavage from the resin support (originally preloaded Wang resin) was performed in methylene chloride containing 5 % TFA, 0.2 % ß-mercaptoethanol, 0.2 % thio anisole and 0.2 % dimethylsulfide. Cleavage of the side chain protection of the

peptide was carried out in a mixture of ethanedithiol : thioanisole : water : trifluoroaceticacid = 250 µl: 500 µl : 500 µl : 10 ml for 1.5 hours at room temperature. After that the peptide was precipitated and washed three times with diethylether, and lyophilized.

The synthesized crude phospholamban (1-36) peptide was prepurified by high performance liquid chromatography (HPLC) technique with an analytical reversed phase (RP) column (C_8, 20 µm, 4.6 mm x 30 mm i.d. Perkin-Elmer, Applied Biosystems Brownlee TM column). A linear gradient of acetonitrile (0-100% in 30 min.) in 0.1% TFA was used for elution.

The repurified peptide was futher purified by HPLC RP-chromatography using a C_{18} Kromasil, 5 µm (1.0 x 25 cm) column. The peptide was eluted using a stepwise gradient of acetonitrile, 0.075% TFA (3-30%, in 10 min, 30-50% in 120min.) in 0.1% TFA.

The purified phospholamban (1-36) peptide was characterized by SDS-PAGE followed by Coomassie brilliant blue staining. Western blot analysis was done by using the commercial monoclonal anti-PLB antibody (Upstate Biotechnology). The purified RP-chromatography peaks containing the peptide was further analyzed by mass spectrometry (MALDI-TOF) in reflector mode with a BIFLEX™ mass spectrometer using a 337nm nitrogen laser. The samples were applied in a solution containing 30% acetonitrile/0.1% TFA together with a droplet of sinapinic acid matrix for mass spectrometry analysis. The total amount of purified protein was estimated according to Bradford and also based on RP-chromatography using ß-lactoglobulin as a standar reference. The purified peptides were lyophilized and the dry powder was estimated by weight before analysis of the 3-dimensional structure.

Obtaining NMR spectra of phospholamban (1-36)

^{1}H-NMR spectra were acquired at 400.13 MHz and at 599.86 MHz on a Bruker ARX400 and a Varian UNITY 600 NMR spectrometer respectively. 1D and 2D NMR spectra were obtained for a 3 mM solution of the 36-a.a. fragment of PLB in the solvent mixture H_2O:D_2O:d_3-TFE (63:7:30) containing 6 mM d_{10}-DTT to prevent disulphide formation. The pH was adjusted to 3.00±0.02 (uncorrected for deuterium isotope effects) with microliter amounts of NaOD. COSY, TOCSY (30 - 90 ms) and NOESY (40 - 400 ms) spectra were recorded at 2, 7, 17 and 27°C, by the States-TPPI method using a spectral width of 8.5 ppm. The 2D data was weighted and Fourier transformed to 2 k x 1 k real point matrices. The transmitter presaturated (2.0 s) residual solvent line

was reduced by deconvolution. The spectra were referenced to the residual solvent signal (4.75 ppm at 27°C, -10 ppb/°C). A series of ten 1D spectra was acquired at different temperatures (ranging from 2 to 47°C).

Assignment of the NMR spectra of phospholamban (1-36)

The spin-system and sequential assignments were derived according to Wüthrich, K. et al. (1986) NMR of Proteins and Nucleic Acids, John Wiley & Sons, Inc., New York, by use of COSY, TOCSY and NOESY spectra acquired at 12, 17 and 27°C. Differences in the temperature dependences of the amido proton chemical shifts were sufficient to unravel resonance overlap. Stereospecific assignments for non-degenerated methylenes were deduced from coupling constants $J_{H\alpha H\beta}$ measured from the COSY spectra and from intra residual NOE-cross peak intensities.

Phospholamban (1-36) structure generation and refinement

A series of NOESY spectra was acquired at 17°C with five different mixing times (50, 80, 120, 160, and 200 ms). The integrated cross peak intensities (I) were used in a NOESY-built-up-analysis. Distance restraints were extracted from the inital slope of a second-order polynomial curve fitted to the volumes of the cross peaks integrated from the NOE-series, with the initial condition $I_{(\tau m=0)}=0$. Intra methylene and sequential NOEs served for the calibration. The distances were initially classified as short (1.8-2.5 Å), medium (1.8-3.5 Å) or long (3.0-6.0 Å) for the generation of the first set of structures. When a distance could not be calculated from the built-up curve, owing to a partial (> 20 %) overlap, a poor signal-to-noise ratio or disturbances, it was only required that the distance was < 5.0 Å. The upper bounds were extended by 1.0 Å for each pseudo atom. The restraint data were supplemented with distance restraints, which were based on strong, medium and weak NOEs, from the 150 ms NOE-spectrum acquired at 12°C.

Coupling constants (*J*) were measured by the *J*-doubling method (McIntyre, L. et al. (1992) J Magn Reson 96, 425-431) from fine structures of COSY cross peaks. Dihedrals ϕ and χ, which were characterised by intermediate *J*, were not constrained but small and large $J_{NH\alpha}$ and $J_{H\alpha H\beta}$ were related to staggered conformers (± 30 degrees) on the basis of Karplus functions and intra residual NOEs (Karplus, M. (1963) J . Am. Chem. Soc., 85, 2870). The H-H distance and dihedral angle restraints were calculated and the data were imported into the software InsightII (Molecular Simulations, Inc.) in order to generate, evaluate and refine the structures. Simulated NOESY spectra were

back calculated. The protein coordinate files were analysed by the software PROMOTIF v2.0 (Hutchinson, G. (1995), v2.0 Ed., available by anonymous ftp on 128.40.46.11).

Structures were generated by distance geometry (DGII) followed by simulated annealing (force field AMBER) (Havel, T. et al. (1979) Biopolymers 18, 73). A set of structures was computed. The structures with the least restraint violations were used to back calculate NOE-matrices. If the Hα-chemical shift of consequent residues in the segment characterised by NOEs typical of α-helices departed from the corresponding random coil value more than -0.2 ppm, also the correspondent dihedrals ψ were constrained (± 60 degrees). A new set of structures was subsequently calculated. From this new family of structures only those structures with no violations over 0.2 Å were accepted.

Assignment results

The complete spin-system and sequential assignments were obtained under the experimental conditions described. The assignments are listed in Table V (annexed to the present application) showing H-chemical shifts of PLB (1-36) in 54% H_2O / 6% D_2O / 30% d_3-TFE, pH 3.05 at 17°C, wherein the staggered conformations are denoted by a line under the chemical shift of $C_\beta H$ in an anti-configuration and by a dashed line in a gauche-configuration (-60 degree) to $C_\alpha H$.

Fig. 7 is a summary of the observed sequential and medium-range NOE connectivities for PLB(1-36) in 54% H_2O / 6% D_2O / 30% d_3-TFE, at pH 3.05 at 17°C., wherein assignments were made from NOESY spectra acquired at 120, 160 and 200 ms mixing times. Sequential NOEs are represented by shaded blocks. Medium-range NOEs are represented by arrows connecting the appropriate residues. Open circles denote $^3J_{NH\alpha CH}$ coupling constants smaller than 7 Hz. The secondary shift (Δδ) of αCH is defined as the difference between the observed chemical shift and the random coil chemical shift for each residue. Negative (upfield) Δδ values are associated with α-helical secondary structure and positive (downfield) Δδ values with β-structure according to Wishart et al., Biochemistry (1992), 31, 1647-1651.

In total 723 NOEs were assigned. All the 34 possible intra NH-$C_\alpha H$ correlations were observed in the finger print region. Most of the corresponding NOEs were fairly strong and comparable to sequential NH_{i+1}-$C_\alpha H_i$ NOEs (Fig. 7). Many sequential NH_i-NH_{i+1} and NH_i-NH_{i+2} NOEs were present. Numerous $C_\alpha H_i$-NH_{i+3} and some $C_\alpha H_i$-NH_{i+4} NOEs were crowded in the finger print region of the NOESY spectra. Furthermore, there were a number of $C_\alpha H_i$-$C_\beta H_{i+3}$ cross peaks. NOEs derived from interactions longer than i > i+4 were observed only for protons of Met20.

J-couplings between NH and $C_\alpha H$ were small for most residues. Due to overlap of resonances or weak intenstity of COSY cross peaks it was not possible to measure accurate values for all residues but the couplings were below 7-8 Hz with the exception of the residues at the N- and C-terminus and in the center of PLB (1-36).

The central region of the PLB(1-36) does not show a helical character. Namely, the $\delta_{C\alpha H}$ values of the residues Glu19, Met20 and Pro21 were not significantly smaller than their random coil values. Glu19 and Met20 were mostly devoid of the NOEs typical of a helical structure, and there were unambiguous strong sequential NOEs between $C_\alpha H$ of Glu19 and NH of Met20, and between $C_\alpha H$ of Met20 and $C_\delta Hs$ of Pro21. Furthermore, the NOE between $C_\alpha H$ of Ile18 and NH of Glu19 is strong, even when partially buried in the crowded finger print region. All this implies that the central region of PLB(1-36) assumes an extended-like conformation. The extended segment is, nevertheless, short. Thr17 and Gln22 show NOEs and coupling constants characteristic of residues in an α-helix, and there are NOEs from the side chain protons of Glu19 and Met20 to the protons of the adjacent residues in the N- and C-terminal helices. We conclude that the N- and C-terminal α-helices are separated by a turn at Ile18, Glu19, Met20, and Pro21. The proline is in a *trans*-conformation. A tight turn, which would result the axes of the N- and C-terminal helices being parallel, is not possible. There were no unambiguous NOEs between the N- and C-terminal helices.

Structure of PLB (1-36)

The structure of PLB (1-36) was determined from 599 distances and 50 dihedral restraints excluding those that were defined more accurately by the covalent structure alone. These redundant NOE-derived restraints were consistent with the covalently imposed distance limits, which indicated that the calibration of distances was reasonable. On average there were 16.6 non-trivial NOE-derived restraints per residue. The residues Lys3-Ile18 of the N-terminal helix had on average a few restraints less per residue than the residues Gln22-Cys36 in the C-terminal helix. This is at least partly due to the fact that there were on average more protons with non-degenerated shifts per residue in the C-terminal helix than in the N-terminal helix (Table V). For the residues Ile18-Pro21, which confine the turn, there were about as many restraints per residue as there were for the residues in the N-terminal helix.

The structure generation resulted in a family of structures all of which show a helix-turn-helix motif. The root mean square deviation was computed from the family of 20 structures with no distance violations above 0.2 Å and no dihedral violations. Fig.

9 shows the quality of the structure of PLB(1-36) obtained by NOE data wherein RMSD per residue and the number of restraints per residue is shown.

Since no unambiguous long range NOEs were found between the N- and C-terminal helices, the family of structures displayed a dispersion of atomic coordinates in the remote parts of the N- and C-terminal helices. The mutual orientation of the helices was constrained only by the short range distance restraints in the turn. Therefore, RMSD per residue was computed separately i) for the N-terminal helix plus the turn (a.a. 1-21) and ii) for the C-terminal helix plus the turn (18-36). The RMSD represented roughly an inverse correlation with the number of restraints per residue, as expected. In average the atoms in the N-terminal helix were defined to a precision of 1.3 Å (backbone only) and of 2.3 Å (all atoms) and in the C-terminal helix to a precision of 0.8 Å (backbone only) and of 1.9 Å (all atoms). The smallest number of distance violations (below 0.2 Å) were observed for structures in which the segment from Cα of Glu19 to Cα of Pro21 is extended, the side chain of Met20 sticks out approximately parallel to the C-terminal helix and the side chain of Glu19 points almost in the opposite direction. In these structures, the plane of the peptide bond Ile18-Glu19 is approximately orthogonal to the plane of the extended segment.

Owing to the structural mobility of the turn, the family of structures displays a dispersion in the relative position of the N- and C-terminal helices. The dispersion is, nevertheless, limited. When the different structures of the family are superimposed on the Cα of the residues in the C-terminal helixes, the axe of the N-terminal is dispersed in a cone with an opening of approximatively 90 degrees, and with a relative angle of about 80 degrees. Similar mutual orientations for two sequential helices, one of which transmembran and the other anfiphatic, have been found or hypothized for many small membrane bound proteins or peptides (Stopar, D. et al. (1996) Biochemistry, 35 (48), 5467-5473).

In some of the structures, the side chain εNH of Arg9, Arg13 and Arg14, whose chemical shifts are nearly independent of *T*, make hydrogen bonds with the adjacent side chain oxygen of Ser10, Ser16 and Thr17. For Arg25, with large $\Delta\delta_{NH}(T)$, there were no obvious candidates for hydrogen bond donors. The side chain NH_2 of the glutamines and asparagines could form hydrogen bond net works parallel to the helical axis.

With regards to the phosphorylation of PLB, we find important that the phosphorylation site Ser16 is readily accessible and exposed to the solvent. Thr17, on the N-terminal helix, is facing the C-terminal helix and appears less exposed to the solvent than Ser16. Due to the pitch of the α-helix, Arg13 and Arg14 are also exposed with orientations that lag 60 degrees in phase with respect to Ser16 and Thr17 on the

same side of the helix. The presence of positively charged residues in the vicinity of a serine or threonine residue is often seen in a substrate for phosphokinases (e.g. in Troponin I).

We find that one side of the N-terminal helix is predominantly polar or hydrophilic. The same is true for the C-terminal helix, whose polar residues are located on one side while leaving the other side dominated by lipophilic side chains. Owing to the relative orientation of the helices, it can be noted that the hydrophilic side of the N-terminal helix faces always the lipophilic side of the C-terminal helix. This defines a pocket which could be described as an amfiphatic armpit. In this pocket, the relative position of the polar residues on the N-terminal and of the lipophilic residues on the C-terminal can be conveniently described by use of two centroids calculated by averaging the coordinates of selected side chains. The coordinates of the side chains of Arg13, Arg9 and Tyr6 were used to build the centroid relative to the N-terminal and the coordinates of the side chains of Phe32 and Phe35 were used to build up the centroid relative to the C-terminal. The distance between these two centroids was calculated for every structure of the family and was 18.5±4.5 Å. The refined structure of PLB (1-36) is shown in Figure 3.

EXAMPLE 2. Structure Of The Cyclic Peptide cP226

Peptide synthesis, cyclization and purification

The linear peptide having the amino acid sequence CYWELEWLPCA was synthesized with an automated peptide synthesizer (Perkin-Elmer, Applied Biosystems 431A) using the fluorenylmethoxycarbonyl-strategy. The synthesis was started from the carboxy-terminal end. The side chain protecting groups employed during the synthesis were: Trityl (Trt) for Cys, tert-Butoxy (OtBu) for Glu, and tert-Butyl (tBu) for Tyr.

The amount of the preloaded resin was 100 µmol and the quantity of the amino-acids at each step of the synthesis was 1 mmol.

The peptide cleavage from the resin support (originally preloaded Wang resin) as well as cleavage of the side chain pretection groups was carried out in a mixture of ethanedithiol : thioanisole : water : trifluoroaceticacid = 250 µl: 500 µl : 500 µl : 10 ml for 1.5 hours at room temperature. After that the peptide was precipitated and washed three times with diethylether, and lyophilized.

The amino-acids and the preloaded resins used for the peptide synthesis were obtained from Novabiochem. Trifluoroacetic-acid (TFA) was produced by Perkin-Elmer, ethanedithiol (EDT) and thioanisole were manufactured by Fluka.

The cyclic peptide cP226 was reconstituted from the linear CYWELEWLPCA peptide by dissolving 0.5 mg/ml the purified peptide into 10 mM $(NH_4)_2CO_3$ and the oxidation of the SH groups of the two cycteine residues to form intramolecular disulphide bridge was achieved by leaving the solution at room temperature for 1-2 days. The reaction was followed by HPLC chromatography from the peaks of the linear and the cyclic peptide was varied as a fuction of time.

The peptides, both the linear and the cyclic cP226, were purified and separated by reverse phase HPLC-chromatography (C8, Aquqpore Octyl, 30 μm, 10x100 mm, Perkin-Elmer) using 30 min linear gradient from 0.1 % TFA to 100 % acetonitrile. The obtained peptides were characterized by mass spectrometry.

NMR spectra of cP226

^{1}H-NMR spectra were acquired at 400.13 MHz and at 599.86 MHz on a Bruker ARX400 and a Varian UNITY 600 NMR spectrometer respectively. 1D and 2D NMR spectra were obtained for a 1 mM solution of the cyclic peptide in water. The pH was adjusted to 6.50±0.02 (uncorrected for deuterium isotope effects) with microliter amounts of NaOD. COSY, TOCSY (30 - 90 ms) and NOESY (200 - 400 ms) spectra were recorded at 5, 10, 15 and 27°C, by the States-TPPI method, using a spectral width of 8.5 ppm. The 2D data was weighted and Fourier transformed to 2 k ∞ 1 k real point matrices. The transmitter presaturated (2.0 s) residual solvent line was reduced by deconvolution. The spectra were referenced to the residual solvent signal (4.75 ppm at 27°C, -10 ppb/°C).

Assignment of the NMR spectra of cP226

The spin-system and sequential assignments were derived according to Wüthrich as in EXAMPLE 1, by use of COSY, TOCSY and NOESY spectra acquired at 5, 10 and 27°C. Differences in the temperature dependences of the amido proton chemical shifts were sufficient to unravel resonance overlap. Stereospecific assignments for non-degenerated methylenes were deduced from coupling constants $J_{H\alpha H\beta}$ measured from the COSY spectra and from intra residual NOE-cross peak intensities.

cP226 Structure Generation And Refinement

A series of NOESY spectra was acquired at 10°C with different mixing times (200, 300, 400 ms). The integrated cross peak intensities (I) were used in a NOESY-built-up-analysis. Distance restraints were extracted from the inital slope of a second-order polynomial curve fitted to the volumes of the cross peaks integrated from the NOE-series, with the initial condition $I_{(\tau_m=0)}=0$. Intra methylene and sequential NOEs

served for the calibration. The distances were initially classified as short (1.8-2.5 Å), medium (1.8-3.5 Å) or long (3.0-6.0 Å) for the generation of the first set of structures. When a distance could not be calculated from the built-up curve, owing to a partial (> 20 %) overlap, a poor signal-to-noise ratio or disturbances, it was only required that the distance was < 5.0 Å. The upper bounds were extended by 1.0 Å for each pseudo atom. The restraint data were supplemented with distance restraints, which were based on strong, medium and weak NOEs, from the 300 ms NOE-spectrum acquired at 10°C.

Coupling constants (*J*) were measured by the *J*-doubling method from fine structures of COSY cross peaks. Dihedrals ϕ and χ, which were characterised by intermediate *J*, were not constrained but small and large $J_{NH\alpha}$ and $J_{H\alpha H\beta}$ were related to staggered conformers (± 30 degrees) on the basis of Karplus functions and intra residual NOEs. The H-H distance and dihedral angle restraints were calculated. Finally, the data were imported into the software InsightII (Molecular Simulations, Inc.) in order to generate, evaluate and refine the structures. Simulated NOESY spectra were back calculated. The protein coordinate files were analysed by the software PROMOTIF v2.0.

Structures were generated by distance geometry (DGII) followed by simulated annealing (force field AMBER). A set of 30 structures was computed. The structures with the least restraint violations were used to back calculate NOE-matrices. Based on the comparison of the back-calculated and experimental NOE-spectra it became possible to unambiguously identify more NOEs and impose corresponding distance restraints. A new set of 30 structures was subsequently calculated. From this new family, 12 structures with at most one violation larger than 0.3 Å were selected and examined further. The distance restraints corresponding to well-resolved cross peaks were refined by an iterative relaxation matrix method (IRMA) based on a structure without restraint violations (>0.2 Å, >0 deg). The upper bounds were kept within at least 10% of the exact distance given by IRMA to take into account the uncertainty in τ_c. The refined restraint set was subsequently used to refine the coordinates by simulated annealing.

The resulting final family of 12 structures was visualized by the graphic software MOLMOL (Koradi, R. et al. (1996) J Mol Graphics 14, 51-55).

Assignment results

The complete spin-system and sequential assignments were obtained under the experimental conditions described. It was necessary to run the NOESY experiments at low temperature (<10°C) and with relatively long mixing time (>300 ms) to induce enough magnetization transfet and visualize the cross peaks. The assignments are listed in Table VI.

cP226 spectra displayed chemical shift dispersion over 8.5 ppm. $C_\alpha H$ shifts ranged from 3.9 to 4.7 ppm and most of the NH shifts were confined between 7.8 and 8.5 ppm, but for Tyr2 and Leu8 the NH resonances were shifted up-field, to 6.9 and 7.3 ppm respectively. There were no signals of methyl groups at very high field (> 0 ppm).

Fig. 10 is a summary of the observed sequential and medium-range NOE connectivities for CP226 in 90% H_2O / 10% D_2O, pH 6.50 at 10°C. The assignments were made from NOESY spectra acquired at 300 and 400 ms mixing times. Sequential NOEs are represented by shaded blocks. Medium-range NOEs are represented by arrows connecting the appropriate residues. Open circles denote $^3J_{NH\alpha CH}$ coupling constants bigger than 8 Hz. The secondary shift ($\Delta\delta$) of αCH is defined as the difference between the observed chemical shift and the random coil chemical shift for each residue. Negative (upfield) and positive (downfield) $\Delta\delta$ values are associated to the secondary structure according to Wishart et al., Biochemistry (1992), 31, 1647-1651.

In total 120 NOEs were assigned. Not all the 9 possible intra NH-$C_\alpha H$ correlations were observed in the finger print region. Most of the corresponding NOEs were fairly weak. Only four sequential NH_i-NH_{i+1} and one NH_i-NH_{i+2} NOEs were present. Some NH_{i+n}-$C_\beta H_i$ were visible in the NOESY spectra and facilitated the sequential assignment. The secondary shift ($\Delta\delta$) of αCH, defined as the difference between the observed chemical shift and the random coil chemical shift for each residue, gave evidence of bended structure (Fig. 10). NOEs derived from interactions longer than i > i+4 (across the cycle) were observed for protons of the side chains of Trp3 and Leu8 and for protons of Tyr2 and Cys10.

J-couplings between NH and C_aH (measured from the COSY cross peaks) were large for most residues. The couplings for all residues were above 8 Hz, suggesting that the ϕ angles have predominantly values of 120 ± 30°.The proline was in a trans-conformation.

Structure of cP226

The structure of cP226 was determined from 110 distances and 8 dihedral restraints excluding those that were defined more accurately by the covalent structure alone. These redundant NOE-derived restraints were consistent with the covalently imposed distance limits, which indicated that the calibration of distances was reasonable. On average there were 10 non-trivial NOE-derived restraints per residue. The residues in the central part of the peptide (from Trp3 to Leu8) had more restrain per residue than the average. This is at least partly due to the fact that there were on average more protons with non-degenerated shifts per residue in that zone.

The structure generation resulted in a family of structures all of which show bend-coil-bend motif (MOLMOL). The root mean square deviation was computed from the family of 12 structures with no distance violations above 0.3 Å and no dihedral violations. The small distance restraint violations occurred primarily among the side chain groups, e.g. the tyrosine side chain. This may be a result of excessive mobility in these parts, which could give rise to non-simultaneous NOEs. RMSD per residue was computed and represented roughly an inverse correlation with the number of restraints per residue, as expected. In average the atoms were defined to a precision of 0.96 Å (backbone only) and of 2.02 Å (all atoms) and, if calculed only for the portion from Trp3 to Trp7, to a precision of 0.72 Å (backbone only) and of 1.87 Å (all atoms) (Table VII).

The lipophilic side chains of Trp3, Leu5, Trp7 and Leu8 were clustered on one side of the cyclic peptide, leaving the most of the polar carbonyl and amine groups of the backbone on the other side.

The structure of CP226 shown in this report was docked on the structure of PLB (1-36) described above. The comparison of the two structures confirm the hypothesis that the two glutamate residues on CP226 may partecipate to the binding by coupling with Arg9 and Arg 13 on PLB (1-36), exposing the lipophilic cluster of PC226 to the lipophilic outer part of the C-terminal helix of PLB(1-36).

Fig. 11 shows a family of 12 structures of CP226 deduced from NMR data. The backbones, the heavy atoms of the Trp3 and Trp7 side chains, the heavy atoms of the Glu4 and Glu6 side chains, the carbon β of Glu4 and Glu6 is shown. The distance between the beta carbons of the two glutamate residues (Fig. 11) was highly conservative (8.3 ± 0.9 Å). This information can be useful to design small molecules in which two acetate residues mimic the position of Glu4 and Glu6 on CP226. In the

same way, the distance of the lipophilic cluster from the two glutamate residues will also be useful in the drug design process.

EXAMPLE 3. Activity assays

Experiment 1. Effect on calcium uptake into the SR vesicles prepared from cardiac and fast skeletal muscle

The inhibitory effect of a given compound on phospholamban can be demonstrated by measuring the effect of the compound on calcium uptake into the SR vesicles prepared from cardiac tissue and into SR vesicles prepared from fast skeletal muscle (psoas m.). Both kind of SR vesicles contain Ca^{2+}-ATPase but the vesicles from the fast skeletal muscle do not contain phospholamban (Hoh JFY, "Muscle fiber types and function", Current Opinion in Rheumatology, 4:801-808, 1992). An increase in the calcium uptake into the SR vesicles prepared from cardiac tissue but not into the SR vesicles prepared from fast skeletal muscle indicates that the compound relieves the inhibitory effect of phospholamban on SR Ca^{2+}-ATPase and thus acts as a phospholamban inhibitor. Since phospholamban represses both the rates of relaxation and contraction in the mammalian heart through its inhibitory effects on the cardiac SR Ca^{2+}-ATPase, a compound relieving these effects is potentially useful in the treatment of heart failure.

Method

Guinea pigs (10-12) were decapited. Their hearts or the psoas muscles were excised, washed in ice-cold 0.9 % NaCl and cut into pieces in a buffer containing 20 mM Tris-maleate, 0.3 M sucrose, pH 7.0. Thereafter tissue pieces were homogenized with Polytron and further with Potter (10 strokes). The homogenate was centrifugated at 1000 g for 15 min at 4 °C. The supernatant was collected and the pellet was resuspended into 5 ml of the buffer (20 mM Tris-maleate, 0.3 M sucrose, pH 7.0) and recentrifugated at 1000 g for 10 min at 4 °C. The obtained supernatant was combined with the earlier collected supernatant and centrifugated once again at 10 000 g for 20 min at 4 °C. The final supernatant was filtered into a bottle equipped with a magnetic stirrer. KCl was added to the filtered supernatant to achieve the final concentration of 0.6 M (at 4 °C). The obtained solution was centrifugated at 100 000 g for 60 min at 4 °C. The pellet was suspended in 5 ml of the buffer containing 20 mM Tris-maleate, 0.3 M sucrose, pH 7.0 and centrifugated at 100 000 g for 60 min at 4 °C. The obtained pellet was suspended in 5 ml of buffer containing 20 mM Tris-maleate, 0.3 M sucrose,

0.1 M KCl, pH 7.0 and stored at -80 °C until use. The protein concentration was also measured in order to standardise the separately prepared vesicle preparations.

In the calcium uptake assay, the fluorescent indicator, fluo-3 was used to detect the decrease of the extravesicular Ca^{2+}-concentration, when the SR Ca^{2+}ATPase was transferring Ca^{2+} from the extravesicular space into the SR-vesicles.

The SR-vesicles obtained above (50 µg protein/ml) were pre-incubated with or without the test compound at 37 °C for 5 min in the assay buffer containing 40 mM imidazole, 95 mM KCl, 5 mM NaN_3, 5 mM $MgCl_2$, 0.5 mM EGTA, 5 mM potassium oxalate, 2 µM ruthenium red, 5 µM fluo-3, pH 7.0. The free calcium was adjusted to 0.1 µM or to 0.04 µM by $CaCl_2$. The reaction was initiated by adding ATP (5 mM). The final reaction volume was 1.5 ml. The fluorescence of reaction mixture was measured for 3 min by using the excitation and emission wavelengths of 510 nm and 530 nm, respectively.

Results

Figures 12A and 12B show the effect of the compound of Example 1c (50 and 100 µM) on the Ca^{2+} uptake rate into the cardiac (A) and fast skeletal muscle (B) SR vesicles. It can be seen that the compound of the invention accelerated the calcium uptake into the cardiac SR vesicles but did not change the calcium uptake into the SR vesicle prepared from the fast skeletal muscle.

Table VIII shows the effects of various compounds of the invention on the Ca^{2+} uptake rate into the cardiac (A) and fast skeletal muscle (B) SR vesicles. The experiments were carried out at 0.1 µM and 0.04 µM free calcium concentrations, respectively.

Table VIII. Stimulation (%) of the Ca^{2+} uptake into the vesicle preparations obtained from the ventricular myocardium (A) and fast skeletal muscle (B) of the guinea-pig heart.

Compound of Example No. (100 μM)	The stimulation (%) of Ca^{2+} uptake A	B
3c**	51	0
2c	26	-1
7c	5	-17
8g*	18	0
11b	28	nd
12	32	nd
13d***	23	nd
14c*	18	nd
18e	13	nd
21	11	nd
23****	20	nd

*10 μM, **20 μM, ***50 μM, ****5 μM
nd=not determined

Experiment 2. The effects on the left ventricular pressure derivatives

Method

Guinea-pigs of either sex weighing 300-400 g were used in the study. After the guinea-pig was sacrificed by a blow on the skull and decapitated the heart was rapidly excised. The heart was then rinsed in cold oxygenated perfusion buffer. A cannula was inserted into the aorta and secured with a ligature. Retrograde perfusion began as soon as the heart was placed in a thermostatically controlled moist chamber of the Langendorff apparatus. Modified Tyrode solution (37 °C), equilibrated in a thermostatically controlled bulb oxygenator with carbogen (95 % O_2 and 5% CO_2) was used as a perfusion buffer. The composition of the Tyrode solution was (in mM): NaCl 135; $MgCl_2$ x $6H_2O$ 1; KCl 5; $CaCl_2$ x $2H_2O$ 2; $NaHCO_3$ 15; Na_2HPO_4 x $2H_20$ 1; glucose 10; pH 7.3-7.4. The experiments were carried out under constant pressure condition (50 mmHg). After a short prestabilization (10 min) a latex balloon (size 4) was carefully placed into the left ventricle through the left pulmonary vein and the left atrium. The latex balloon was attached to a stainless-steel cannula coupled with a pressure transducer. The latex balloon, the cannula and the chamber of the pressure transducer were filled with ethylene glycol / water (1:1) mixture avoiding any air-

bubble. The isovolumetric left ventricular pressure was recorded through the pressure transducer. At the beginning of the experiment, the volume of the balloon was adjusted to obtain a diastolic pressure of approximately 5 mmHg. Before starting the experiment, the heart was allowed to stabilise further for 30 - 50 min with vehicle (0.1% DMSO) in the perfusion buffer.

After 15 min baseline recording various concentrations of the test compound were added to the perfusion buffer at 15 min intervals. The concentration range of 0.3 - 30 μM was tested. The vehicle concentration (0.1% DMSO) was kept constant throughout the experiment.

Results

The EC_{50} values and maximum effects (% change from baseline) of various compounds of the invention on left ventricular systolic pressure are given in Table IX.

TABLE IX. The EC_{50} values and maximum effects (% change from baseline) on left ventricular systolic pressure.

Compound of Example No.	EC_{50} (μM)	maximum effect (%)
1c	9	+52 at 30 μM
3c	4	+63 at 10 μM
5c	>10	+14 at 30 μM
6c	0.5	+25 at 10 μM
7c	2.5	+29 at 10 μM
8g	2	+64 at 10 μM
9d	5	+50 at 30 μM
12	5	+22 at 10 μM
13d	10	+48 at 30 μM
14c	1.5	+25 at 10 μM
15c	3	+37 at 10 μM
16c	10	+57 at 30 μM
18e	10	+35 at 30 μM
19e	6	+39 at 30 μM

EXAMPLE 4.

The preparation of PLB deactivators is described below by the following non-limiting examples.

Example 1. Preparation of 3-Benzyl-5,7-bis[(1*H* -tetrazol-5-yl)-methoxy]-4-methyl-2*H* -1-benzopyran-2-one

a) 3-Benzyl-5,7-dihydroxy-4-methyl-2*H* -1-benzopyran-2-one

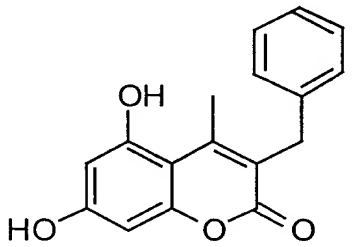

A solution of phloroglucinol dihydrate (20 g) and ethyl 2-benzylaceto-acetate (27.5 ml) in ethanol (320 ml) was treated with dry HCl at 0°C for five hours and the solution was kept at that temperature overnight. The yellow solution was concentrated and triturated with water, the solids filtered, washed with water and dried. The resulting hydrate was thrice evaporated to dryness from toluene, triturated with pethroleum ether (bp. 40-60°C) and filtered. Yield 33,4 g (96 %). Melting point 258-260 °C.

^{1}H-NMR (DMSO-d_6, 400MHz): 2.525 (s, 3H, CH_3), 3.887 (s, 2 H, CH_2Ph), 6.171 (d, 1H, J = 2,4 Hz), 6.274 (d, 1H, J = 2,4 Hz), 7.167-7.279 (m, 5H, Ph), 10.2 (s, 1H, OH), 10.47 (s, 1H, OH).

b) 3-Benzyl-5,7-bis(cyanomethoxy)-4-methyl-2*H* -1-benzopyran-2-one

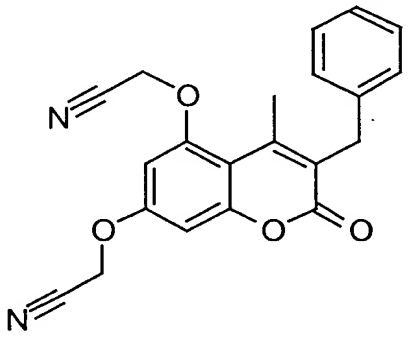

Chloracetonitrile (6.86 g), potassium carbonate (23.9 g) and 12.2 g of the product from example 1a were stirred in 120 ml of DMF at 100°C under nitrogen for two hours. The reaction mixture was cooled and poured into ice water. The solids were filtered and washed with water. Yield 13.8 g (88 %). Melting point 147-154°C.

^{1}H-NMR (DMSO-d_6, 400MHz): 2.525 (s, 3H, CH_3), 3.969 (s, 2H, CH_2Ph), 5.307 (s, 2H, OCH_2CN), 5.314 (s, 2H, OCH_2CN), 6.814 (d, 1 H, J = 2.5 Hz), 6.940 (d, 1H, J = 2.5 Hz), 7.18-7.292 (m, 5H, Ph).

c) 3-Benzyl-5,7-bis[(1*H* -tetrazol-5-yl)methoxy]-4-methyl-2*H* -1-benzopyran-2-one

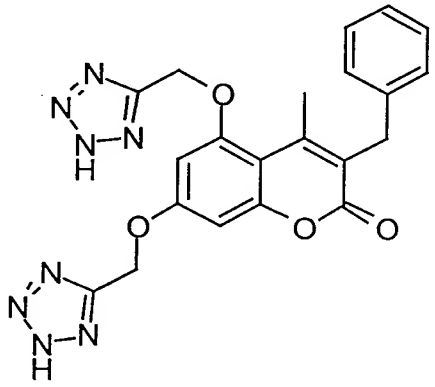

The product from example 1b (1 g), sodium azide (0.42 g) and ammonium chloride (0.34 g) were stirred in DMF (5 ml) under nitrogen at 100 °C for 5 hours. The reaction mixture was allowed to cool down and then poured into ice water. The pH of the solution was adjusted to 10-11 and then the solution either extracted once with ethyl acetate or filtered through CELITE. The solution was acidified to pH 2 with hydrochloric acid, kept at 5°C and filtered. Yield 0.96 g (81 %). Melting point 229-233°C.

^{1}H-NMR (DMSO-d_6, 400MHz): 2.468 (s, 3H, CH_3), 3.937 (s, 2H, CH_2Ph), 5.596 (s, 2H, OCH_2Tet), 5.602 (s, 2H, OCH_2Tet), 6.832 (d, 1H, J = 2.4 Hz), 6.851 (d, 1H, J = 2.4 Hz), 7.171-7.283 (m, 5H, Ph).

Example 2. Preparation of 7,8,9,10-Tetrahydro-1,3-bis[(1*H* -tetrazol-5-yl)methoxy]-7-phenyl-6H-dibenzo[b,d]pyran-6-one

a) 7,8,9,10-Tetrahydro-1,3-dihydroxy-7-phenyl-6H-dibenzo[b,d]pyran-6-one

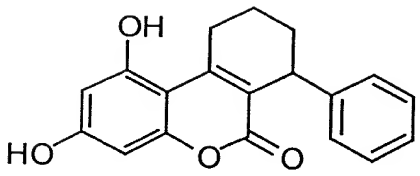

A solution of phloroglucinol (0.7 g) and 2-ethoxycarbonyl-3-phenylcyclohexanone (1,5 g) in ethanol was treated with dry HCl as described in example 1a. The product was first recrystallized from ethanol-water (1:1) and then triturated with ether. Yield 0.61 g.

^{1}H-NMR (DMSO-d_6, 400MHz): 1.38-1.52 (m, 1H), 1.57-1.66 (m, 1H), 1.69-1.78 (m, 1H), 1.86-1.96 (m, 1H), 2.9-3.02 (m, 1H), 3.3-3.4 (m,1H), 4.050 (b, 1H), 6.157 (d, 1H, J = 2.4 Hz), 6.297 (d, 1H, J = 2.4 Hz), 7.076-7.265 (m, 5H), 10.153 (s, 1H), 10.456 (s, 1H).

b) 7,8,9,10-Tetrahydro-1,3-bis(cyanomethoxy)-7-phenyl-6H-dibenzo[b,d]pyran-6-one

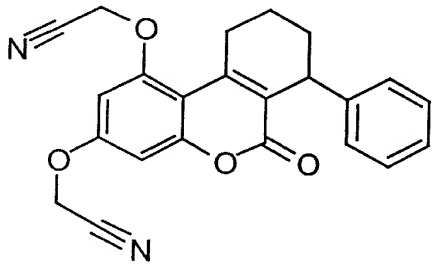

The product from example 2a (0.5 g) was treated with chloroaceto-nitrile (0.25 g) and potassium carbonate (1.12g) in DMF (5 ml) as described in example 1b. Yield 0.6 g.

^{1}H-NMR (DMSO-d_6, 400MHz): 1.38-1.58 (m, 1H), 1.6-1.7 (m, 1H), 1.7-1.76 (m, 1H), 1.89-1.99 (m, 1H), 2.9-3.03 (m, 1H), 3.2-3.28 (m 1H), 4.111(b, 1H), 5.314 (s, 2H), 5.349 (s, 2H), 6.840 (d, 1H, J = 2.5 Hz), 6.925 (d, 1H, J = 2.5 Hz), 7.108-7.274 (m, 5H).

c) 7,8,9,10-Tetrahydro-1,3-bis[(1*H* -tetrazol-5-yl)methoxy]- 7-phenyl- 6H-dibenzo[b,d]pyran-6-one

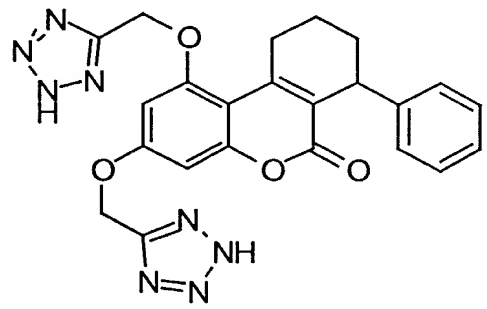

The product from example 2b (0.6 g) was treated with sodium azide (0.2 g) and ammonium chloride (0.17 g) in DMF (5 ml) as in example 1c. The product was recrystallized from a mixture of DMF, ethanol and water (approximately 1:2:3). Yield 0.41 g. Melting point: 153-154°C.

^{1}H-NMR (DMSO-d_6, 400MHz): 1.38-1.5 (m, 1H), 1.5-1.6 (m, 1H), 1.69-1.76 (m, 1H), 1.87-1.96 (m, 1H), 2.9-3.05 (m, 1H), 3.2-3.3 (m, 1H), 4.094 (b, 1H), 5.602 (s, 2H), 5.643 (s, 2H), 6.832 (d, 1H, J = 2.3 Hz), 6.851 (d, 1H, J = 2.3.Hz), 7.089-7.212 (m, 5H).

Example 3. Preparation of 3-Benzyl-5,7-bis[(2,5-dihydro-5-oxo-4*H* -1,2,4-oxadiazol-3-yl)- methoxy]-4-methyl-2*H* -1-benzopyran-2-one

a) 3-Benzyl-5,7-bis[(hydroxyamidino)methoxy]-4-methyl-2*H* -1-benzopyran-2-one

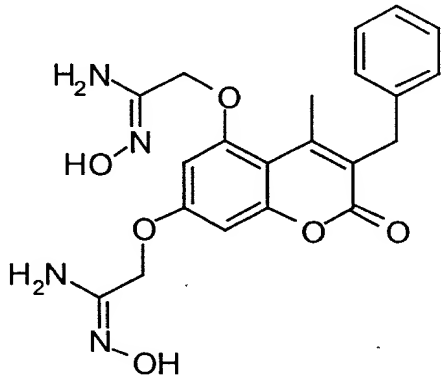

Triethylamine (1.94 ml) was added to a suspension of hydroxylamine hydrochloride (0.97 g) in DMSO (2 ml) and the resulting mixture stirred at room temperature for thirty minutes. The crystals were filtered and washed with THF. The filtrate was concentrated and the product from example 1b (0.5 g) added. This solution was kept at 75 °C overnight. The reaction mixture was treated with ice water, the pH

adjusted to 11 and the solids filtered, washed with water, and dried. Yield 0.5 g. Melting point: 155-160°C.

^{1}H-NMR (DMSO-d_6, 400MHz): 2.56 (s, 3H, CH_3), 3.938 (s, 2H), 4.466 (s, 2H), 4.486 (s, 2H), 5.565 (s, H, NH_2), 5.709 (s, 2H, NH_2), 6.658 (d, 1H, J = 2.4 Hz), 6.692 (d, 1H, J = 2.4 Hz), 7.168-7.284 (m, 5H, Ph), 9.346 (s, 1H, OH), 9.362 (s, 1H, OH).

b) 3-Benzyl-5,7-bis[(ethoxycarbonyloxyamidino)methoxy]-4-methyl- 2*H* -1-benzopyran-2-one

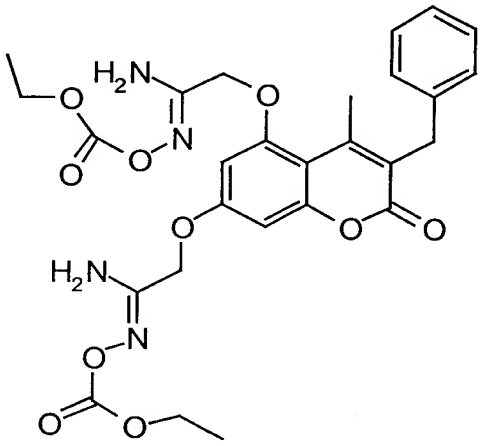

Ethyl chloroformiate (0.45 ml) was added to a solution of the product from example 3a (1 g) and pyridin (0.38 ml) in DMF (5 ml) at 0°C. The reaction mixture was kept at that temperature for an additional 30 minutes and then ice water added. The solids were filtered and washed with water. Yield 1.63 g. Melting point 87-92°C.

^{1}H-NMR (DMSO-d_6, 400MHz): 1.215-1.256 (m, 6H), 2.553 (s, 3H), 3.947 (s, 2H), 4.140-4.198 (m, 4H), 4.566 (s, 2H), 4.599 (s, 2H), 6.688 (d, 1H, J = 2.4 Hz), 6.718 (d, 1H, J = 2.4 Hz), 6.792 (b, 2H, NH_2), 6.818 (b, 2H, NH_2), 7.171-7.285 (m, 5H).

c) 3-Benzyl-5,7-bis[(2,5-dihydro-5-oxo-4*H* -1,2,4-oxadiazol-3-yl)- methoxy]-4-methyl-2*H* -1-benzopyran-2-one

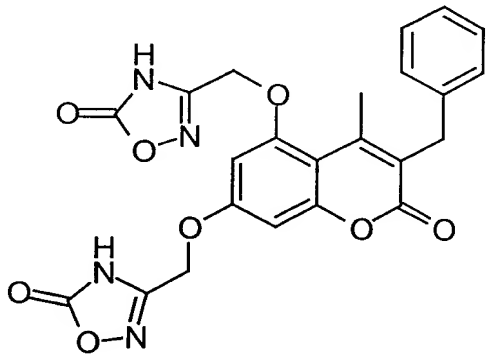

The product from the previous example (1.5 g) and DBU (0.8 ml) in DMF (5 ml) was stirred at room temperature overnight. The reaction mixture was treated with ice water and acidified. The solids were filtered and washed with water. The resulting solid mass was taken in 0.1 N sodium hydroxide solution, treated with activated carbon and finally acidified. Yield 0.64 g. Melting point: 130-136°C.

^{1}H-NMR (DMSO-d_6, 400MHz): 2.524 (s, 3H), 3.954 (s, 2H), 5.187 (s, 2H), 5.215 (s, 2H), 6.748 (d, 1H, J = 2.4 Hz), 6.834 (d, 1H, J = 2.4 Hz), 7.158-7.289 (m, 5H), 12.8 (b, 2H).

Example 4. Preparation of 7,8,9,10-Tetrahydro-bis[(1*H* -tetrazol-5-yl)methoxy] -1,3-dihydroxy-6H-dibenzo[b,d]pyran-6-one

a) 7,8,9,10-Tetrahydro-1,3-dihydroxy-6H-dibenzo[b,d]pyran-6-one

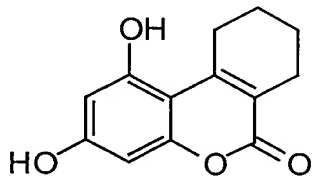

Phloroglucinol (1 g) and ethyl 2-oxocyclohexane carboxylate (1.32 g) were stirred in 75 % sulfuric acid (10 ml) overnight, the mixture poured into ice water and filtered. Yield: 1.55 g.

^{1}H-NMR (DMSO-d_6, 400MHz): 1.65 (b, 4H), 2.345 (b, 2H), 3.037 (b, 2H), 6.138 (d, 1H, J = 2.4 Hz), 6.245 (d, 1H, J = 2.4 Hz), 10.069 (b, 1H, OH), 10.322 (s, 1H, OH).

b) 7, 8, 9, 10-Tetrahydro-bis(cyanomethoxy)-1,3-dihydroxy-6H-dibenzo[b,d]pyran-6-one

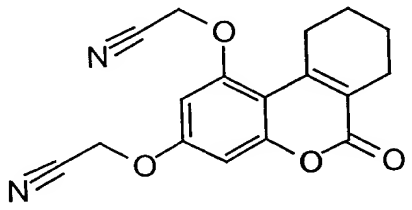

The product from the previous example (0.5 g), chloroacetonitrile (0.34 g) and potassium carbonate (1.5 g) in DMF (5 ml) were reacted as in example 1b. Yield: 0.44 g.

^{1}H-NMR (DMSO-d_6, 400MHz): 1.68 (b, 4H), 2.41 (b, 2H), 3.00 (b, 2H), 5.297 (s, 2H), 5.309 (s, 2H), 6.797 (d, 1H, J = 2.4 Hz), 6.899 (d, 1H, J = 2.4 Hz).

c) 7,8,9,10-Tetrahydro-bis[(1*H* -tetrazol-5-yl)methoxy] -1,3-dihydroxy-6H-dibenzo[b,d]pyran-6-one

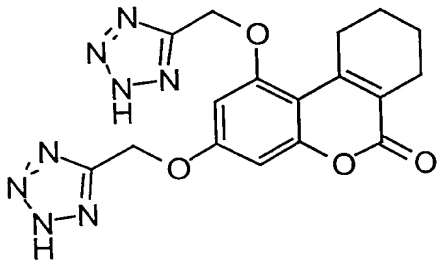

The product from the previous example (0.4 g) was treated with sodium azide (0.18 g) and ammonium chloride (0.14 g) in DMF (2.5 ml) as in example 1c. The product was recrystallized from ethanol-DMF (1:1). Yield 0.17 g. Melting point 283-286°C.

^{1}H-NMR (DMSO-d_6, 400MHz): 1.626 (b, 4H), 2.393 (b, 2H), 2.971 (b, 2H), 5.583 (s, 2H), 5.599 (s, 2H), 6.811 (s, 2H).

Example 5. Preparation of 5,7-Bis[(1*H*-tetrazol-5-yl)methoxy]-4-phenyl-2*H*-1-benzopyran-2-one

a) 5,7-Dihydroxy-4-phenyl-2*H*-1-benzopyran-2-one

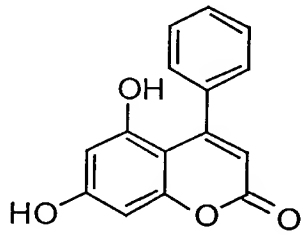

A solution of phloroglucinol (2.00 g) and ethyl benzoylacetate (3.05 g) in ethanol (30 ml) was treated with dry HCl as described in example 1a. The product was recrystallized from ethanol-water (1:1). Yield 3.0 g (75 %).

^{1}H-NMR (DMSO-d$_6$, 300 MHz): 5.739 (s, 1H, CH=C), 6.155 (d, 1H, J = 2.3 Hz), 6.263 (d, 1H, J = 2.3 Hz), 7.305-7.381 (m, 5H, Ph), 10.084 (s, 1H, OH), 10.368 (s, 1H, OH).

b) 5,7-Bis(cyanomethoxy)-4-phenyl-2*H*-1-benzopyran-2-one

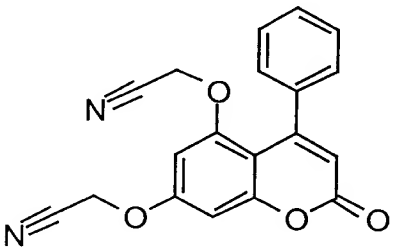

The product from previous example (1.00 g) was treated with chloroaceto-nitrile (0.62 g) and potassium carbonate (2.72 g) in DMF (5 ml) as described in example 1b. The reaction mixture was poured into ice water and the mixture extracted with ethyl acetate. Ethyl acetate was washed with 1 M NaOH, dried with sodium sulfate and evaporated. The product was recrystallized from isopropanol. Yield 0.41 g (31 %).

^{1}H-NMR (DMSO-d$_6$, 300 MHz): 4.845 (s, 2H, OCH$_2$CN), 5.344 (s, 2H, OCH$_2$CN), 6.086 (s, 1H, CH=C), 6.770 (d, 1H, J = 2.4 Hz), 7.040 (d, 1H, J = 2.4 Hz), 7.320-7.443 (m, 5H, Ph).

c) 5,7-Bis[(1*H*-tetrazol-5-yl)methoxy]-4-phenyl-2*H*-1-benzopyran-2-one

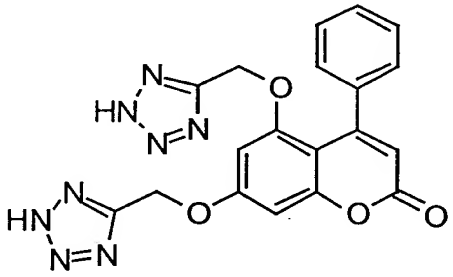

The product from previous example (0.40g) was treated with sodium azide (0.16 g) and ammonium chloride (0.14 g) in DMF (2 ml) at 100 °C for 2 hours. The product was isolated as described in example 1c. Yield: 0.40 g (79 %). Melting point 222-224 °C.

^{1}H-NMR (DMSO-d$_6$, 400 MHz): 5.148 (s, 2H, OCH$_2$Tet), 5.649 (s, 2H, OCH$_2$Tet), 5.968 (s, 1H, CH=C), 6.811 (d, 1H, J = 2.3 Hz), 6.962 (d, 1H, J = 2.3 Hz), 6.994-7.185 (m, 5H, Ph).

Example 6. Preparation of 7,8,9,10-Tetrahydro-1,3-bis[(1*H*-tetrazol-5-yl)methoxy]-8-phenyl-6*H*- dibenzo[b,d]pyran-6-one

a) 7,8,9,10-Tetrahydro-1,3-dihydroxy-8-phenyl-6*H*-dibenzo[b,d]pyran-6-one

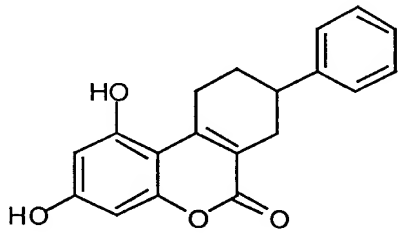

A solution of phloroglucinol (1.56 g) and ethyl 2-oxo-5-phenylcyclo-hexane-carboxylate (2.52 g) in ethanol (25 ml) was treated with dry HCl as described in example 1a. The precipitate was filtered and washed with water and EtOH. Yield 1.0 g (32 %).

^{1}H-NMR (DMSO-d$_6$, 400 MHz): 1.72-1.82 (m, 1H), 2.01 (b, 1H), 2.317-2.387 (m, 1H), 2,707-2,763 (m, 1H), 2,830 (b, 1H), 3,041 (b, 1H), 3.35 and 3.40 (b, 1H), 6.174 (d, 1H, J = 2.3 Hz), 6.277 (d, 1H, J = 2.3 Hz), 7.200-7.350 (m, 5H, Ph), 10.131 (s, 1H, OH), 10.401 (s, 1H, OH).

b) 7,8,9,10-Tetrahydro-1,3-bis(cyanomethoxy)-8-phenyl-6*H*-dibenzo[b,d]pyran-6-one

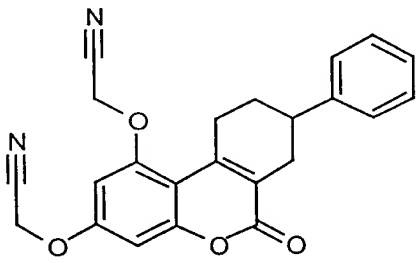

The product from previous example (1.0 g) was treated with chloro-acetonitrile (0.57 g) and potassium carbonate (1.0 g) in DMF (5 ml) as described in example 1b. DMF was evaporated and residue dissolved in EtOAc. Ethyl acetate was washed with 1 M NaOH, dried with sodium sulfate and evaporated. The product was recrystallized from acetone-isopropanol (1:3). Yield 0.50 g (40 %).

^{1}H-NMR (DMSO-d$_6$, 300 MHz): 1.75-1.88 (m, 1H), 2.05 (b, 1H), 2.38-2.48 (m, 1H), 2.77-2.85 (m, 1H), 2.90 (b, 1H), 3.07 (b, 1H), 3.22 and 3.28 (b, 1H), 5.316 (s, 2H, OCH_2CN), 5.331 (s, 2H, OCH_2CN), 6.829 (d, 1H, J = 2.5 Hz), 6.939 (d, 1H, J = 2.5 Hz), 7.210-7.380 (m, 5H, Ph).

c) 7,8,9,10-Tetrahydro-1,3-bis[(1*H*-tetrazol-5-yl)methoxy]-8-phenyl-6*H*-dibenzo[b,d]pyran-6-one

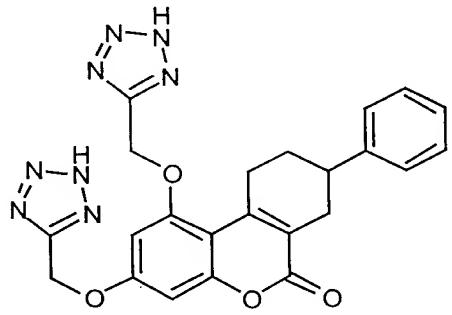

The product from previous example (0.30 g) was treated with sodium azide (0.10 g) and ammonium chloride (0.09 g) in DMF (2 ml) at 100 °C for 3.5 hours. The product was isolated in the same manner as in example 1c. Yield 0.30 g (82 %). Melting point 235-245 °C.

^{1}H-NMR (DMSO-d$_6$, 400 MHz): 1.70-1.80 (m, 1H), 1.96 (b, 1H), 2.38-2.446 (m, 1H), 2.836 (m, 2H), 3.052 (b, 1H), 3.252 and 3.301 (b, 1H), 5.604 (s, 2H, OCH_2CN), 5.632 (s, 2H, OCH_2CN), 6.827 (d, 1H, J = 2.5 Hz), 6.858 (d, 1H, J = 2.5 Hz), 7.209-7.351 (m, 5H, Ph).

Example 7. Preparation of 5,7-Bis[(1*H*-tetrazol-5-yl)methoxy]-4-methyl-3-(2-phenylethyl)-2*H*-1benzopyran-2-one

a) 5,7-Dihydroxy-4-methyl-3-(2-phenylethyl)-2*H*-1-benzopyran-2-one

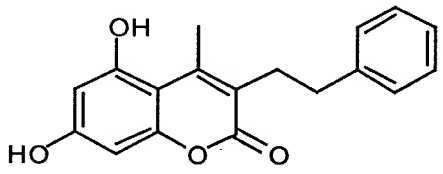

A solution of phloroglucinol (0.87 g) and ethyl 2-(2-phenylethyl)-acetoacetate (1.62 g) in ethanol (30 ml) was treated with dry HCl as described in example 1a. Yield: 1.77 g (87 %). Melting point 248-252 °C.

^{1}H-NMR (DMSO-d_6, 300 MHz): 2.413 (s, 3H, CH_3), 2.652-2.782 (m, 4H, CH_2CH_2), 6.151 (d, 1H, J = 2.4 Hz), 6.256 (d, 1H, J = 2.4 Hz), 7.183-7.304 (m, 5H, Ph), 10.137 (s, 1H, OH), 10.369 (s, 1H, OH).

b) 5,7-Bis(cyanomethoxy)-4-methyl-3-(2-phenylethyl)-2*H*-1-benzopyran-2-one

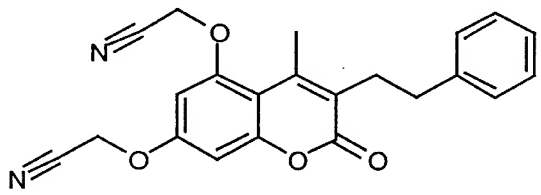

The product from previous example (0.90 g) was treated with chloroacetonitrile (0.48 g) and potassium carbonate (2.1 g) in DMF (5 ml) at 100 °C for 0.5 hours. The product was isolated as described in example 1b. Yield 1.00 g (88 %). Melting point 179-183 °C.

^{1}H-NMR (DMSO-d_6, 300 MHz): 2,384 (s, 3H, CH_3), 2.699-2,754 (m, 2H, CH_2CH_2), 2.805-2.841 (m, 2H, CH_2CH_2), 5,302 (s, 4H, OCH_2CN), 6,790 (d, 1H, J = 2.5 Hz), 6.909 (d, 1H, J = 2.5 Hz), 7.190-7.307 (m, 5H, Ph).

c) 5,7-Bis[(1*H*-tetrazol-5-yl)methoxy]-4-methyl-3-(2-phenylethyl)-2*H*-1benzopyran-2-one

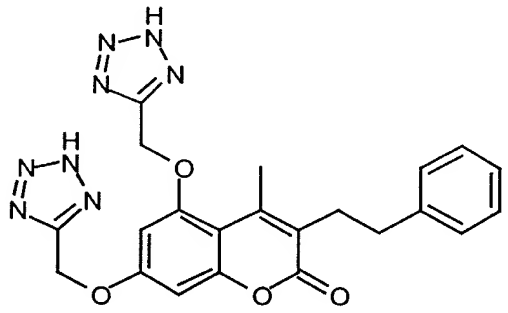

The product from previous example (0.40g) was treated with sodium azide (0.15 g) and ammonium chloride (0.12 g) in DMF (2 ml) at 100 °C for 2.5 hours. The product was isolated as described in example 1c. Yield 0.385 g (78 %). Melting point 248-250 °C.

^{1}H-NMR (DMSO-d_6, 400 MHz): 2.368 (s, 3H, CH_3), 2.668-2.707 (m, 2H, CH_2CH_2), 2.783-2.822 (m, 2H, CH_2CH_2), 5.593 (s, 2H, OCH_2Tet), 5.604 (s, 2H, OCH_2Tet), 6.819 (d, 1H, J = 2.3 Hz), 6.834 (d, 1H, J = 2.3 Hz), 7.161-7.291 (m, 5H, Ph).

Example 8. Preparation of 5,7-Bis[(1H-tetrazol-5-yl)methoxy]-1,3-dibenzyl-4-methyl-2(1H)-quinolinone

a) 2-Benzyl-3-oxobutanoic acid 3,5-dimethoxyanilid

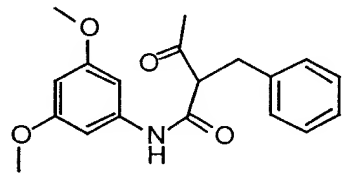

3,5-Dimethoxyaniline (5 g) was added in portions to a preheated (160 °C) ethyl 2-benzyl acetoacetate (15 ml) under nitrogen and kept at that temperature for 60 minutes. The cooled solution was diluted with heptane-ethyl ether and filtered. Yield 5.2 g (49 %).

^{1}-H-NMR (DMSO-d_6, 300 MHz): 2.183 (s, 3H), 3.069 (d, 2H, J = 7.2 Hz), 3.923 (t, 1H, J = 7.2 Hz), 6.616 (dd. 1H, J = 2.3 Hz), 6.765 (d, 2H, J = 2.3 Hz), 7.13-7.3 (m, 5H), 10.123 (s, 1H).

b) 3-Benzyl-5,7-dimethoxy-4-methyl-2(1H)-quinolinone

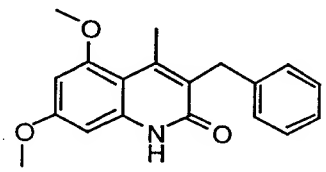

The product from the previous example (1.2 g) was added to a preheated (85 °C) methanesulfonic acid (3.5 ml) and kept at that temperature for 15 minutes. The solution was allowed to cool and then treated with ice water. The product was filtered, washed with sodium bicarbonate and water. Yield 1.08 g (95 %).

^{1}-H-NMR (300 MHz):2.486 (s, 3H), 3.785 (s, 3H), 3.808 (s, 3H), 3.985 (s, 2H), 6.315 (d, 1H, J = 2.4 Hz), 6.472 (d, 1H, J = 2.4 Hz), 7.1-7.3 (m, 5 H), 11.52 (s, 1H).

c) 3-Benzyl-5,7-dihydroxy-4-methyl-2(1H)-quinolinone

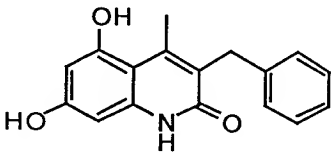

The product from the previous example (1 g) was refluxed under nitrogen in pyridine hydrochloride (5 g) for twenty minutes. The reaction mixture was treated with water and the product filtered. Yield 0.9 g (100 %). Melting point: 307 - 312 °C.

^{1}-H-NMR (300 MHz):2.503 (s, 3H), 3.942 (s, 2H), 6.102 (d, 1H, J = 2.3 Hz), 6.187 (d, 1H, J = 2.3 Hz), 7.1-7.25 (m, 5H), 9.725 (s, 1H), 9.984 (s, 1H), 11.285 (s, 1H).

d) 1,3-Dibenzyl-5,7-dimethoxy-4-methyl-2(1H)-quinolinone

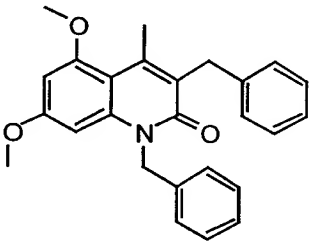

The product from the example 8b (1 g), potassium t-butoxide (0.62 g) and benzyl bromide (0.68 ml) were stirred in DMSO (10 ml) at 60 °C for 4 hours. The reaction mixture was treated with water, extracted with toluene and evaporated. The product was triturated with ethyl ether and filtered. Yield 0.5 g (39 %).

^{1}-H-NMR (400 MHz):2.537 (s, 3H), 3.708 (s, 3H), 3.826 (s, 3H), 4.124 (s, 2H), 5.56 (b, 2H), 6.413-6.434 (m, 2H), 7.154- 7.332 (m, 10H).

e) 1,3-Dibenzyl-5,7-dihydroxy-4-methyl-2(1H)-quinolinone.

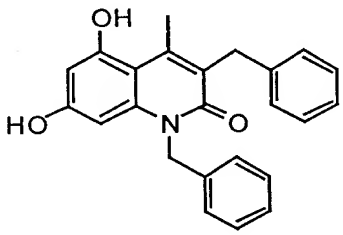

The product from the previous example (2 g) was treated with pyridine hydrochloride (10 g) as described in example 8c. The product was extracted with ethyl acetate and evaporated. Yield 1,4 g (75 %).

^{1}-H-NMR (400 MHz):2.570 (s, 3H), 4.076 (s, 2H), 5.450 (b, 2H), 6.135 (d, 1H, J = 2.2 Hz), 6.199 (d, 1H, J = 2.2 Hz), 7.128 - 7.333 (m, 10 H), 9.83 (b, 1H), 10.166 (s, 1H).

f) 5,7-Bis(cyanomethoxy)-1,3-dibenzyl-4-methyl-2(1H)-quinolinone.

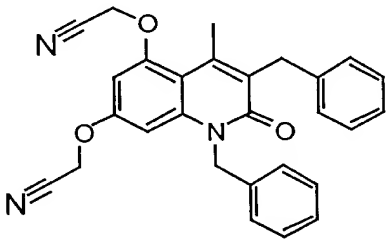

The product from the previous example (1.4 g) was treated with chloroacetonitrile (0.76 g) and K_2CO_3 (2.5 g) in DMF (20 ml) as described in example 1b. Yield 1.5 g (89 %).

^{1}-H-NMR (400 MHz):2.555 (s, 3H), 4.146 (s, 2H), 5.214 (s, 2H), 5.275 (s, 2H), 5.578 (s, 2H), 6.735 (s, 2H), 7.13-7.33 (m, 10H).

g) 5,7-Bis[(1H-tetrazol-5-yl)methoxy]-1,3-dibenzyl-4-methyl-2(1H)-quinolinone.

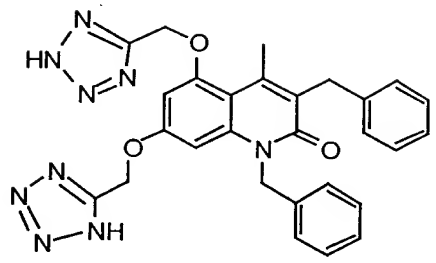

The product from the previous example (1.3 g) was treated with sodium azide (0.41 g) and ammonium chloride (0.34 g) as described in example 1c. Yield: 0.69 g (45 %).

^{1}-H-NMR (400 MHz):2.471 (s, 3H), 4.113 (s, 2H), 5.477 (s, 2H), 5.55 (b, 2H), 5.574 (s, 2H), 6.670 (d, 1H, J = 2.1 Hz), 6.775 (d, 1H, J = 2.1 Hz), 7.13-7.32 (m, 10 H).

Example 9. Preparation of 5,7-Bis[(1H-tetrazol-5-yl)methoxy] -3-benzyl-1,4-dimethyl-2(1H)-quinolinone.

a) 3-Benzyl-5,7-dimethoxy-1,4-dimethyl-2(1H)-quinolinone.

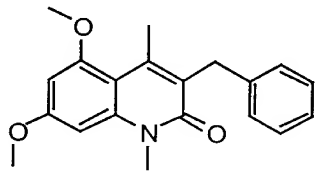

The product from example 8b (0.5 g), t-BuOK (0.2 g) and methyl iodide (0.4 ml) were stirred in DMSO (5 ml) at 35 °C for two days. The reaction mixture was treated with water and extracted with toluene. The product was purified by column chromatography using toluene-ethyl acetate-acetic acid 8 : 2: 1 as the eluent. Yield 0.24 g (46 %).

^{1}-H-NMR (300 MHz):2.51 (s, 3H), 3.632 (s, 2H), 3.846 (s, 3H), 3.896 (s, 3H), 4.047 (s, 2H), 6.468 (d, 1H, J = 2.3 Hz), 6.558 (d, 1H, J = 2.3 Hz), 7.1-7.26 (m, 5H).

b) 3-Benzyl-5,7-dihydroxy-1,4-dimethyl-2(1H)-quinolinone.

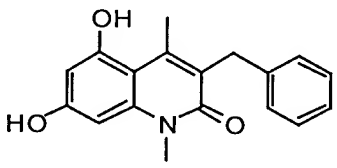

The product from the previous example (0.2 g) was treated with pyridine hydrochloride (2 g) as described in example 8c and the product extracted with ethyl acetate. Yield 0.16 g (89 %).

^{1}-H-NMR (400 MHz):2.567 (s, 3H), 3.515 (s, 3H), 4.005 (s, 2H), 6.244 (d, 1H, J = 2.3 Hz), 6.268 (d, 1H, J = 2.3 Hz), 7.08-7.25 (m. 5H), 9.879 (s, 1H), 10.113 (s,1H).

c) 5,7-Bis(cyanomethoxy)-3-benzyl-1,4-dimethyl-2(1H)-quinolinone.

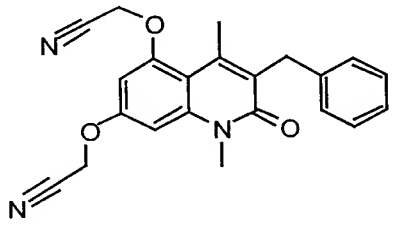

The product from the previous example (0.15 g), chloroacetonitrile 0.08 g) and K_2CO_3 (0.28 g) were reacted in DMF (2 ml) as described in example 1b. Yield 0.16 g (84 %).

^{1}-H-NMR (400 MHz): 2.524 (s, 3H), 3.658 (s, 3H), 4.079 (s, 2H), 5.292 (s, 2H), 5.379 (s, 2H), 6.766 (d, 1H, J = 2.3 Hz), 6.855 (d, 1H, J = 2.3 Hz), 7.13-7.24 (m 5H).

d) 5,7-Bis[(1H-tetrazol-5-yl)methoxy] -3-benzyl-1,4-dimethyl-2(1H)-quinolinone.

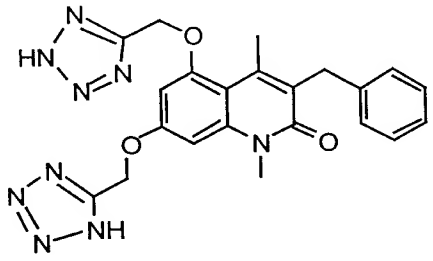

The product from the previous example (0.15 g) was treated with NaN_3 (57 mg) and NH_4Cl (47 mg) in DMF (2 ml) as described in example 1c. Yield 0.115 g. Melting point: 250-253°C.

^{1}-H-NMR (400 MHz): 2.451 (s, 3H), 3.649 (s, 3H), 4.042 (s, 2H), 6.792 (d, 1H, J = 2.2 Hz), 6.833 (d, 1H, J = Hz), 7.1-7.25 (m, 5H).

Example 10. Preparation of 3-Benzyl-5,7-bis[(2-methyl-1*H* -tetrazol-5-yl)methoxy]-4-methyl-2*H* -1-benzopyran-2-one and the three isomers.

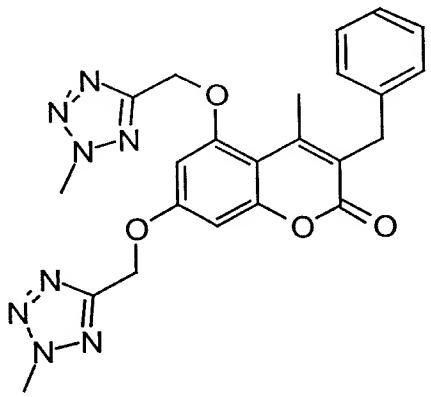

0.07 ml of methyl iodide was added to a solution of 0.2 g of the product from example 1c and 0.31 g of K_2CO_3 in 2 ml of DMF and the mixture stirred at room temperature for 4 hours. The reaction mixture was poured into ice water and filtered. Yield 0.2 g as a mixture of four regioisomers, melting point 71-76°C.

^{1}H-NMR (DMSO-d_6, 400MHz): 2.47 (s, CH_3), 2.48 (s, CH_3), 3.93 (s, CH_2Ph), 4.11 (s, NCH_3), 4.12 (s, NCH_3), 4.15 (s, NCH_3), 4.38 (s, NCH_3), 4.40 (s, NCH_3), 5.51 (s, OCH_2), 5.52 (s, OCH_2), 5.62 (s, OCH_2), 5.67 (s, OCH_2), 6.84-6.91 (m, 2H), 7.16-7.28 (m,5H, Ph).

Example 11. Preparation of 3-Benzyl-5,7-bis[1-(1 *H* -tetrazol-5-yl)ethoxy]4-methyl-2 *H* -1-benzopyran-2-one, mixture of stereoisomers

a) 3-Benzyl-5,7-bis-[(1-cyano)ethoxy)-4-methyl-2 *H* -1-benzopyran- 2-one

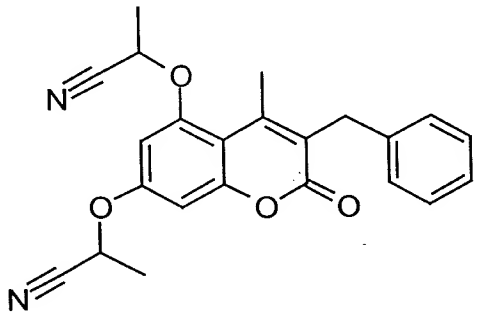

The product from example 1a (1 g), 2-chlorpropionitrile (0.7 g) and potassium carbonate (2 g) were heated in DMF (15 ml) under nitrogen at 110°C for sixty minutes. The mixture was treated with water, filtered and washed with 1 N NaOH and water. Yield 1.2 g.

^{1}H-NMR (DMSO-d_6, 300MHz): 1.74-1.78 (t + t, 6 H, CH-C**H**$_3$), 2.53 (s, 3 H), 3.97 (s, 2H), 5.58-5.66 (m, 2H, C**H**-CH$_3$), 6.87 (m, 1H), 6.99 (d, 1H), 7.18-7.31 (m, 5H).

b) 3-Benzyl-5,7-bis[1-(1 *H* -tetrazol-5-yl)ethoxy]4-methyl-2 *H* -1-benzopyran-2-one, mixture of stereoisomers.

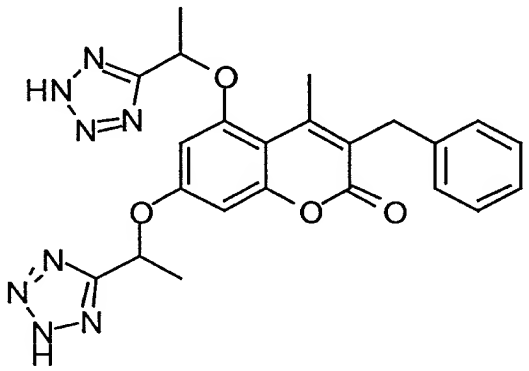

The product from the previous example (0.5 g), sodium azide (0.18 g) and ammonium chloride (0.15 g) were heated in DMF (7 ml) at 100 °C for 90 minutes. The product was treated with water, extracted with ethyl acetate and evaporated. Yield 0.57 g. Melting point 91-104°C.

^{1}H-NMR (DMSO-d_6, 300MHz): 1.69-1.77 (m, 6 H, CH-C**H**$_3$), 2.54 (s, 3H), 3.94 (s, 2H), 6.10-6.17 ((m, 2H, C**H**-CH$_3$), 6.65 (dd, 1H), 6.74 (dd, 1H), 7.13-7.30 (m, 5H).

Example 12. Preparation of 5,7-Bis(carboxymethoxy)-1,3-dibenzyl-4-methyl-2(1H)-quinolinone

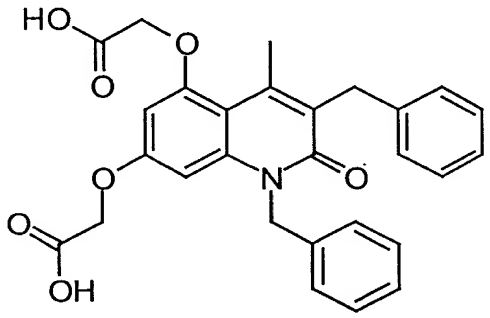

The product from example 8f (0.2 g) was refluxed in a solution of concentrated hydrochloric acid (3 ml) and acetic acid (2 ml) for one hour. The product was filtered at 25 °C. Yield 0.14 g.

^{1}H-NMR (300 Mhz, DMSO-d$_6$): 2.63 (s, CH3), 4.14 (s, 2H, CH_2Ph), 4.66 (s, 2 H, OCH_2COOH), 4.79 (s, 2H, OCH_2COOH), 5.53 (s, 2H, NCH_2Ph), 6.41 (d, 1H, J = 2.2 Hz), 6.45 (d, 1H, J = 2.2 Hz), 7.13-7.34 (m, 10 H, Ph).

Example 13. Preparation of 3-Benzyl-5,7-bis[(1H-tetrazol-5-yl)methoxy]-1-(4-fluorobenzyl)-4-methyl-2(1H)-quinolinone

a) 1-Benzyl-5,7-dimethoxy-3-(4-fluorobenzyl)-4-methyl-2(1H)-quinolinone

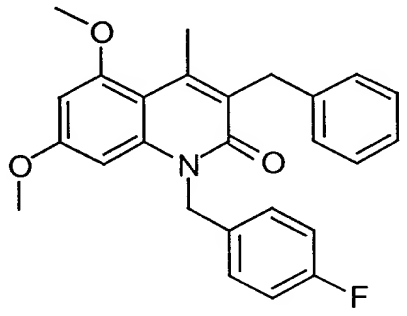

The product from example 8b (2 g), potassium -tert-butoxide (0.87 g) and 4-fluorobenzylchloride (1.12 g) were heated in DMSO (20 ml) at 60 °C for three hours as in example 8d. Yield 1.28 g.

^{1}H-NMR (400 Mhz, DMSO-d$_6$): 2.53 (s, 3H), 3.73 (s, 3H), 3.83 (s, 3H), 5.55 (s, 2H), 6.43 (s, 2H), 7.12-7.2 (m, 5 H), 7.26-7.28 (m, 4H).

b) 3-Benzyl-5,7-dihydroxy-1-(4-fluorobenzyl)-4-methyl-2(1H)-quinolinone

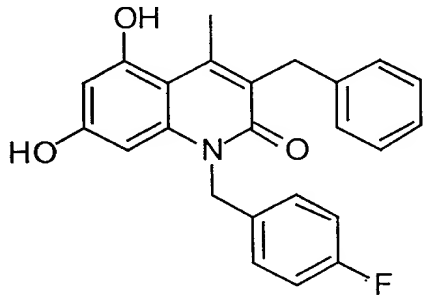

The product from previous example (1.25 g) were heated in pyridine hydrochloride (12.5 g) at about 225 °C for 9 minutes. Yield 1 g.

^{1}H-NMR (300 Mhz, DMSO-d$_6$): 2.56 (s, 3H), 4.07 (s, 2H), 5.4 (b, 2H), 6.13 (d, 1H, J = 2.1 Hz), 6.20 (d, 1H, J = 2.1 Hz), 7.12-7.28 (m, 9H), 9.88 (s, 1H), 10.22 (s, 1H).

c) 3-Benzyl-5,7-Bis(cyanomethoxy)-1-(4-fluorobenzyl) -4-methyl-2(1H)-quinolinone

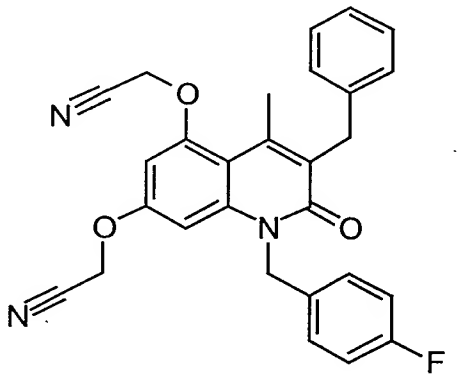

The product from the previous example (1 g), $ClCH_2CN$ (0.43 g) and K_2CO_3 (1.42 g) were heated in DMF (8 ml) at 120 °C for one hour. Yield 0.94 g.

^{1}H-NMR (300 Mhz, DMSO-d$_6$): 2.55 (s, 3H), 4.14 (s, 2H), 5.25 (s, 2H), 5.28 (s, 2H), 5.57 (s, 2H), 6.74 (s, 2H, ArH), 7.1 -7.3 (m, 9H).

d) 3-Benzyl-5,7-bis[(1H-tetrazol-5-yl)methoxy]-1-(4-fluorobenzyl)-4-methyl-2(1H)-quinolinone

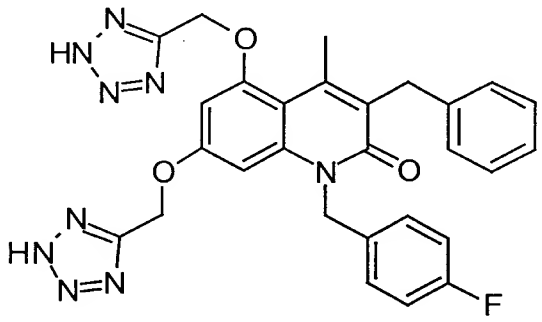

The product from the previous example (0.5 g), sodium azide (0.14 g) and ammonium chloride (0.12 g) were heated in DMF (5 ml) at 120 °C for 90 min. The product was triturated with acetonitrile. Yield 0.28 g. Melting point: 126-132 °C.

^{1}H-NMR (300 Mhz, DMSO-d$_6$): 2.48 (s, 3H), 4.11 (s, 2H), 5.51 (s, 2H), 5.55 (s, 2H), 5.58 (s, 2H), 6.67 (d, 1H, J = 2.1 Hz), 6.78 (d, 1H, J = 2.1 Hz).

Example 14. Preparation of 5,7-Bis[(1*H*-tetrazol-5-yl)methoxy]-3-(4-chlorobenzyl)-4-methyl-2*H*-1-benzopyran-2-one

a) 3-(4-Chlorobenzyl)-5,7-dihydroxy-4-methyl-2*H*-1-benzopyran-2-one

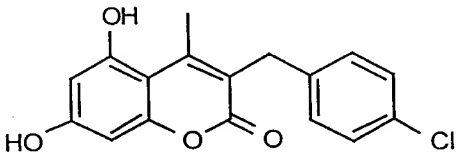

A solution of phloroglucinol (1.57 g) and ethyl 2-(4-chlorobenzyl)-acetoacetate (3.18 g) in ethanol (25 ml) was treated with dry HCl at 0 °C for 1.5 hours and the solution was kept at that temperature overnight. Solvent was evaporated and the precipitate triturated with water. Yield 3.87 g (98 %). Melting point 270-278 °C.

^{1}H-NMR (DMSO-d$_6$, 300 MHz): 2.52 (s, 3H, CH_3), 3.87 (s, 2H, CH_2), 6.17 (d, 1H, J = 2.4 Hz), 6.28 (d, 1H, J = 2.4 Hz), 7.18-7.34 (m, 4H, Ph), 10.21 (s, 1H, OH), 10.48 (s, 1H, OH).

b) 5,7-Bis(cyanomethoxy)-3-(4-chlorobenzyl)-4-methyl-2*H*-1-benzopyran-2-one

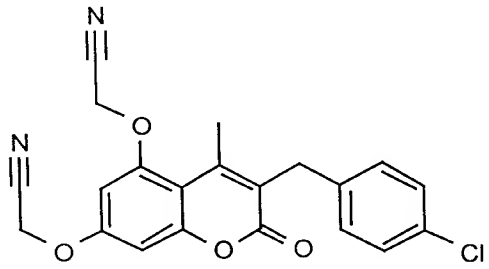

The product from the previous example (1.00 g), chloroacetonitrile (0.50 g) and potassium carbonate (2.18 g) were heated in DMF (5 ml) at 100 °C for 30 minutes. The product was isolated as described in example 1b. Yield 0.90 g (72 %).

^{1}H-NMR (DMSO-d$_6$, 300 MHz): 2.52 (s, 3H, CH_3), 3.95 (s, 2H, CH_2), 5.308 (s, 2H, OCH_2CN), 5.312 (s, 2H, OCH_2CN), 6.81 (d, 1H, J = 2.5 Hz), 6.94 (d, 1H, J = 2.5 Hz), 7.22-7.33 (m, 4H, Ph).

c) 5,7-Bis[(1*H*-tetrazol-5-yl)methoxy]-3-(4-chlorobenzyl)-4-methyl-2*H*-1-benzopyran-2-one

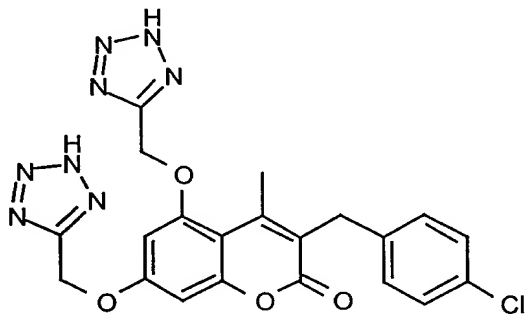

The product from the previous example (0.40 g), sodium azide (0.14 g) and ammonium chloride (0.11 g) were heated in DMF (2 ml) at 100 °C for 2 hours. The product was isolated as in example 1c. Yield 0.40 g (82 %).

^{1}H-NMR (DMSO-d_6, 300 MHz): 2.46 (s, 3H, CH_3), 3.92 (s, 2H, CH_2), 5.602 (s, 2H, OCH_2Tet), 5.609 (s, 2H, OCH_2Tet), 6.83 (d, 1H, J = 2.5 Hz), 6.85 (d, 1H, J = 2.5 Hz), 7.20-7.33 (m, 4H, Ph).

Example 15. Preparation of 5,7-Bis[(1*H*-tetrazol-5-yl)methoxy]-3-(4-nitrobenzyl)-4-methyl-2*H*-1-benzopyran-2-one

a) 5,7-Dihydroxy-4-methyl-3-(4-nitrobenzyl)-2*H*-1-benzopyran-2-one

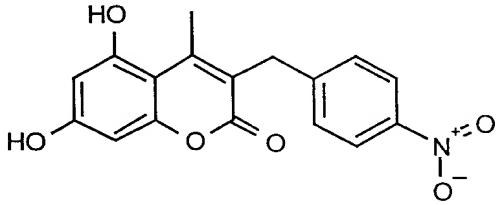

A solution of phloroglucinol (0.48 g) and ethyl 2-(4-nitrobenzyl)aceto-acetate (1.00 g) in ethanol (150 ml) was treated with dry HCl at 0 °C for 7.5 hours and the solution was kept at that temperature overnight. Solvent was evaporated and the precipitate triturated with water. Yield 0.63 g (51 %). Melting point 280-285 °C.

^{1}H-NMR (DMSO-d_6, 300 MHz): 2.53 (s, 3H, CH_3), 4.03 (s, 2H, CH_2), 6.19 (d, 1H, J = 2.4 Hz), 6.29 (d, 1H, J = 2.4 Hz), 7.40-7.51 and 8.11-8.17 (m, 4 H, Ph), 10.25 (s, 1H, OH), 10.52 (s, 1H, OH).

b) 5,7-Bis(cyanomethoxy)-3-(4-nitrobenzyl)-4-methyl-2*H*-1-benzopyran-2-one

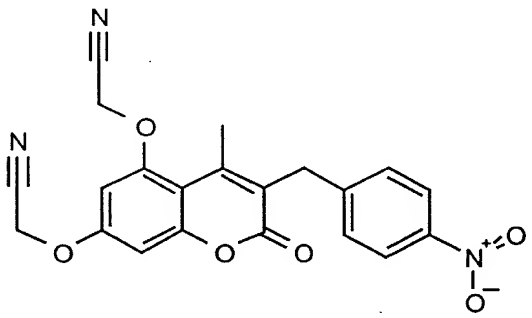

The product from the previous example (0.57 g), chloroacetonitrile (0.27 g) and potassium carbonate (1.20 g) were heated in DMF (2 ml) at 100 °C for 50 minutes. The product was isolated as described in example 1b. Yield 0.47 g (67 %). Melting point 178-185 °C.

^{1}H-NMR (DMSO-d_6, 400 MHz): 2.53 (s, 3H, CH_3), 4.11 (s, 2H, CH_2), 5.319 (s, 2H, OCH_2CN), 5.323 (s, 2H, OCH_2CN), 6.83 (d, 1H, J = 2.4 Hz), 6.96 (d, 1H, J = 2.4 Hz), 7.48-7.53 and 8.12-8.16 (m, 4H, Ph).

c) 5,7-Bis[(1*H*-tetrazol-5-yl)methoxy]-3-(4-nitrobenzyl)-4-methyl-2*H*-1-benzopyran-2-one

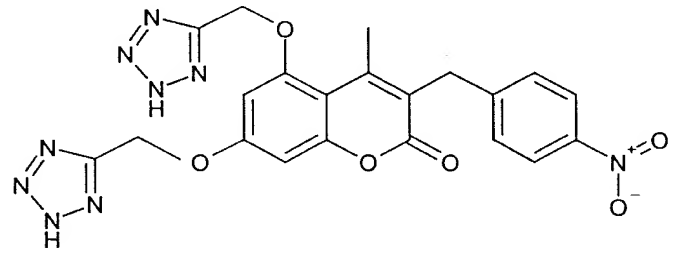

The product from the previous example (0.38 g), sodium azide (0.12 g) and ammonium chloride (0.11 g) were heated in DMF (3 ml) at 100 °C for 2 hours. The product was isolated as described in example 1c. Yield 0.25 g (54 %). Melting point 240-244 °C.

^{1}H-NMR (DMSO-d_6, 400 MHz): 2.47 (s, 3H, CH_3), 4.08 (s, 2H, CH_2), 5.611 (s, 2H, OCH_2Tet), 5.623 (s, 2H, OCH_2Tet), 6.85 (d, 1H, J = 2.4 Hz), 6.87 (d, 1H, J = 2.4 Hz), 7.46-7.50 and 8.12-8.16 (m, 4H, Ph).

Example 16. Preparation of 5,7-Bis[(1*H*-tetrazol-5-yl)methoxy]-3-cyclopentyl-4-methyl-2*H*-1-benzopyran-2-one

a) 3-Cyclopentyl-5,7-dihydroxy-4-methyl-2*H*-1-benzopyran-2-one

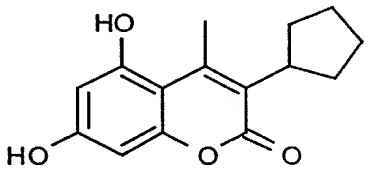

A solution of phloroglucinol (2.00 g) and ethyl 2-cyclopentylaceto-acetate (3.14 g) in ethanol (40 ml) was treated with dry HCl at 0 °C for 2.5 hours and the solution kept at that temperature overnight. Solvent was evaporated and the precipitate purified with flash chromatography eluting with toluene-EtOAc-AcOH (8:1:1). Yield 1.22 g (29 %).

^{1}H-NMR (DMSO-d_6, 300 MHz): 1.50-1.88 (m, 8H, -$(CH_2)_4$-), 2.57 (s, 3H, CH_3), 3.25 (m, 1H, CH), 6.11 (d, 1H, J = 2.4 Hz), 6.25 (d, 1H, J = 2.4 Hz), 10.25 (b, 2H, OH).

b) 5,7-Bis(cyanomethoxy)-3-cyclopentyl-4-methyl-2*H*-1-benzopyran-2-one

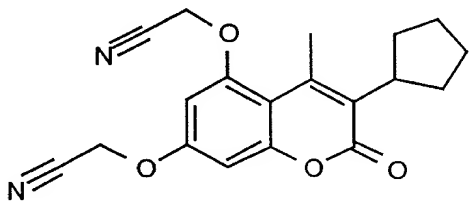

The product from the previous example (0.50 g), chloroacetonitrile (0.31 g) and potassium carbonate (0.61 g) were heated in DMF (2 ml) at 80 °C for 40 minutes. The product was isolated as described in example 1b. Yield 0.56 g (86 %).

^{1}H-NMR (DMSO-d_6, 300 MHz): 1.55-1.90 (m, 8H, -$(CH_2)_4$-), 2.56 (s, 3H, CH_3), 3.37 (m, 1H, CH), 5.29 (s, 2H, OCH_2CN), 5.31 (s, 2H, OCH_2CN), 6.75 (d, 1H, J = 2.5 Hz), 6.88 (d, 1H, J = 2.5 Hz).

c) 5,7-Bis[(1*H*-tetrazol-5-yl)methoxy]-3-cyclopentyl-4-methyl-2*H*-1-benzopyran-2-one

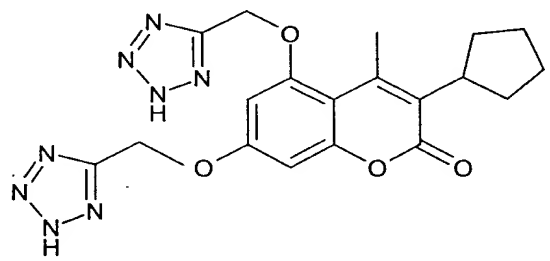

The product from the previous example (0.30 g), sodium azide (0.13 g) and ammonium chloride (0.11 g) were heated in DMF (1 ml) at 100 °C for 1.5 hours. The product was isolated as described in example 1c. Yield 0.30 g (80 %). Melting point 248-252 °C.

^{1}H-NMR (DMSO-d$_6$, 400 MHz): 1.53-1.89 (m, 8H, -(CH$_2$)$_4$-), 2.51 (s, 3H, CH$_3$), 3.34 (m, 1 H, CH), 5.59 (s, 2H, OCH$_2$Tet), 5.61 (s, 2H, OCH$_2$Tet), 6.80 (s, 2H).

Example 17. Preparation of 5,7-Bis[(1*H*-tetrazol-5-yl)methoxy]-4-methyl-3-(1-naphtylmethyl)-2*H*-1-benzopyran-2-one

a) 5,7-dihydroxy-4-methyl-3-(1-naphtylmethyl)-2*H*-1-benzopyran-2-one

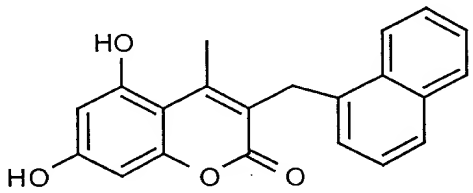

A solution of phloroglucinol (0.47 g) and ethyl 2-(1-naphtylmethyl)-acetoacetate (1.00 g) in ethanol (20 ml) was treated with dry HCl at 0 °C for 3 hours and the solution kept at that temperature overnight. Solvent was evaporated and the precipitate triturated with water and recrystallized from isopropanol-water (1:1). Yield 0,96 g (78 %). Melting point 275-280 °C.

^{1}H-NMR (DMSO-d$_6$, 400 MHz): 2.45 (s, 3H, CH$_3$), 4.32 (s, 2H, CH$_2$), 6.23 (d, 1H, J = 2.5 Hz), 6.32 (d, 1 H, J = 2.5 Hz), 6.97-8.25 (m, 7H, Naph), 10.26 (s, 1H, OH), 10.53 (s, 1H, OH).

b) 5,7-Bis(cyanomethoxy)-4-methyl-3-(1-naphtylmethyl)-2*H*-1-benzopyran-2-one

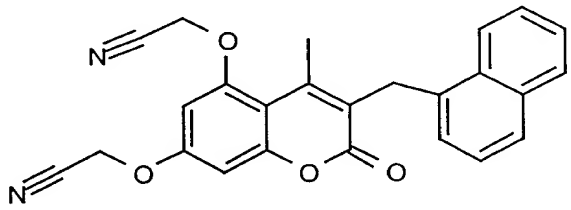

The product from the previous example (0.80 g), chloroacetonitrile (0.36 g) and potassium carbonate (0.66 g) were heated in DMF (4 ml) at 100 °C for 1 hour. The product was isolated as in example 1b. Yield 0.30 g (30 %).

^{1}H-NMR (DMSO-d$_6$, 300 MHz): 2.45 (s, 3H, CH_3), 4.40 (s, 2H, CH_2), 5.34 (s, 2H, OCH_2CN), 5.36 (s, 2H, OCH_2CN), 6.86 (d, 1H, J = 2.5 Hz), 7.010 (d, 1H, J = 2.5 Hz), 7.016-8.27 (m, 7H, Naph).

c) 5,7-Bis[(1*H*-tetrazol-5-yl)methoxy]-4-methyl-3-(1-naphtylmethyl)-2*H*-1-benzopyran-2-one

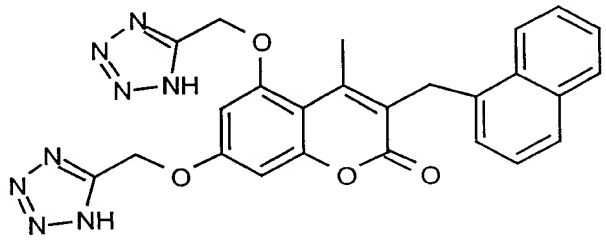

The product from the previous example (0.25 g), sodium azide (0.080 g) and ammonium chloride (0.072 g) were heated in DMF (2 ml) at 100 °C for 2.5 hours. The product was isolated as described in example 1c. Yield 0.11 g (36 %). Melting point 164-174 °C.

^{1}H-NMR (DMSO-d$_6$, 300 MHz): 2.40 (s, 3H, CH_3), 4.37 (s, 2H, CH_2), 5.63 (s, 2H, OCH_2Tet), 5.65 (s, 2H, OCH_2Tet), 6.87 (d, 1H, J = 2.5 Hz), 6.92 (d, 1H, J = 2.5 Hz), 6.98-8.26 (m, 7H, Naph).

Example 18. Preparation of 1-Benzyl-5,7-bis-[(1*H*-tetrazol-5-yl)-methoxy]-4-methyl-2(1H)-quinolinone

a) 5,7-Dimethoxy-4-methyl-2(1H)-quinolinone

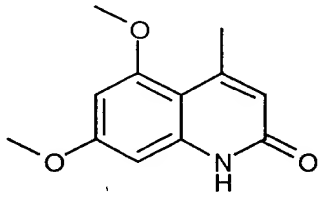

tert-Butyl acetoacetate (1.58 g) was heated to 120 °C and 3,5-dimethoxyaniline (1.53 g) dissolved in xylene (4 ml) was added. The mixture was heated at 120-130 °C for 20 minutes and then cooled to room temperature. Methanesulfonic acid (2 ml) was added and the mixture was stirred at ambient temperature for 10 minutes. Water (40 ml) was added and the precipitate filtered and dried. Yield 1.31 g (60 %).

^{1}H-NMR (DMSO-d_6, 300 MHz): 2.50 (s, 3H, CH_3), 3.79 (s, 3H, OCH_3), 3.83 (s, 3H, OCH_3), 6.03 (s, 1H, CH=C), 6.31 (d, 1H, J = 2.3 Hz), 6.45 (d, 1H, J = 2.3 Hz), 11.4 (b, 1H, NH).

b) 1-Benzyl-5,7-dimethoxy-4-methyl-2(1H)-quinolinone

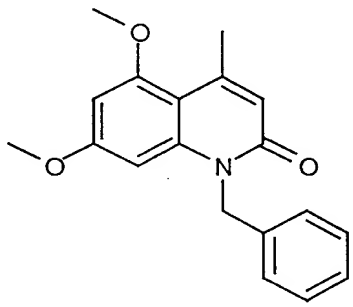

The product from the previous example (1.20 g) was suspended to DMSO (15 ml) and *t*-BuOK (0.68 g) and benzylbromide (1.03 g) were added. Reaction mixture was stirred at ambient temperature overnight. Water was added and the product extracted to EtOAc. EtOAc was dried and evaporated to dryness. The product was recrystallized from toluene. Yield 0.80 g (47 %).

^{1}H-NMR (DMSO-d_6, 300 MHz): 2.55 (d, 3H, J = 1.1 Hz, CH_3), 3.71 (s, 3H, OCH_3), 3.84 (s, 3H, OCH_3), 5.48 (b, 2H, NCH_2), 6.29 (d, 1H, J = 1.1 Hz, CH=C), 6.4 (s, 2H), 7.18-7.33 (m, 5H, Ph).

c) 1-Benzyl-5,7-dihydroxy-4-methyl-2(1H)-quinolinone

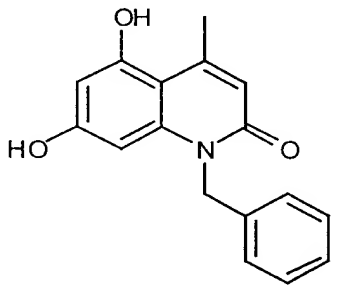

The product from the previous example (0.69 g) was dissolved to CH_2Cl_2 (14 ml) and the reaction mixture cooled to -20 °C. BBr_3 (2.4 g) in CH_2Cl_2 (1M solution) was added and the mixture was allowed to warm to ambient temperature during the night. The precipitate was filtered, washed with CH_2Cl_2 and dissolved to EtOAc. EtOAc was washed with dilute HCl, dryed and evapotated to dryness. Yield 0.34 g (54 %).

^{1}H-NMR (DMSO-d_6, 300 MHz): 2.56 (d, 3H, J = 1.0 Hz, CH_3), 5.33 (b, 2H, NCH_2), 6.11 (d, 1H, J = 2.1 Hz), 6.13 (d, 1H, J = 1.0 Hz, CH=C), 6.17 (d, 1H, J = 2.1 Hz), 7.12-7.34 (m, 5H, Ph), 9.90 (b, 1H, OH), 10.22 (s, 1H, OH).

d) 1-Benzyl-5,7-bis(cyanomethoxy)-4-methyl-2(1H)-quinolinone

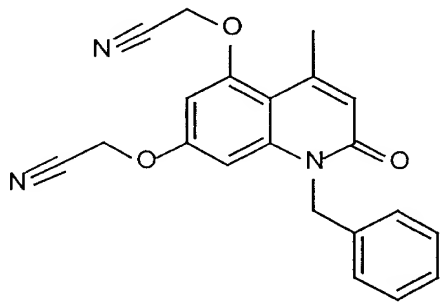

The product from the previous example (0.34 g), chloroacetonitrile (0.13 g) and potassium carbonate (0.34 g) were heated in DMF (2 ml) at 100 °C for 1.5 hours. Water was added and the precipitate filtered and dried. The product was recrystallized from isopropanol. Yield 0.20 g (46 %).

^{1}H-NMR (DMSO-d_6, 400 MHz): 2.57 (s, 3H, CH_3), 5.22 (s, 2H, OCH_2CN), 5.30 (s, 2H, OCH_2CN), 5.50 (b, 2H, NCH_2), 6.42 (s, 1H, CH=C), 6.70 (d, 1H, J = 2.1 Hz), 6.73 (d, 1H, J = 2.1 Hz), 7.21-7.32 (m, 5H, Ph).

e) 1-Benzyl-5,7-bis-[(1*H*-tetrazol-5-yl)methoxy]-4-methyl-2(1H)-quinolinone

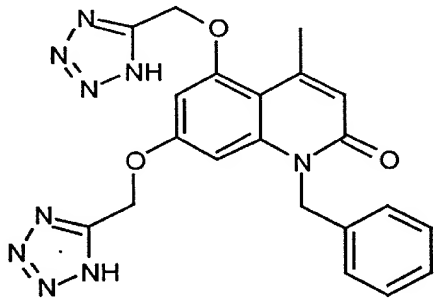

The product from the previous example (0.20 g), sodium azide (0.072 g) and ammonium chloride (0.060 g) were heated in DMF (2 ml) at 100 °C for 3 hours. The product was isolated as described in example 1c. Yield 0.21 g (85 %). Melting point 246-249 °C.

^{1}H-NMR (DMSO-d_6, 400 MHz): 2.50 (s, 3H, CH_3), 5.48 (b, 4H, OCH_2Tet, NCH_2), 5.60 (s, 2H, OCH_2Tet), 6.34 (s, 1H, CH=C), 6.64 (d, 1H, J = 1.9 Hz), 6.77 (d, 1H, J = 1.9 Hz), 7.18-7.32 (m, 5H, Ph).

Example 19. Preparation of 1-Benzyl-5,7-bis[1*H*-tetrazol-5-yl)methoxy]-3-(2-fluorobenzyl)-4-methyl-2(1H)-quinolinone

a) 5,7-Dimethoxy-3-(2-fluorobenzyl)-4-methyl-2(1H)-quinolinone

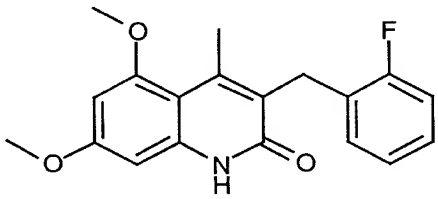

Ethyl 2-(2-fluorobenzyl)acetoacetate (2.5 g) in xylene (1 ml) was heated to 150 °C and 3,5- dimethoxyaniline (1.46 g) in xylene (4 ml) was added in small portions during 30 minutes. The reaction mixture was heated at 160 °C for 3 hours and then cooled to room temperature. Methanesulfonic acid (1.7 ml) was added and the mixture was stirred at ambient temperature for 30 minutes. Water was added and the precipitate filtered and dried. The product was triturated with warm ethanol. Yield 0.64 g (21 %).

^{1}H-NMR (DMSO-d_6, 300 MHz): 2.45 (s, 3H), 3.79 (s, 3H), 3.82 (s, 3H), 3.97 (s, 2H), 6.33 (d, 1H, J = 2.4 Hz), 6.48 (d, 1H, J = 2.4 Hz), 6.90-7.25 (m, 4H), 11.61 (s, 1H).

b) 1-Benzyl-5,7-dimethoxy-3-(2-fluorobenzyl)-4-methyl-2(1H)-quinolinone

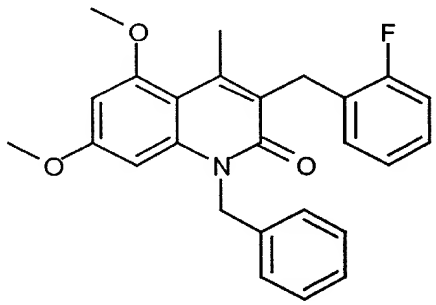

The product from the previous example (0.62 g) was treated with *t*-BuOK (0.23 g) and benzylbromide (0.36 g) in DMSO (12 ml) at 60 °C for 2.5 hours. The product was isolated as described in example 18b. Yield 0.39 g (49 %).

^{1}H-NMR (DMSO-d_6, 400 MHz): 2.51 (s, 3H), 3.72 (s, 3H), 3.84 (s, 3H), 4.11 (s, 2H), 5.55 (b, 2H), 6.433 (d, 1H, J = 2.1 Hz), 6.443 (d, 1H, J = 2.1 Hz), 6.97-7.33 (m, 9H).

c) 1-Benzyl-5,7-dihydroxy-3-(2-fluorobenzyl)-4-methyl-2(1H)-quinolinone

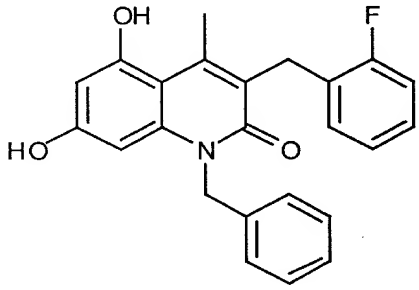

The product from the previous example (0.34 g) was treated with BBr_3 (8.48 g) in CH_2Cl_2 (7 ml) as described in example 18c. Yield 0.30 g (82 %).

^{1}H-NMR (DMSO-d_6, 400 MHz): 2.55 (s, 3H), 4.06 (s, 2H), 5.40 (b, 2H), 6.13 (d, 1H, J = 2.1 Hz), 6.22 (d, 1H, J = 2.1 Hz), 6.97-7.33 (m, 9H), 10.3 (b, 2H).

d) 1-Benzyl-5,7-bis(cyanomethoxy)-3-(2-fluorobenzyl)-4-methyl-2(1H)-quinolinone

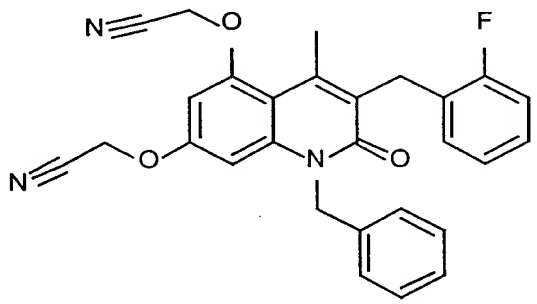

The product from the previous example (0.21 g), chloroacetonitrile (0.086 g) and potassium carbonate (0.37 g) were heated in DMF (2 ml) at 100 °C for 2 hours. The product was isolated as described in example 1b. Yield 0.18 g (71 %).

^{1}H-NMR (DMSO-d$_6$, 400 MHz): 2.53 (s, 3H), 4.13 (s, 2H), 5.23 (s, 2H), 5.29 (s, 2H), 5.57 (b, 2H), 6.746 (d, 1H, J = 2.3 Hz), 6.756 (d, 1H, J = 2.3 Hz), 7.00-7.32 (m, 9H).

e) 1-Benzyl-5,7-bis[1*H*-tetrazol-5-yl)methoxy]-3-(2-fluorobenzyl)-4-methyl-2(1H)-quinolinone

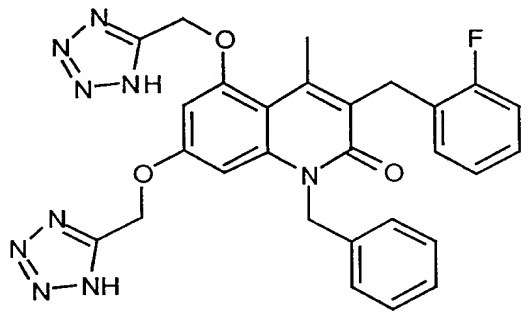

The product from the previous example (0.17 g), sodium azide (0.051 g) and ammonium chloride (0.042 g) were heated in DMF at 100 °C for 3 hours. The product was isolated as described in example 1c. Yield 0.17 g (85 %). Melting point 135-140 °C.

^{1}H-NMR (DMSO-d$_6$, 400 MHz): 2.46 (s, 3H), 4.10 (s, 2H), 5.48 (s, 2H), 5.51 (b, 2H), 5.59 (s, 2H), 6.68 (d, 1H, J = 2.2 Hz), 6.79 (d, 1H, J = 2.2 Hz), 6.99-7.32 (m, 9H).

Example 20. Preparation of 1-Benzyl-5,7-bis[1*H*-tetrazol-5-yl)-methoxy]-4-methyl-3-(2-phenylethyl)-2(1H)-quinolinone

a) 5,7-Dimethoxy-4-methyl-3-(2-phenylethyl)-2(1H)-quinolinone

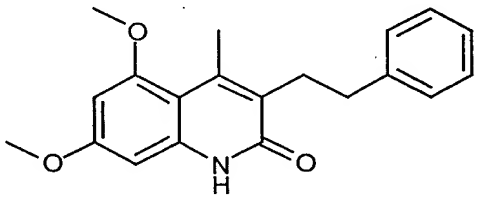

Ethyl 2-(2-phenylethyl)acetoacetate (2.70 g) in xylene (5 ml) was treated with 3,5-dimethoxyaniline (1.60 g) at 150 °C as described in example 19a. Methanesulfonic acid (4.0 ml) was added at room temperature and the mixture heated at 80 °C for 1 hour. The product was isolated as described in example 19a. Yield 1.38 g (41 %).

^{1}H-NMR (DMSO-d_6, 400 MHz): 2.45 (s, 3H), 2.64-2.68 (m, 2H), 2.82-2.86 (m, 2H), 3.78 (s, 3H), 3.81 (s, 3H), 6.30 (d, 1H, J = 2.3 Hz), 6.45 (d, 1H, J = 2.3 Hz), 7.18-7.30 (m, 5H), 11.45 (s, 1H).

b) 1-Benzyl-5,7-dimethoxy-4-methyl-3-(2-phenylethyl)-2(1H)-quinolinone

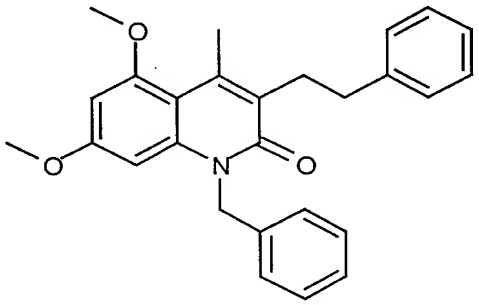

The product from the previous example (0.61 g), *t*-BuOK (0.24 g) and benzylbromide (0.36 g) were heated in DMSO (12 ml) at 60 °C for 2 hours. The product was isolated as described in example 18b. Yield 0.31 g (40 %).

^{1}H-NMR (DMSO-d_6, 400 MHz): 2.51 (s, 3H), 2.73-2.77 (m, 2H), 2.96-3.00 (m, 2H), 3.70 (s, 3H), 3.83 (s, 3H), 5.55 (b, 2H), 6.40 (s, 2H), 7.17-7.33 (m, 10 H).

c) 1-Benzyl-5,7-dihydroxy-4-methyl-3-(2-phenylethyl)-2(1H)-quinolinone

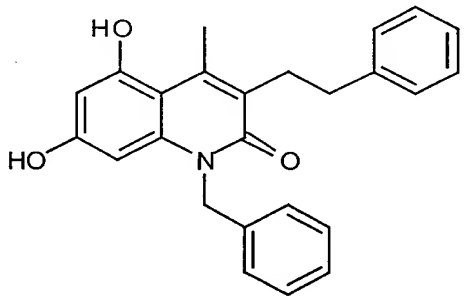

The product from the previous example (0.31 g) was treated with BBr_3 (0.75 g) in CH_2Cl_2 (5 ml) as in example 18c. Yield 0.26 g (89 %).

^{1}H-NMR (DMSO-d_6, 300 MHz): 2.56 (s, 3H), 2.69-2.75 (m, 2H), 2.90-2.95 (m, 2H), 5.39 (b, 2H), 6.08 (d, 1H, J = 2.0 Hz), 6.19 (d, 1H, J = 2.0 Hz), 7.11-7.33 (m, 10H), 10.2 (b, 2H).

d) 1-Benzyl-5,7-bis(cyanomethoxy)-4-methyl-3-(2-phenylethyl)-2(1H)-quinolinone

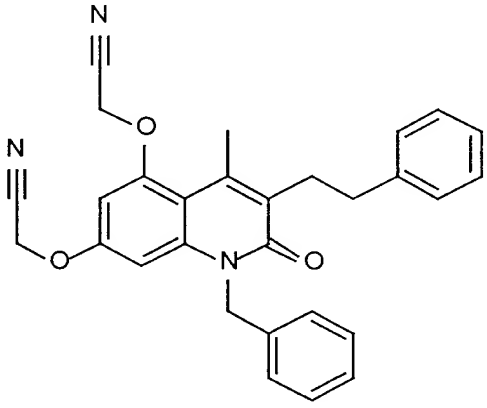

The product from the previous example (0.22 g), chloroacetonitrile (0.091 g) and potassium carbonate (0.39 g) were heated at 100 °C for 2 hours. The product was isolated as in example 1b. Yield 0.20 g (76 %).

^{1}H-NMR (DMSO-d_6, 400 MHz): 2.50 (s, 3H), 2.73-2.77 (m, 2H), 2.98-3.02 (m, 2H), 5.21 (s, 2H), 5.29 (s, 2H), 5.56 (b, 2H), 6.70 (d, 1H, J = 2.1 Hz), 6.72 (d, 1H, J = 2.1 Hz), 7.18-7.33 (m, 10H).

e) 1-Benzyl-5,7-bis[1*H*-tetrazol-5-yl)methoxy]-4-methyl-3-(2-phenylethyl)-2(1H)-quinolinone

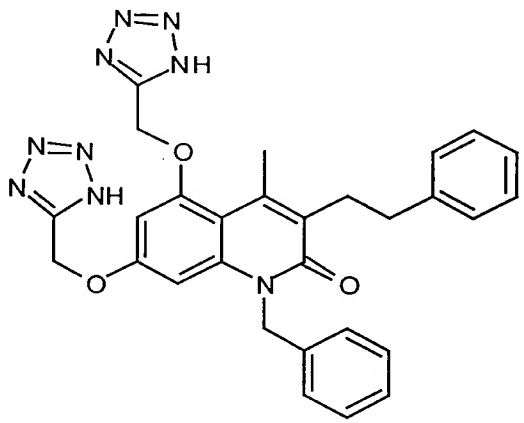

The product from the previous example (0.19 g), sodium azide (0.057 g) and ammonium chloride (0.047 g) were heated in DMF at 100 °C for 3 hours. The product was isolated as described in example 1c. Yield 0.18 g (78 %). Melting point 215-218 °C.

^{1}H-NMR (DMSO-d_6, 400 MHz): 2.46 (s, 3H), 2.70-2.74 (m, 2H), 2.95-2.99 (m, 2H), 5.47 (s, 2H), 5.54 (b, 2H), 5.57 (s, 2H), 6.64 (d, 1H, J = 2.0 Hz), 6.77 (d, 1H, J = 2.0 Hz), 7.16-7.33 (m, 10H).

Example 21. Preparation of 5,7-Bis(aminocarbonylmethoxy)-1,3-dibenzyl-4-methyl-2(1H)-quinolinone.

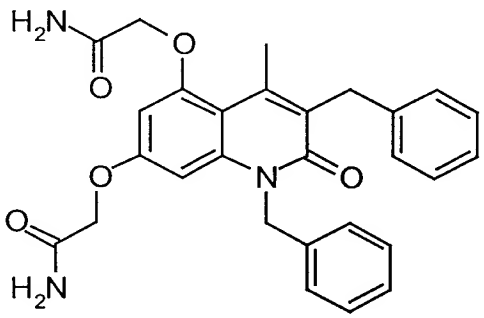

The mixture of 5,7-dihydroxy-1,3-dibenzyl-4-methyl-2(1H)-quinolinone (0.5 g), potassium carbonate (0.9 g) and 2-chloroacetamide (0.25 g) in DMF (6.5 ml) were reacted at 100 °C for two hours. The reaction mixture was treated with ice water and filtered. The product was triturated with hot ethanol. Yield: 0.32 g. Melting point 252-253°C.

^{1}H-NMR (400 MHz, DMSO-d_6): 2.63 (s, 3H, CH3), 4.13 (s, 2H, $PhCH_2$), 4.37 (s, 2H, OCH_2), 4.55 (s, 2H, OCH_2), 5.54 (s, 2H, NCH_2Ph), 6.40 (d, 1H, J = 2 Hz,

ArH), 6.53 (d, 1H, J = 2 Hz, ArH), 7.13-7.33 (m, 10 H, Ph), 7.44 (d, 2H, J = 65 Hz, $CONH_2$), 7.47 (d, 2H, J = 68 Hz, $CONH_2$).

Example 22. Preparation of 5,7-Bis(ethoxycarbonylmethoxy)-1,3-dibenzyl-4-methyl-2(1H)-quinolinone.

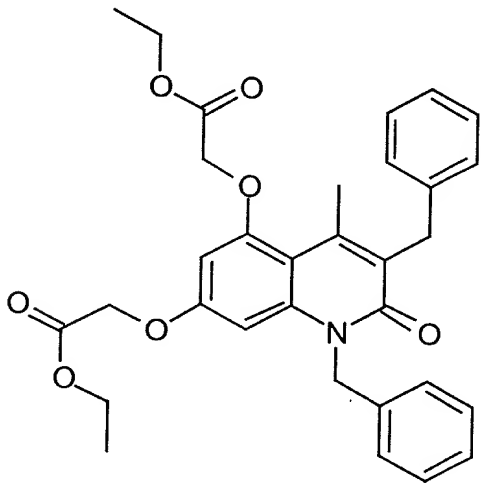

The mixture of 5,7-dihydroxy-1,3-dibenzyl-4-methyl-2(1H)-quinolinone (1 g), ethyl 2-bromoacetate (0.63 ml) and potassium carbonate (1.49 g) in DMF (5 ml) was heated under nitrogen at 110 °C for three hours, poured into ice water and filtered. The resulting solid material was triturated with ether and filtered again. Yield: 1.03 g, melting point 113-116 °C.

^{1}H-NMR (400 MHz, DMSO-d_6): 1.15 (t, 3H, CH_3CH_2, J = 7.1 Hz), 1.20 (t, 3H, CH_3CH_2, J = 7.1 Hz), 2.63 (s, 3H, CH3), 4.03 (q, 2H, CH_2CH_3, J = 7.1 Hz), 4.13 (s, 2H, CH_2Ph), 4.17 (q, 2H, CH_2CH_3, J = 7.1 Hz), 4.78 (s, 2H, OCH_2), 4.90 (s, 2H, OCH_2), 6.41 (d, 1H, J = 2.2 Hz), 6.44 (d, 1H, J = 2.2 Hz), 7.13-7.33 (m, 10 H, Ph).

Example 23. Preparation of 5,7-Bis(hydroxyaminocarbonylmethoxy)-1,3-dibenzyl-4-methyl-2(1H)-quinolinone

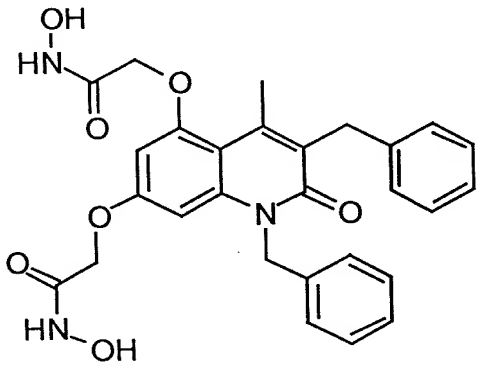

The product from the previous example (0.3 g), hydroxylamine hydrochloride (0.32 g) and 5 N NaOH (1.05 ml) were reacted in ethanol (8 ml) at 50 °C for six hours. The reaction mixture was treated with water and made basic (pH 10) and filtered. The filtrate was acidified to pH 2 and filtered. Yield: 0.2 g, melting point 121-127°C.

^{1}H-NMR (400 MHz, DMSO-d6): the tautomeric forms of hydroxamic acid are seen in OCH_2-signals: 2.63 (s,3H, CH3), 4.13 (S, 2H, CH_2Ph), 4.41 (s, 2H, OCH_2), 4.54 (s, 2H,OCH_2), 4.64 (s, 2H, HON=C(OH)CH_2O), 4.65 (s, 2H, HON=C(OH)CH_2O), 4.77 (s, 2H, HON=C(OH)CH_2O), 4.78 ((s, 2H, HON=C(OH)CH_2O), 5.54 (s, 2H, NCH_2Ph), 6.38-6.54 (m, 2H, ArH), 7.14-7.34 (m, 10 H, Ph), 9.05 (b, 2H, NOH), 10.84 (s, 1H, HONHCO), 10.88 (s, 1H, HONHCO).

EXAMPLE 5. Design of PLB inhibitors

The three dimensional structure determined for phospholamban can be used as a target for selecting compounds that bind to the protein. In order to have good affinity for phospholamban, the ligand should have steric and electrostatic complementarity with the target. Especially, good electrostatic and/or hydrogen bonding interactions should be formed with the sites S1 and S2, and good hydrophobic interactions should be formed with the sites S3 and S4. Any of the various computer programs and databases available for such purpose can be used to design compounds that fullfill these requirements. The structure-based approaches include *de Novo* design, computer-based selection of ligands that are complementary with the target and computer-aided optimization of lead molecules. The detection of the PLB binding compounds can proceed by using the following steps:

1. The target region of the protein is selected. The binding model of the effective phospholamban deactivator peptide, cP226, can be used to define an area on the phospholamban surface which can function as a target for phospholamban deactivators. Especially, this determines the side chains of phospholamban which can interact with the compounds to be designed.

2. Small molecules which are complementary to the binding site can be docked to the target by using available software, such as e.g. Ludi, DOCK or LeapFrog. Computer databases of three-dimensional structures of small molecules or molecular fragments can be used in the docking. Such an approach gives molecules or fragments that have good interactions with the various parts of the target area.

3. Different small molecules or fragments that bind to the target area can be linked together or one can incorporate new side chains and/or functional groups to them, so that one gets a single, larger molecule. The resulting new compound is likely to have better affinity to the target than the smaller molecules.

4. One can also select a proper scaffold and dock that by using an interactive molecular graphics system near the binding site of the protein. One can then add new fragments and functional groups to the scaffold, so that the new groups form good interactions with the target surface.

5. The cyclic peptide cP226 is an example of a compound which binds to the ligand binding site of phospholamban. The structure of cP226 can be used as a model for designing new compounds with affinity to phospholamban. Any of the well defined methods for designing peptidomimetics or, more generally, peptide mimics can be used to design such compounds.

A limited number of compounds can be selected through the process outlined above. Anyone skilled with the art would be able to identify such compounds by using the three dimensional structure of phospholamban stored in a computer system. The compounds can be then synthetized and tested for their ability to deactivate phosholamban in an assay similar to that outlined in example 3.

TABLE I. Orthogonal three dimensional coordinates in Ångströms for the cyclic peptide cP226

Residue	Atom	X	Y	Z
1 CYS	N	-4.500	-5.816	1.065
1 CYS	CA	-3.913	-5.081	2.195
1 CYS	HN1	-4.805	-6.727	1.378
1 CYS	HN2	-5.291	-5.300	0.706
1 CYS	HN3	-3.811	-5.926	0.337
1 CYS	HA	-4.673	-5.015	2.974
1 CYS	C	-3.521	-3.665	1.797
1 CYS	O	-4.275	-2.984	1.106
1 CYS	CB	-2.716	-5.833	2.773
1 CYS	SG	-1.186	-5.807	1.793
1 CYS	HB1	-2.485	-5.381	3.737
1 CYS	HB2	-3.005	-6.870	2.943
1 CYS	LG1	-0.868	-6.293	2.143
1 CYS	LG2	-1.298	-5.206	1.500
2 TYR	N	-2.334	-3.230	2.226
2 TYR	CA	-1.822	-1.920	1.877
2 TYR	HN	-1.741	-3.845	2.764
2 TYR	HA	-2.467	-1.466	1.124
2 TYR	C	-0.427	-2.065	1.301
2 TYR	O	-0.005	-3.170	0.967
2 TYR	CB	-1.782	-1.016	3.105
2 TYR	HB1	-0.796	-0.552	3.147
2 TYR	HB2	-2.524	-0.231	2.974
2 TYR	CG	-2.052	-1.724	4.413
2 TYR	CD1	-3.368	-1.863	4.872
2 TYR	HD1	-4.192	-1.509	4.270
2 TYR	CD2	-0.987	-2.180	5.200
2 TYR	HD2	0.031	-2.071	4.855
2 TYR	CE1	-3.619	-2.453	6.116

2	TYR	HE1	-4.634	-2.555	6.471
2	TYR	CE2	-1.238	-2.769	6.445
2	TYR	HE2	-0.415	-3.115	7.053
2	TYR	CZ	-2.553	-2.901	6.905
2	TYR	OH	-2.798	-3.464	8.124
2	TYR	HH	-1.998	-3.726	8.585
3	TRP	N	0.295	-0.949	1.195
3	TRP	CA	1.639	-0.990	0.666
3	TRP	HN	-0.084	-0.061	1.491
3	TRP	HA	2.012	-2.004	0.800
3	TRP	C	2.542	-0.026	1.422
3	TRP	O	2.112	0.623	2.372
3	TRP	CB	1.614	-0.654	-0.821
3	TRP	HB1	0.826	-1.238	-1.296
3	TRP	HB2	1.378	0.404	-0.929
3	TRP	CG	2.892	-0.918	-1.546
3	TRP	CD1	3.831	0.008	-1.830
3	TRP	CD2	3.402	-2.178	-2.077
3	TRP	NE1	4.877	-0.580	-2.512
3	TRP	CE2	4.664	-1.934	-2.681
3	TRP	HD1	3.772	1.053	-1.559
3	TRP	HE1	5.708	-0.104	-2.833
3	TRP	CE3	2.933	-3.504	-2.103
3	TRP	HE3	1.978	-3.737	-1.655
3	TRP	CZ2	5.421	-2.947	-3.276
3	TRP	HZ2	6.378	-2.724	-3.723
3	TRP	CZ3	3.684	-4.528	-2.696
3	TRP	HZ3	3.302	-5.538	-2.700
3	TRP	CH2	4.927	-4.255	-3.280
3	TRP	HH2	5.501	-5.051	-3.731
4	GLU	N	3.799	0.056	0.982
4	GLU	CA	4.812	0.899	1.576
4	GLU	HN	4.087	-0.499	0.192
4	GLU	HA	5.405	0.313	2.216
4	GLU	C	4.236	2.017	2.406
4	GLU	O	4.787	2.431	3.423

4	GLU	CB	5.698	1.448	0.481
4	GLU	CG	6.679	0.389	-0.014
4	GLU	CD	7.595	0.956	-1.091
4	GLU	OE1	7.249	0.790	-2.281
4	GLU	OE2	8.627	1.545	-0.704
4	GLU	HB1	5.027	1.763	-0.302
4	GLU	HB2	6.242	2.305	0.856
4	GLU	HG1	7.290	0.056	0.824
4	GLU	HG2	6.128	-0.462	-0.411
5	LEU	N	3.135	2.522	1.889
5	LEU	CA	2.622	3.813	2.150
5	LEU	HN	2.818	2.140	1.031
5	LEU	HA	3.362	4.435	2.574
5	LEU	C	1.437	3.723	3.079
5	LEU	O	1.552	3.459	4.275
5	LEU	CB	2.300	4.379	0.776
5	LEU	HB1	1.233	4.331	0.644
5	LEU	HB2	2.784	3.725	0.059
5	LEU	CG	2.893	5.759	0.516
5	LEU	HG	3.808	5.818	1.092
5	LEU	CD1	3.275	5.906	-0.959
5	LEU	HD11	4.091	5.223	-1.199
5	LEU	HD12	2.426	5.670	-1.594
5	LEU	HD13	3.598	6.928	-1.157
5	LEU	CD2	1.924	6.871	0.916
5	LEU	HD21	1.572	6.707	1.933
5	LEU	HD22	2.430	7.834	0.854
5	LEU	HD23	1.076	6.877	0.232
6	GLU	N	0.310	4.034	2.475
6	GLU	CA	-0.797	4.584	3.234
6	GLU	HN	0.545	4.337	1.543
6	GLU	HA	-0.766	4.194	4.238
6	GLU	C	-2.174	4.334	2.625
6	GLU	O	-3.182	4.404	3.326
6	GLU	CB	-0.517	6.066	3.324
6	GLU	CG	-1.394	6.792	4.342

6	GLU	CD	-1.241	6.210	5.741
6	GLU	OE1	-2.246	5.654	6.235
6	GLU	OE2	-0.124	6.332	6.290
6	GLU	HB1	0.541	6.185	3.551
6	GLU	HB2	-0.707	6.444	2.332
6	GLU	HG1	-1.101	7.841	4.360
6	GLU	HG2	-2.436	6.722	4.036
7	TRP	N	-2.229	4.100	1.315
7	TRP	CA	-3.460	4.217	0.555
7	TRP	HN	-1.368	3.977	0.804
7	TRP	HA	-4.317	4.129	1.222
7	TRP	C	-3.504	3.121	-0.491
7	TRP	O	-4.454	2.344	-0.558
7	TRP	CB	-3.485	5.577	-0.150
7	TRP	HB1	-4.435	5.670	-0.675
7	TRP	HB2	-3.431	6.359	0.607
7	TRP	CG	-2.379	5.797	-1.141
7	TRP	CD1	-1.059	5.740	-0.857
7	TRP	CD2	-2.452	6.056	-2.579
7	TRP	NE1	-0.316	5.931	-1.995
7	TRP	CE2	-1.127	6.116	-3.086
7	TRP	HD1	-0.629	5.529	0.104
7	TRP	HE1	0.688	5.926	-2.054
7	TRP	CE3	-3.486	6.229	-3.517
7	TRP	HE3	-4.514	6.191	-3.189
7	TRP	CZ2	-0.832	6.315	-4.430
7	TRP	HZ2	0.208	6.311	-4.723
7	TRP	CZ3	-3.203	6.453	-4.874
7	TRP	HZ3	-4.014	6.590	-5.573
7	TRP	CH2	-1.880	6.491	-5.336
7	TRP	HH2	-1.673	6.653	-6.384
8	LEU	N	-2.458	3.080	-1.316
8	LEU	CA	-2.399	2.215	-2.463
8	LEU	HN	-1.741	3.788	-1.251
8	LEU	HA	-3.342	2.268	-2.987
8	LEU	C	-2.138	0.775	-2.047

8	LEU	O	-2.050	0.466	-0.861
8	LEU	CB	-1.377	2.801	-3.420
8	LEU	HB1	-1.919	3.553	-3.985
8	LEU	HB2	-0.627	3.313	-2.838
8	LEU	CG	-0.697	1.810	-4.364
8	LEU	HG	-1.411	1.066	-4.715
8	LEU	CD1	0.486	1.139	-3.660
8	LEU	HD11	0.148	0.611	-2.770
8	LEU	HD12	0.958	0.428	-4.336
8	LEU	HD13	1.216	1.894	-3.367
8	LEU	CD2	-0.166	2.597	-5.559
8	LEU	HD21	0.377	1.929	-6.226
8	LEU	HD22	-0.999	3.047	-6.099
8	LEU	HD23	0.503	3.385	-5.211
9	PRO	N	-2.105	-0.108	-3.045
9	PRO	CA	-2.388	-1.520	-2.908
9	PRO	CD	-2.238	0.281	-4.432
9	PRO	HA	-3.411	-1.651	-2.592
9	PRO	HD1	-1.244	0.463	-4.841
9	PRO	HD2	-2.849	1.180	-4.534
9	PRO	C	-1.489	-2.327	-2.003
9	PRO	O	-0.712	-1.817	-1.200
9	PRO	CB	-2.321	-2.090	-4.308
9	PRO	HB1	-2.906	-3.003	-4.418
9	PRO	HB2	-1.278	-2.261	-4.524
9	PRO	CG	-2.874	-0.932	-5.115
9	PRO	HG1	-3.943	-0.968	-4.924
9	PRO	HG2	-2.647	-0.998	-6.179
10	CYS	N	-1.663	-3.631	-2.196
10	CYS	CA	-1.012	-4.692	-1.465
10	CYS	HN	-2.332	-3.890	-2.912
10	CYS	HA	-0.585	-4.387	-0.542
10	CYS	C	0.010	-5.351	-2.349
10	CYS	O	1.190	-5.013	-2.406
10	CYS	CB	-2.057	-5.730	-1.120
10	CYS	SG	-1.557	-6.937	0.133

10	CYS	HB1	-2.248	-6.248	-2.047
10	CYS	HB2	-2.961	-5.214	-0.820
10	CYS	LG1	-2.185	-7.126	0.309
10	CYS	LG2	-0.911	-6.990	-0.068
11	ALA	N	-0.563	-6.322	-3.032
11	ALA	CA	0.071	-7.137	-4.047
11	ALA	HN	-1.541	-6.400	-2.791
11	ALA	HA	-0.700	-7.659	-4.614
11	ALA	C	0.986	-8.164	-3.395
11	ALA	O	1.316	-7.956	-2.208
11	ALA	OXT	1.336	-9.138	-4.095
11	ALA	CB	0.852	-6.232	-4.994
11	ALA	HB1	1.630	-5.713	-4.434
11	ALA	HB2	1.304	-6.831	-5.783
11	ALA	HB3	0.172	-5.502	-5.433

END

TABLE III. Orthogonal three dimensional coordinates in Ångströms for the phospholamban (1-36) peptide

Residue		Atom	X	Y	Z
1	MET	N	-18.883	-3.493	9.020
1	MET	CA	-17.518	-3.957	8.653
1	MET	HN1	-19.536	-4.279	9.119
1	MET	HN2	-18.890	-2.989	9.914
1	MET	HN3	-19.280	-2.863	8.314
1	MET	HA	-16.901	-3.038	8.626
1	MET	C	-17.415	-4.543	7.212
1	MET	O	-16.572	-4.081	6.439
1	MET	CB	-16.875	-4.826	9.772
1	MET	HB1	-15.795	-4.924	9.547
1	MET	HB2	-16.893	-4.265	10.726
1	MET	CG	-17.422	-6.248	10.031
1	MET	SD	-19.151	-6.241	10.562
1	MET	CE	-18.991	-5.887	12.325
1	MET	HG1	-17.330	-6.874	9.124
1	MET	HG2	-16.810	-6.758	10.798
1	MET	HE1	-19.984	-5.878	12.809
1	MET	HE2	-18.374	-6.655	12.827
1	MET	HE3	-18.521	-4.900	12.492
2	GLU	N	-18.254	-5.533	6.842
2	GLU	CA	-18.265	-6.128	5.478
2	GLU	HN	-18.900	-5.856	7.571
2	GLU	HA	-17.210	-6.282	5.173
2	GLU	C	-18.948	-5.225	4.401
2	GLU	O	-19.754	-4.342	4.720
2	GLU	CB	-18.906	-7.547	5.541
2	GLU	CG	-20.416	-7.627	5.896
2	GLU	CD	-21.035	-8.987	5.590
2	GLU	OE1	-21.495	-9.191	4.444
2	GLU	OE2	-21.070	-9.854	6.489

2	GLU	HB1	-18.746	-8.031	4.557
2	GLU	HB2	-18.337	-8.184	6.246
2	GLU	HG1	-20.571	-7.388	6.963
2	GLU	HG2	-20.990	-6.864	5.338
3	LYS	N	-18.664	-5.521	3.116
3	LYS	CA	-19.464	-5.049	1.948
3	LYS	HN	-17.993	-6.291	3.013
3	LYS	HA	-19.008	-5.581	1.092
3	LYS	C	-19.248	-3.539	1.622
3	LYS	O	-18.370	-3.219	0.818
3	LYS	CB	-20.930	-5.587	1.997
3	LYS	CG	-21.709	-5.508	0.666
3	LYS	CD	-23.177	-5.990	0.736
3	LYS	CE	-23.411	-7.513	0.856
3	LYS	NZ	-23.320	-8.021	2.243
3	LYS	HB1	-20.905	-6.644	2.322
3	LYS	HB2	-21.495	-5.058	2.788
3	LYS	HG1	-21.711	-4.458	0.320
3	LYS	HG2	-21.169	-6.068	-0.122
3	LYS	HD1	-23.726	-5.441	1.525
3	LYS	HD2	-23.662	-5.662	-0.204
3	LYS	HE1	-24.420	-7.750	0.465
3	LYS	HE2	-22.711	-8.069	0.201
3	LYS	HZ1	-22.376	-7.928	2.639
3	LYS	HZ2	-23.954	-7.523	2.880
3	LYS	HZ3	-23.558	-9.017	2.311
4	VAL	N	-20.017	-2.625	2.249
4	VAL	CA	-19.844	-1.150	2.084
4	VAL	HN	-20.672	-3.020	2.932
4	VAL	HA	-19.723	-0.979	0.995
4	VAL	C	-18.532	-0.595	2.734
4	VAL	O	-17.763	0.075	2.042
4	VAL	CB	-21.166	-0.392	2.460
4	VAL	HB	-21.981	-0.865	1.880
4	VAL	CG1	-21.148	1.087	2.010
4	VAL	HG11	-22.125	1.579	2.173

4	VAL	HG12	-20.389	1.679	2.555
4	VAL	HG13	-20.921	1.182	0.931
4	VAL	CG2	-21.594	-0.469	3.946
4	VAL	HG21	-22.587	-0.009	4.106
4	VAL	HG22	-21.672	-1.514	4.297
4	VAL	HG23	-20.886	0.051	4.615
5	GLN	N	-18.257	-0.895	4.022
5	GLN	CA	-16.969	-0.532	4.685
5	GLN	HN	-18.970	-1.467	4.487
5	GLN	HA	-16.753	0.525	4.431
5	GLN	C	-15.708	-1.326	4.214
5	GLN	O	-14.609	-0.764	4.263
5	GLN	CB	-17.126	-0.595	6.230
5	GLN	HB1	-16.134	-0.491	6.711
5	GLN	HB2	-17.470	-1.605	6.519
5	GLN	CG	-18.072	0.452	6.870
5	GLN	HG1	-19.093	0.350	6.454
5	GLN	HG2	-18.189	0.209	7.943
5	GLN	CD	-17.577	1.906	6.777
5	GLN	OE1	-16.699	2.331	7.525
5	GLN	NE2	-18.118	2.697	5.865
5	GLN	HE21	-17.754	3.655	5.830
5	GLN	HE22	-18.828	2.281	5.254
6	TYR	N	-15.837	-2.578	3.722
6	TYR	CA	-14.754	-3.255	2.953
6	TYR	HN	-16.798	-2.934	3.726
6	TYR	HA	-13.836	-3.179	3.569
6	TYR	C	-14.429	-2.578	1.577
6	TYR	O	-13.246	-2.405	1.284
6	TYR	CB	-15.073	-4.771	2.823
6	TYR	HB1	-15.450	-5.161	3.789
6	TYR	HB2	-15.922	-4.917	2.126
6	TYR	CG	-13.870	-5.631	2.391
6	TYR	CD1	-12.947	-6.081	3.342
6	TYR	HD1	-13.093	-5.867	4.391
6	TYR	CD2	-13.656	-5.919	1.038

6	TYR	HD2	-14.351	-5.571	0.287
6	TYR	CE1	-11.820	-6.795	2.944
6	TYR	HE1	-11.109	-7.135	3.683
6	TYR	CE2	-12.526	-6.633	0.642
6	TYR	HE2	-12.364	-6.840	-0.406
6	TYR	CZ	-11.608	-7.066	1.594
6	TYR	OH	-10.486	-7.749	1.203
6	TYR	HH	-10.543	-7.928	0.261
7	LEU	N	-15.435	-2.177	0.768
7	LEU	CA	-15.228	-1.333	-0.448
7	LEU	HN	-16.377	-2.392	1.118
7	LEU	HA	-14.505	-1.879	-1.083
7	LEU	C	-14.618	0.088	-0.187
7	LEU	O	-13.755	0.514	-0.959
7	LEU	CB	-16.568	-1.276	-1.239
7	LEU	HB1	-16.964	-2.304	-1.362
7	LEU	HB2	-17.320	-0.763	-0.607
7	LEU	CG	-16.545	-0.600	-2.641
7	LEU	HG	-16.134	0.421	-2.532
7	LEU	CD1	-17.977	-0.449	-3.189
7	LEU	HD11	-18.471	-1.427	-3.341
7	LEU	HD12	-18.616	0.136	-2.501
7	LEU	HD13	-17.989	0.081	-4.159
7	LEU	CD2	-15.670	-1.352	-3.665
7	LEU	HD21	-16.014	-2.391	-3.823
7	LEU	HD22	-15.676	-0.852	-4.652
7	LEU	HD23	-14.613	-1.398	-3.347
8	THR	N	-15.020	0.793	0.895
8	THR	CA	-14.337	2.035	1.379
8	THR	HN	-15.786	0.362	1.425
8	THR	HA	-14.401	2.775	0.558
8	THR	C	-12.813	1.822	1.687
8	THR	O	-11.983	2.555	1.144
8	THR	CB	-15.125	2.633	2.591
8	THR	OG1	-16.503	2.806	2.270
8	THR	HB	-15.061	1.931	3.445

8	THR	HG1	-16.535	3.486	1.594
8	THR	CG2	-14.620	4.006	3.070
8	THR	HG21	-14.652	4.764	2.265
8	THR	HG22	-15.233	4.389	3.908
8	THR	HG23	-13.579	3.955	3.436
9	ARG	N	-12.454	0.800	2.491
9	ARG	CA	-11.040	0.367	2.694
9	ARG	HN	-13.242	0.262	2.868
9	ARG	HA	-10.475	1.248	3.056
9	ARG	C	-10.279	-0.141	1.422
9	ARG	O	-9.068	0.074	1.342
9	ARG	CB	-10.986	-0.704	3.816
9	ARG	CG	-11.336	-0.195	5.239
9	ARG	CD	-11.278	-1.278	6.331
9	ARG	NE	-12.399	-2.249	6.225
9	ARG	CZ	-12.453	-3.428	6.870
9	ARG	NH1	-13.518	-4.178	6.704
9	ARG	NH2	-11.493	-3.881	7.666
9	ARG	HB1	-9.966	-1.132	3.864
9	ARG	HB2	-11.641	-1.555	3.549
9	ARG	HG1	-10.627	0.611	5.509
9	ARG	HG2	-12.331	0.292	5.247
9	ARG	HD1	-10.296	-1.790	6.290
9	ARG	HD2	-11.320	-0.790	7.325
9	ARG	HE	-13.225	-2.039	5.652
9	ARG	HH12	-14.259	-3.806	6.101
9	ARG	HH11	-13.535	-5.071	7.209
9	ARG	HH21	-10.677	-3.270	7.781
9	ARG	HH22	-11.642	-4.793	8.108
10	SER	N	-10.946	-0.787	0.443
10	SER	CA	-10.354	-1.132	-0.884
10	SER	HN	-11.942	-0.946	0.641
10	SER	HA	-9.439	-1.724	-0.697
10	SER	C	-9.924	0.093	-1.755
10	SER	O	-8.816	0.081	-2.300
10	SER	CB	-11.306	-2.070	-1.661

10	SER	OG	-11.499	-3.303	-0.971
10	SER	HB1	-12.283	-1.585	-1.840
10	SER	HB2	-10.895	-2.294	-2.663
10	SER	HG	-12.151	-3.796	-1.475
11	ALA	N	-10.757	1.151	-1.848
11	ALA	CA	-10.344	2.469	-2.403
11	ALA	HN	-11.651	1.031	-1.357
11	ALA	HA	-9.966	2.296	-3.429
11	ALA	C	-9.219	3.223	-1.619
11	ALA	O	-8.321	3.776	-2.259
11	ALA	CB	-11.608	3.341	-2.539
11	ALA	HB1	-12.075	3.558	-1.559
11	ALA	HB2	-11.379	4.314	-3.012
11	ALA	HB3	-12.378	2.857	-3.170
12	ILE	N	-9.242	3.226	-0.266
12	ILE	CA	-8.172	3.838	0.586
12	ILE	HN	-10.056	2.754	0.145
12	ILE	HA	-8.006	4.865	0.200
12	ILE	C	-6.795	3.099	0.438
12	ILE	O	-5.794	3.779	0.207
12	ILE	CB	-8.658	4.011	2.076
12	ILE	HB	-8.948	3.006	2.440
12	ILE	CG1	-9.901	4.950	2.214
12	ILE	HG11	-10.620	4.757	1.398
12	ILE	HG12	-9.602	6.005	2.066
12	ILE	CG2	-7.544	4.533	3.028
12	ILE	HG21	-7.887	4.618	4.075
12	ILE	HG22	-6.669	3.857	3.055
12	ILE	HG23	-7.174	5.529	2.721
12	ILE	CD1	-10.686	4.819	3.530
12	ILE	HD11	-11.582	5.467	3.523
12	ILE	HD12	-11.037	3.782	3.694
12	ILE	HD13	-10.086	5.112	4.410
13	ARG	N	-6.728	1.753	0.563
13	ARG	CA	-5.468	0.976	0.354
13	ARG	HN	-7.628	1.294	0.749

13	ARG	HA	-4.726	1.433	1.041
13	ARG	C	-4.830	1.090	-1.073
13	ARG	O	-3.613	1.260	-1.173
13	ARG	CB	-5.630	-0.486	0.871
13	ARG	CG	-6.342	-1.498	-0.063
13	ARG	CD	-6.640	-2.883	0.549
13	ARG	NE	-7.896	-2.883	1.345
13	ARG	CZ	-8.627	-3.976	1.626
13	ARG	NH1	-8.236	-5.216	1.363
13	ARG	NH2	-9.800	-3.810	2.198
13	ARG	HB1	-6.139	-0.472	1.855
13	ARG	HB2	-4.622	-0.886	1.095
13	ARG	HG1	-7.266	-1.050	-0.471
13	ARG	HG2	-5.699	-1.654	-0.950
13	ARG	HD1	-6.722	-3.609	-0.283
13	ARG	HD2	-5.789	-3.231	1.168
13	ARG	HE	-8.340	-1.998	1.613
13	ARG	HH12	-7.314	-5.315	0.927
13	ARG	HH11	-8.879	-5.974	1.620
13	ARG	HH21	-10.096	-2.844	2.364
13	ARG	HH22	-10.347	-4.658	2.382
14	ARG	N	-5.647	1.040	-2.150
14	ARG	CA	-5.205	1.316	-3.547
14	ARG	HN	-6.640	0.917	-1.918
14	ARG	HA	-4.382	0.609	-3.774
14	ARG	C	-4.654	2.762	-3.783
14	ARG	O	-3.574	2.899	-4.362
14	ARG	CB	-6.387	0.954	-4.492
14	ARG	CG	-6.046	0.936	-6.002
14	ARG	CD	-7.241	0.641	-6.935
14	ARG	NE	-7.781	-0.743	-6.818
14	ARG	CZ	-7.326	-1.813	-7.495
14	ARG	NH1	-6.304	-1.776	-8.341
14	ARG	NH2	-7.927	-2.967	-7.304
14	ARG	HB1	-6.779	-0.047	-4.223
14	ARG	HB2	-7.232	1.648	-4.313

14	ARG	HG1	-5.635	1.922	-6.287
14	ARG	HG2	-5.227	0.217	-6.196
14	ARG	HD1	-8.058	1.355	-6.720
14	ARG	HD2	-6.959	0.862	-7.983
14	ARG	HE	-8.576	-0.946	-6.202
14	ARG	HH12	-5.856	-0.864	-8.466
14	ARG	HH11	-6.046	-2.656	-8.800
14	ARG	HH21	-8.716	-2.973	-6.649
14	ARG	HH22	-7.566	-3.769	-7.830
15	ALA	N	-5.366	3.815	-3.329
15	ALA	CA	-4.859	5.215	-3.352
15	ALA	HN	-6.249	3.572	-2.865
15	ALA	HA	-4.610	5.460	-4.404
15	ALA	C	-3.580	5.502	-2.503
15	ALA	O	-2.687	6.192	-2.996
15	ALA	CB	-6.019	6.148	-2.948
15	ALA	HB1	-5.723	7.211	-3.012
15	ALA	HB2	-6.898	6.024	-3.608
15	ALA	HB3	-6.360	5.965	-1.911
16	SER	N	-3.471	4.962	-1.270
16	SER	CA	-2.253	5.080	-0.420
16	SER	HN	-4.293	4.425	-0.965
16	SER	HA	-2.050	6.162	-0.292
16	SER	C	-0.958	4.438	-1.011
16	SER	O	0.081	5.105	-1.033
16	SER	CB	-2.595	4.527	0.984
16	SER	OG	-1.533	4.766	1.904
16	SER	HB1	-2.808	3.441	0.942
16	SER	HB2	-3.513	5.000	1.382
16	SER	HG	-0.749	4.360	1.526
17	THR	N	-1.011	3.178	-1.503
17	THR	CA	0.124	2.551	-2.246
17	THR	HN	-1.934	2.731	-1.438
17	THR	HA	1.023	2.737	-1.625
17	THR	C	0.453	3.189	-3.638
17	THR	O	1.637	3.295	-3.969

17	THR	CB	-0.014	0.998	-2.268
17	THR	OG1	1.246	0.419	-2.593
17	THR	HB	-0.270	0.656	-1.245
17	THR	HG1	1.437	0.690	-3.494
17	THR	CG2	-1.058	0.403	-3.230
17	THR	HG21	-1.179	-0.683	-3.070
17	THR	HG22	-2.050	0.867	-3.099
17	THR	HG23	-0.770	0.546	-4.287
18	ILE	N	-0.556	3.629	-4.427
18	ILE	CA	-0.333	4.400	-5.692
18	ILE	HN	-1.497	3.496	-4.036
18	ILE	HA	0.698	4.211	-6.053
18	ILE	C	-0.421	5.946	-5.379
18	ILE	O	-1.236	6.672	-5.957
18	ILE	CB	-1.288	3.908	-6.852
18	ILE	HB	-2.305	4.271	-6.603
18	ILE	CG1	-1.395	2.357	-7.037
18	ILE	HG11	-1.526	1.871	-6.054
18	ILE	HG12	-0.444	1.948	-7.427
18	ILE	CG2	-0.883	4.538	-8.215
18	ILE	HG21	-0.844	5.641	-8.182
18	ILE	HG22	0.115	4.193	-8.547
18	ILE	HG23	-1.597	4.290	-9.020
18	ILE	CD1	-2.570	1.867	-7.901
18	ILE	HD11	-2.470	2.172	-8.958
18	ILE	HD12	-2.641	0.764	-7.888
18	ILE	HD13	-3.536	2.260	-7.531
19	GLU	N	0.446	6.441	-4.470
19	GLU	CA	0.634	7.888	-4.165
19	GLU	HN	1.033	5.726	-4.025
19	GLU	HA	0.850	8.416	-5.116
19	GLU	C	1.890	7.939	-3.246
19	GLU	O	1.773	7.912	-2.015
19	GLU	CB	-0.615	8.561	-3.518
19	GLU	CG	-0.502	10.091	-3.331
19	GLU	CD	-1.757	10.709	-2.714

19	GLU	OE1	-1.821	10.833	-1.471
19	GLU	OE2	-2.681	11.079	-3.471
19	GLU	HB1	-1.509	8.364	-4.140
19	GLU	HB2	-0.836	8.082	-2.544
19	GLU	HG1	0.364	10.339	-2.690
19	GLU	HG2	-0.306	10.582	-4.302
20	MET	N	3.097	7.953	-3.849
20	MET	CA	4.367	7.766	-3.099
20	MET	HN	3.066	7.947	-4.874
20	MET	HA	4.229	8.109	-2.058
20	MET	C	5.500	8.612	-3.764
20	MET	O	5.912	8.250	-4.873
20	MET	CB	4.774	6.264	-3.011
20	MET	HB1	4.730	5.784	-4.006
20	MET	HB2	5.837	6.193	-2.714
20	MET	CG	3.968	5.437	-1.993
20	MET	SD	4.791	3.860	-1.711
20	MET	CE	4.009	3.366	-0.164
20	MET	HG1	3.884	5.980	-1.034
20	MET	HG2	2.935	5.259	-2.347
20	MET	HE1	4.407	2.394	0.179
20	MET	HE2	4.198	4.113	0.628
20	MET	HE3	2.916	3.266	-0.289
21	PRO	N	6.082	9.682	-3.136
21	PRO	CA	7.307	10.353	-3.661
21	PRO	CD	5.577	10.289	-1.885
21	PRO	HA	7.190	10.566	-4.742
21	PRO	HD1	5.491	9.562	-1.057
21	PRO	HD2	4.577	10.737	-2.051
21	PRO	C	8.610	9.505	-3.466
21	PRO	O	8.564	8.355	-3.015
21	PRO	CB	7.264	11.689	-2.884
21	PRO	HB1	8.254	12.168	-2.762
21	PRO	HB2	6.636	12.421	-3.431
21	PRO	CG	6.612	11.360	-1.542
21	PRO	HG1	6.162	12.247	-1.057

21	PRO	HG2	7.367	10.953	-0.842
22	GLN	N	9.775	10.079	-3.825
22	GLN	CA	11.099	9.383	-3.763
22	GLN	HN	9.684	11.028	-4.202
22	GLN	HA	11.033	8.583	-4.525
22	GLN	C	11.482	8.638	-2.439
22	GLN	O	11.949	7.500	-2.513
22	GLN	CB	12.223	10.322	-4.282
22	GLN	HB1	13.148	9.727	-4.407
22	GLN	HB2	11.966	10.640	-5.311
22	GLN	CG	12.550	11.578	-3.435
22	GLN	HG1	11.630	12.168	-3.268
22	GLN	HG2	12.884	11.281	-2.422
22	GLN	CD	13.588	12.498	-4.093
22	GLN	OE1	13.260	13.333	-4.933
22	GLN	NE2	14.855	12.373	-3.736
22	GLN	HE21	15.067	11.660	-3.030
22	GLN	HE22	15.516	13.007	-4.196
23	GLN	N	11.241	9.236	-1.255
23	GLN	CA	11.413	8.552	0.061
23	GLN	HN	10.841	10.178	-1.328
23	GLN	HA	12.430	8.113	0.051
23	GLN	C	10.448	7.350	0.351
23	GLN	O	10.910	6.324	0.858
23	GLN	CB	11.447	9.600	1.208
23	GLN	HB1	12.280	10.306	1.013
23	GLN	HB2	11.743	9.086	2.143
23	GLN	CG	10.154	10.415	1.475
23	GLN	HG1	9.839	10.931	0.549
23	GLN	HG2	9.316	9.735	1.719
23	GLN	CD	10.320	11.475	2.574
23	GLN	OE1	10.799	12.580	2.329
23	GLN	NE2	9.928	11.173	3.800
23	GLN	HE21	9.539	10.235	3.942
23	GLN	HE22	10.049	11.909	4.503
24	ALA	N	9.143	7.463	0.030

24	ALA	CA	8.159	6.359	0.204
24	ALA	HN	8.886	8.352	-0.413
24	ALA	HA	8.289	5.956	1.227
24	ALA	C	8.290	5.147	-0.774
24	ALA	O	8.102	4.010	-0.329
24	ALA	CB	6.748	6.969	0.163
24	ALA	HB1	6.615	7.761	0.924
24	ALA	HB2	6.522	7.421	-0.821
24	ALA	HB3	5.969	6.209	0.360
25	ARG	N	8.632	5.358	-2.064
25	ARG	CA	9.043	4.252	-2.981
25	ARG	HN	8.743	6.347	-2.322
25	ARG	HA	8.300	3.441	-2.842
25	ARG	C	10.430	3.587	-2.668
25	ARG	O	10.540	2.365	-2.801
25	ARG	CB	8.889	4.651	-4.473
25	ARG	CG	9.786	5.799	-5.012
25	ARG	CD	10.177	5.685	-6.502
25	ARG	NE	11.091	4.541	-6.782
25	ARG	CZ	12.421	4.541	-6.578
25	ARG	NH1	13.108	5.603	-6.180
25	ARG	NH2	13.079	3.421	-6.783
25	ARG	HB1	7.831	4.908	-4.677
25	ARG	HB2	9.054	3.736	-5.072
25	ARG	HG1	9.259	6.756	-4.857
25	ARG	HG2	10.708	5.894	-4.408
25	ARG	HD1	9.264	5.572	-7.115
25	ARG	HD2	10.627	6.636	-6.847
25	ARG	HE	10.720	3.637	-7.092
25	ARG	HH12	12.567	6.460	-6.027
25	ARG	HH11	14.116	5.475	-6.041
25	ARG	HH21	12.529	2.612	-7.087
25	ARG	HH22	14.087	3.441	-6.595
26	GLN	N	11.453	4.350	-2.215
26	GLN	CA	12.697	3.779	-1.612
26	GLN	HN	11.240	5.353	-2.152

26 GLN	HA	13.138	3.102	-2.365
26 GLN	C	12.484	2.907	-0.334
26 GLN	O	13.148	1.878	-0.206
26 GLN	CB	13.749	4.894	-1.344
26 GLN	HB1	13.273	5.724	-0.787
26 GLN	HB2	14.530	4.520	-0.653
26 GLN	CG	14.472	5.467	-2.589
26 GLN	HG1	15.030	6.376	-2.295
26 GLN	HG2	13.724	5.828	-3.317
26 GLN	CD	15.422	4.491	-3.305
26 GLN	OE1	15.071	3.875	-4.309
26 GLN	NE2	16.638	4.327	-2.815
26 GLN	HE21	16.862	4.843	-1.957
26 GLN	HE22	17.228	3.639	-3.294
27 LYS	N	11.548	3.264	0.572
27 LYS	CA	11.074	2.367	1.667
27 LYS	HN	11.088	4.160	0.371
27 LYS	HA	11.940	2.194	2.336
27 LYS	C	10.559	0.961	1.203
27 LYS	O	10.956	-0.041	1.801
27 LYS	CB	10.012	3.154	2.484
27 LYS	CG	9.566	2.501	3.813
27 LYS	CD	8.426	3.241	4.552
27 LYS	CE	6.988	2.966	4.055
27 LYS	NZ	6.636	3.687	2.812
27 LYS	HB1	9.132	3.324	1.842
27 LYS	HB2	10.393	4.168	2.720
27 LYS	HG1	9.272	1.447	3.652
27 LYS	HG2	10.446	2.449	4.483
27 LYS	HD1	8.466	2.914	5.609
27 LYS	HD2	8.630	4.328	4.599
27 LYS	HE1	6.828	1.878	3.918
27 LYS	HE2	6.273	3.264	4.847
27 LYS	HZ1	6.751	4.702	2.914
27 LYS	HZ2	7.225	3.398	2.022
27 LYS	HZ3	5.663	3.522	2.532

28	LEU	N	9.719	0.878	0.145
28	LEU	CA	9.260	-0.418	-0.438
28	LEU	HN	9.490	1.779	-0.290
28	LEU	HA	8.796	-0.997	0.384
28	LEU	C	10.403	-1.321	-1.004
28	LEU	O	10.505	-2.475	-0.581
28	LEU	CB	8.156	-0.187	-1.513
28	LEU	HB1	8.584	0.438	-2.322
28	LEU	HB2	7.934	-1.155	-2.004
28	LEU	CG	6.803	0.435	-1.064
28	LEU	HG	7.002	1.418	-0.596
28	LEU	CD1	5.909	0.683	-2.295
28	LEU	HD11	5.692	-0.251	-2.848
28	LEU	HD12	4.935	1.125	-2.018
28	LEU	HD13	6.384	1.382	-3.009
28	LEU	CD2	6.044	-0.436	-0.042
28	LEU	HD21	5.068	0.007	0.230
28	LEU	HD22	5.844	-1.452	-0.431
28	LEU	HD23	6.607	-0.550	0.901
29	GLN	N	11.255	-0.816	-1.925
29	GLN	CA	12.406	-1.595	-2.475
29	GLN	HN	11.082	0.162	-2.182
29	GLN	HA	11.991	-2.584	-2.755
29	GLN	C	13.567	-1.934	-1.484
29	GLN	O	14.147	-3.014	-1.607
29	GLN	CB	12.883	-1.003	-3.833
29	GLN	HB1	13.599	-1.706	-4.301
29	GLN	HB2	12.019	-1.021	-4.524
29	GLN	CG	13.475	0.432	-3.883
29	GLN	HG1	12.803	1.117	-3.337
29	GLN	HG2	13.438	0.795	-4.926
29	GLN	CD	14.910	0.617	-3.360
29	GLN	OE1	15.141	1.212	-2.310
29	GLN	NE2	15.908	0.140	-4.084
29	GLN	HE21	15.657	-0.353	-4.946
29	GLN	HE22	16.847	0.271	-3.695

30	ASN	N	13.883	-1.064	-0.500
30	ASN	CA	14.859	-1.363	0.589
30	ASN	HN	13.357	-0.182	-0.525
30	ASN	HA	15.789	-1.718	0.103
30	ASN	C	14.394	-2.487	1.576
30	ASN	O	15.180	-3.393	1.865
30	ASN	CB	15.209	-0.024	1.297
30	ASN	HB1	14.313	0.381	1.811
30	ASN	HB2	15.459	0.741	0.538
30	ASN	CG	16.411	-0.079	2.257
30	ASN	OD1	17.565	-0.101	1.835
30	ASN	ND2	16.175	-0.094	3.557
30	ASN	HD21	15.192	-0.090	3.848
30	ASN	HD22	17.001	-0.122	4.163
31	LEU	N	13.133	-2.449	2.059
31	LEU	CA	12.510	-3.577	2.815
31	LEU	HN	12.579	-1.645	1.742
31	LEU	HA	13.171	-3.801	3.673
31	LEU	C	12.370	-4.919	2.020
31	LEU	O	12.617	-5.979	2.598
31	LEU	CB	11.135	-3.137	3.397
31	LEU	HB1	10.484	-2.835	2.550
31	LEU	HB2	10.622	-4.020	3.828
31	LEU	CG	11.136	-2.012	4.471
31	LEU	HG	11.710	-1.150	4.082
31	LEU	CD1	9.702	-1.513	4.733
31	LEU	HD11	9.051	-2.309	5.141
31	LEU	HD12	9.685	-0.673	5.453
31	LEU	HD13	9.225	-1.143	3.806
31	LEU	CD2	11.790	-2.446	5.800
31	LEU	HD21	11.766	-1.636	6.552
31	LEU	HD22	11.283	-3.323	6.245
31	LEU	HD23	12.853	-2.715	5.665
32	PHE	N	12.006	-4.880	0.720
32	PHE	CA	11.945	-6.085	-0.153
32	PHE	HN	11.808	-3.940	0.359

32	PHE	HA	11.330	-6.832	0.380
32	PHE	C	13.325	-6.763	-0.442
32	PHE	O	13.428	-7.981	-0.273
32	PHE	CB	11.156	-5.718	-1.445
32	PHE	HB1	10.236	-5.162	-1.176
32	PHE	HB2	11.739	-4.989	-2.041
32	PHE	CG	10.748	-6.916	-2.322
32	PHE	CD1	11.529	-7.286	-3.422
32	PHE	HD1	12.424	-6.733	-3.671
32	PHE	CD2	9.607	-7.664	-2.009
32	PHE	HD2	8.994	-7.398	-1.160
32	PHE	CE1	11.181	-8.394	-4.190
32	PHE	HE1	11.800	-8.686	-5.026
32	PHE	CE2	9.262	-8.773	-2.778
32	PHE	HE2	8.387	-9.355	-2.525
32	PHE	CZ	10.049	-9.138	-3.867
32	PHE	HZ	9.787	-10.004	-4.457
33	ILE	N	14.353	-6.004	-0.883
33	ILE	CA	15.663	-6.564	-1.345
33	ILE	HN	14.134	-5.006	-0.980
33	ILE	HA	15.384	-7.289	-2.133
33	ILE	C	16.495	-7.409	-0.317
33	ILE	O	17.181	-8.344	-0.739
33	ILE	CB	16.489	-5.449	-2.086
33	ILE	HB	15.776	-4.903	-2.735
33	ILE	CG1	17.557	-6.044	-3.052
33	ILE	HG11	17.119	-6.899	-3.603
33	ILE	HG12	18.393	-6.481	-2.473
33	ILE	CG2	17.113	-4.397	-1.130
33	ILE	HG21	17.525	-3.530	-1.679
33	ILE	HG22	16.366	-3.996	-0.425
33	ILE	HG23	17.934	-4.823	-0.524
33	ILE	CD1	18.119	-5.067	-4.098
33	ILE	HD11	17.319	-4.642	-4.731
33	ILE	HD12	18.660	-4.224	-3.631
33	ILE	HD13	18.834	-5.575	-4.772

34	ASN	N	16.432	-7.113	1.000
34	ASN	CA	17.066	-7.958	2.057
34	ASN	HN	15.817	-6.323	1.227
34	ASN	HA	18.139	-8.016	1.783
34	ASN	C	16.596	-9.450	2.131
34	ASN	O	17.449	-10.334	2.262
34	ASN	CB	17.063	-7.233	3.433
34	ASN	HB1	17.629	-7.850	4.158
34	ASN	HB2	17.675	-6.313	3.346
34	ASN	CG	15.701	-6.904	4.084
34	ASN	OD1	14.944	-7.786	4.489
34	ASN	ND2	15.366	-5.635	4.221
34	ASN	HD21	16.007	-4.942	3.822
34	ASN	HD22	14.441	-5.462	4.626
35	PHE	N	15.282	-9.732	2.018
35	PHE	CA	14.756	-11.120	1.861
35	PHE	HN	14.679	-8.909	1.899
35	PHE	HA	15.444	-11.796	2.407
35	PHE	C	14.743	-11.669	0.395
35	PHE	O	15.062	-12.848	0.209
35	PHE	CB	13.404	-11.302	2.611
35	PHE	HB1	13.580	-11.112	3.689
35	PHE	HB2	13.142	-12.378	2.592
35	PHE	CG	12.173	-10.489	2.152
35	PHE	CD1	11.351	-10.970	1.126
35	PHE	HD1	11.594	-11.891	0.615
35	PHE	CD2	11.830	-9.300	2.804
35	PHE	HD2	12.449	-8.910	3.599
35	PHE	CE1	10.209	-10.267	0.752
35	PHE	HE1	9.583	-10.638	-0.047
35	PHE	CE2	10.675	-8.610	2.442
35	PHE	HE2	10.412	-7.694	2.952
35	PHE	CZ	9.867	-9.092	1.417
35	PHE	HZ	8.977	-8.551	1.131
36	CYS	N	14.361	-10.862	-0.617
36	CYS	CA	14.287	-11.298	-2.032

36	CYS	C	14.877	-10.182	-2.921
36	CYS	O	16.060	-10.297	-3.312
36	CYS	CB	12.828	-11.666	-2.386
36	CYS	SG	12.713	-12.287	-4.099
36	CYS	OXT	14.177	-9.193	-3.237
36	CYS	HN	14.138	-9.897	-0.344
36	CYS	HA	14.907	-12.202	-2.195
36	CYS	HB1	12.450	-12.455	-1.710
36	CYS	HB2	12.149	-10.800	-2.263
36	CYS	HG	12.819	-11.106	-4.704

END

TABLE IV. Orthogonal three dimensional coordinates in Ångströms for the cP226•phospholamban(1-36) complex

Residue	Atom	X	Y	Z
1 MET	N	-18.366	-10.441	5.382
1 MET	CA	-16.968	-10.052	5.756
1 MET	HN1	-18.363	-11.296	4.808
1 MET	HN2	-18.964	-10.642	6.192
1 MET	HN3	-18.836	-9.728	4.811
1 MET	HA	-17.022	-9.109	6.345
1 MET	C	-16.058	-9.653	4.544
1 MET	O	-15.491	-8.562	4.547
1 MET	CB	-16.367	-11.107	6.732
1 MET	HB1	-15.418	-10.692	7.133
1 MET	HB2	-16.999	-11.196	7.638
1 MET	CG	-16.048	-12.534	6.208
1 MET	SD	-17.501	-13.438	5.624
1 MET	CE	-18.199	-13.998	7.185
1 MET	HG1	-15.303	-12.501	5.387
1 MET	HG2	-15.555	-13.137	6.997
1 MET	HE1	-19.124	-14.578	7.010
1 MET	HE2	-17.490	-14.662	7.714
1 MET	HE3	-18.445	-13.157	7.857
2 GLU	N	-15.964	-10.507	3.518
2 GLU	CA	-15.197	-10.254	2.269
2 GLU	HN	-16.431	-11.415	3.613
2 GLU	HA	-14.384	-9.526	2.462
2 GLU	C	-16.086	-9.579	1.149
2 GLU	O	-16.809	-8.614	1.422
2 GLU	CB	-14.496	-11.624	1.943
2 GLU	CG	-15.304	-12.969	1.947
2 GLU	CD	-16.679	-12.989	1.312
2 GLU	OE1	-16.770	-13.228	0.092
2 GLU	OE2	-17.689	-12.746	2.009

2	GLU	HB1	-13.980	-11.532	0.967
2	GLU	HB2	-13.654	-11.750	2.652
2	GLU	HG1	-14.713	-13.761	1.451
2	GLU	HG2	-15.430	-13.335	2.980
3	LYS	N	-16.030	-10.063	-0.108
3	LYS	CA	-16.999	-9.726	-1.196
3	LYS	HN	-15.594	-10.995	-0.096
3	LYS	HA	-16.597	-10.266	-2.076
3	LYS	C	-16.983	-8.231	-1.670
3	LYS	O	-16.139	-7.854	-2.488
3	LYS	CB	-18.379	-10.400	-0.889
3	LYS	CG	-19.212	-10.831	-2.119
3	LYS	CD	-20.381	-11.791	-1.776
3	LYS	CE	-20.044	-13.300	-1.688
3	LYS	NZ	-19.369	-13.685	-0.411
3	LYS	HB1	-18.203	-11.293	-0.268
3	LYS	HB2	-18.978	-9.753	-0.222
3	LYS	HG1	-19.611	-9.917	-2.608
3	LYS	HG2	-18.563	-11.290	-2.893
3	LYS	HD1	-20.925	-11.444	-0.874
3	LYS	HD2	-21.132	-11.674	-2.584
3	LYS	HE1	-20.986	-13.883	-1.807
3	LYS	HE2	-19.429	-13.605	-2.567
3	LYS	HZ1	-18.360	-13.394	-0.340
3	LYS	HZ2	-19.747	-13.259	0.445
3	LYS	HZ3	-19.300	-14.692	-0.225
4	VAL	N	-17.850	-7.370	-1.113
4	VAL	CA	-17.729	-5.883	-1.250
4	VAL	HN	-18.368	-7.786	-0.332
4	VAL	HA	-17.617	-5.678	-2.335
4	VAL	C	-16.444	-5.249	-0.593
4	VAL	O	-15.841	-4.361	-1.194
4	VAL	CB	-19.085	-5.211	-0.839
4	VAL	HB	-19.895	-5.756	-1.368
4	VAL	CG1	-19.192	-3.746	-1.314
4	VAL	HG11	-20.191	-3.313	-1.113

4	VAL	HG12	-18.450	-3.089	-0.822
4	VAL	HG13	-19.028	-3.652	-2.405
4	VAL	CG2	-19.423	-5.252	0.671
4	VAL	HG21	-20.429	-4.840	0.877
4	VAL	HG22	-19.412	-6.281	1.073
4	VAL	HG23	-18.707	-4.660	1.273
5	GLN	N	-15.991	-5.716	0.586
5	GLN	CA	-14.681	-5.298	1.177
5	GLN	HN	-16.525	-6.517	0.946
5	GLN	HA	-14.601	-4.196	1.093
5	GLN	C	-13.383	-5.831	0.471
5	GLN	O	-12.357	-5.141	0.491
5	GLN	CB	-14.696	-5.643	2.692
5	GLN	HB1	-13.684	-5.487	3.116
5	GLN	HB2	-14.878	-6.728	2.817
5	GLN	CG	-15.703	-4.852	3.575
5	GLN	HG1	-16.738	-4.985	3.209
5	GLN	HG2	-15.711	-5.300	4.586
5	GLN	CD	-15.396	-3.363	3.762
5	GLN	OE1	-14.647	-2.963	4.642
5	GLN	NE2	-15.948	-2.495	2.953
5	GLN	HE21	-15.630	-1.536	3.116
5	GLN	HE22	-16.412	-2.871	2.123
6	TYR	N	-13.412	-7.004	-0.197
6	TYR	CA	-12.392	-7.346	-1.233
6	TYR	HN	-14.349	-7.420	-0.207
6	TYR	HA	-11.396	-7.186	-0.771
6	TYR	C	-12.416	-6.413	-2.498
6	TYR	O	-11.364	-5.894	-2.875
6	TYR	CB	-12.491	-8.863	-1.566
6	TYR	HB1	-12.592	-9.455	-0.636
6	TYR	HB2	-13.426	-9.070	-2.123
6	TYR	CG	-11.270	-9.381	-2.345
6	TYR	CD1	-10.084	-9.668	-1.661
6	TYR	HD1	-10.045	-9.609	-0.583
6	TYR	CD2	-11.292	-9.461	-3.742

6	TYR	HD2	-12.200	-9.241	-4.287
6	TYR	CE1	-8.932	-10.001	-2.366
6	TYR	HE1	-8.027	-10.232	-1.830
6	TYR	CE2	-10.131	-9.785	-4.444
6	TYR	HE2	-10.139	-9.832	-5.524
6	TYR	CZ	-8.947	-10.036	-3.755
6	TYR	OH	-7.791	-10.280	-4.452
6	TYR	HH	-7.019	-10.219	-3.861
7	LEU	N	-13.587	-6.154	-3.113
7	LEU	CA	-13.759	-5.074	-4.135
7	LEU	HN	-14.394	-6.657	-2.722
7	LEU	HA	-13.139	-5.360	-5.005
7	LEU	C	-13.271	-3.631	-3.733
7	LEU	O	-12.609	-2.977	-4.542
7	LEU	CB	-15.245	-5.133	-4.594
7	LEU	HB1	-15.523	-6.180	-4.824
7	LEU	HB2	-15.880	-4.860	-3.731
7	LEU	CG	-15.651	-4.252	-5.804
7	LEU	HG	-15.360	-3.200	-5.603
7	LEU	CD1	-17.176	-4.286	-5.987
7	LEU	HD11	-17.553	-5.304	-6.199
7	LEU	HD12	-17.706	-3.921	-5.088
7	LEU	HD13	-17.502	-3.639	-6.825
7	LEU	CD2	-14.975	-4.703	-7.111
7	LEU	HD21	-15.191	-5.760	-7.352
7	LEU	HD22	-15.308	-4.098	-7.975
7	LEU	HD23	-13.876	-4.592	-7.065
8	THR	N	-13.511	-3.164	-2.491
8	THR	CA	-12.882	-1.929	-1.922
8	THR	HN	-14.206	-3.711	-1.961
8	THR	HA	-13.236	-1.074	-2.530
8	THR	C	-11.312	-1.892	-2.013
8	THR	O	-10.767	-0.964	-2.613
8	THR	CB	-13.426	-1.715	-0.469
8	THR	OG1	-14.849	-1.671	-0.441
8	THR	HB	-13.095	-2.565	0.160

8	THR	HG1	-15.101	-0.841	-0.857
8	THR	CG2	-12.988	-0.414	0.216
8	THR	HG21	-13.230	0.484	-0.384
8	THR	HG22	-13.473	-0.292	1.203
8	THR	HG23	-11.898	-0.399	0.403
9	ARG	N	-10.582	-2.897	-1.486
9	ARG	CA	-9.100	-2.999	-1.688
9	ARG	HN	-11.154	-3.657	-1.099
9	ARG	HA	-8.665	-2.002	-1.470
9	ARG	C	-8.597	-3.341	-3.141
9	ARG	O	-7.489	-2.943	-3.504
9	ARG	CB	-8.480	-3.985	-0.662
9	ARG	CG	-8.679	-3.663	0.845
9	ARG	CD	-7.677	-4.331	1.815
9	ARG	NE	-7.723	-5.828	1.787
9	ARG	CZ	-6.925	-6.617	1.073
9	ARG	NH1	-7.116	-7.891	1.115
9	ARG	NH2	-5.961	-6.190	0.314
9	ARG	HB1	-7.392	-4.020	-0.865
9	ARG	HB2	-8.843	-5.012	-0.870
9	ARG	HG1	-8.611	-2.565	0.992
9	ARG	HG2	-9.719	-3.911	1.140
9	ARG	HD1	-6.654	-3.934	1.650
9	ARG	HD2	-7.914	-3.993	2.846
9	ARG	HE	-8.426	-6.349	2.319
9	ARG	HH12	-7.864	-8.264	1.693
9	ARG	HH11	-6.571	-8.401	0.386
9	ARG	HH21	-5.791	-5.188	0.334
9	ARG	HH22	-5.373	-6.910	-0.147
10	SER	N	-9.350	-4.086	-3.965
10	SER	CA	-9.062	-4.255	-5.423
10	SER	HN	-10.216	-4.451	-3.541
10	SER	HA	-7.998	-4.514	-5.543
10	SER	C	-9.237	-2.985	-6.326
10	SER	O	-8.384	-2.744	-7.184
10	SER	CB	-9.828	-5.503	-5.913

10	SER	OG	-9.313	-6.678	-5.275
10	SER	HB1	-10.914	-5.399	-5.724
10	SER	HB2	-9.719	-5.609	-7.011
10	SER	HG	-9.884	-7.422	-5.502
11	ALA	N	-10.260	-2.142	-6.107
11	ALA	CA	-10.294	-0.755	-6.648
11	ALA	HN	-10.941	-2.461	-5.403
11	ALA	HA	-10.105	-0.797	-7.740
11	ALA	C	-9.225	0.239	-6.059
11	ALA	O	-8.524	0.906	-6.827
11	ALA	CB	-11.743	-0.266	-6.454
11	ALA	HB1	-12.024	-0.198	-5.385
11	ALA	HB2	-11.891	0.739	-6.892
11	ALA	HB3	-12.479	-0.934	-6.942
12	ILE	N	-9.063	0.325	-4.722
12	ILE	CA	-8.073	1.248	-4.069
12	ILE	HN	-9.733	-0.232	-4.175
12	ILE	HA	-8.213	2.243	-4.537
12	ILE	C	-6.563	0.911	-4.365
12	ILE	O	-5.785	1.854	-4.502
12	ILE	CB	-8.421	1.468	-2.546
12	ILE	HB	-8.473	0.468	-2.073
12	ILE	CG1	-9.804	2.172	-2.347
12	ILE	HG11	-10.558	1.710	-3.012
12	ILE	HG12	-9.748	3.226	-2.688
12	ILE	CG2	-7.349	2.290	-1.770
12	ILE	HG21	-7.590	2.410	-0.699
12	ILE	HG22	-6.350	1.816	-1.796
12	ILE	HG23	-7.222	3.309	-2.187
12	ILE	CD1	-10.379	2.121	-0.921
12	ILE	HD11	-11.413	2.512	-0.890
12	ILE	HD12	-10.405	1.088	-0.531
12	ILE	HD13	-9.790	2.730	-0.211
13	ARG	N	-6.116	-0.357	-4.492
13	ARG	CA	-4.688	-0.677	-4.826
13	ARG	HN	-6.837	-1.075	-4.352

13	ARG	HA	-4.087	-0.227	-4.011
13	ARG	C	-4.064	-0.040	-6.124
13	ARG	O	-2.892	0.342	-6.094
13	ARG	CB	-4.446	-2.208	-4.706
13	ARG	CG	-4.985	-3.125	-5.840
13	ARG	CD	-4.694	-4.625	-5.629
13	ARG	NE	-5.635	-5.210	-4.631
13	ARG	CZ	-5.642	-6.473	-4.222
13	ARG	NH1	-4.693	-7.326	-4.456
13	ARG	NH2	-6.651	-6.890	-3.537
13	ARG	HB1	-4.825	-2.556	-3.726
13	ARG	HB2	-3.351	-2.360	-4.640
13	ARG	HG1	-6.065	-2.948	-6.011
13	ARG	HG2	-4.505	-2.820	-6.792
13	ARG	HD1	-4.788	-5.161	-6.598
13	ARG	HD2	-3.634	-4.753	-5.333
13	ARG	HE	-6.427	-4.657	-4.281
13	ARG	HH12	-3.840	-6.971	-4.905
13	ARG	HH11	-4.827	-8.262	-4.029
13	ARG	HH21	-7.482	-6.302	-3.505
13	ARG	HH22	-6.560	-7.869	-3.213
14	ARG	N	-4.825	0.102	-7.229
14	ARG	CA	-4.376	0.917	-8.401
14	ARG	HN	-5.808	-0.154	-7.074
14	ARG	HA	-3.272	0.844	-8.428
14	ARG	C	-4.656	2.464	-8.334
14	ARG	O	-3.866	3.230	-8.890
14	ARG	CB	-4.845	0.244	-9.719
14	ARG	CG	-4.019	0.701	-10.958
14	ARG	CD	-4.063	-0.202	-12.216
14	ARG	NE	-3.844	-1.670	-12.010
14	ARG	CZ	-2.795	-2.247	-11.427
14	ARG	NH1	-1.732	-1.615	-11.038
14	ARG	NH2	-2.842	-3.520	-11.225
14	ARG	HB1	-4.739	-0.853	-9.604
14	ARG	HB2	-5.927	0.412	-9.882

14	ARG	HG1	-4.336	1.727	-11.239
14	ARG	HG2	-2.961	0.842	-10.667
14	ARG	HD1	-5.052	-0.063	-12.698
14	ARG	HD2	-3.349	0.185	-12.973
14	ARG	HE	-4.569	-2.354	-12.237
14	ARG	HH12	-1.739	-0.612	-11.189
14	ARG	HH11	-1.056	-2.146	-10.443
14	ARG	HH21	-3.658	-4.047	-11.522
14	ARG	HH22	-2.019	-3.907	-10.697
15	ALA	N	-5.709	2.944	-7.642
15	ALA	CA	-5.801	4.374	-7.222
15	ALA	HN	-6.269	2.220	-7.179
15	ALA	HA	-5.765	5.005	-8.134
15	ALA	C	-4.644	4.893	-6.290
15	ALA	O	-4.074	5.946	-6.571
15	ALA	CB	-7.199	4.561	-6.603
15	ALA	HB1	-7.394	5.627	-6.376
15	ALA	HB2	-8.010	4.227	-7.279
15	ALA	HB3	-7.305	4.011	-5.651
16	SER	N	-4.250	4.134	-5.248
16	SER	CA	-3.106	4.482	-4.352
16	SER	HN	-4.848	3.315	-5.069
16	SER	HA	-3.235	5.535	-4.049
16	SER	C	-1.638	4.397	-4.935
16	SER	O	-0.702	4.880	-4.297
16	SER	CB	-3.324	3.676	-3.050
16	SER	OG	-2.393	4.057	-2.031
16	SER	HB1	-3.255	2.589	-3.240
16	SER	HB2	-4.345	3.849	-2.656
16	SER	HG	-2.450	5.037	-1.916
17	THR	N	-1.403	3.876	-6.157
17	THR	CA	-0.201	4.263	-6.976
17	THR	HN	-2.258	3.512	-6.589
17	THR	HA	0.636	4.460	-6.276
17	THR	C	-0.319	5.601	-7.802
17	THR	O	0.712	6.218	-8.084

17	THR	CB	0.310	3.069	-7.842
17	THR	OG1	1.531	3.425	-8.481
17	THR	HB	0.520	2.218	-7.163
17	THR	HG1	1.382	4.296	-8.872
17	THR	CG2	-0.615	2.566	-8.957
17	THR	HG21	-0.136	1.754	-9.534
17	THR	HG22	-1.545	2.157	-8.534
17	THR	HG23	-0.896	3.364	-9.669
18	ILE	N	-1.523	6.028	-8.226
18	ILE	CA	-1.764	7.358	-8.891
18	ILE	HN	-2.302	5.493	-7.824
18	ILE	HA	-0.928	7.554	-9.592
18	ILE	C	-1.733	8.562	-7.864
18	ILE	O	-1.063	9.563	-8.116
18	ILE	CB	-3.077	7.284	-9.765
18	ILE	HB	-3.906	7.053	-9.065
18	ILE	CG1	-3.060	6.171	-10.865
18	ILE	HG11	-2.576	5.258	-10.472
18	ILE	HG12	-2.417	6.477	-11.714
18	ILE	CG2	-3.416	8.637	-10.450
18	ILE	HG21	-3.540	9.455	-9.715
18	ILE	HG22	-2.626	8.959	-11.154
18	ILE	HG23	-4.364	8.600	-11.016
18	ILE	CD1	-4.448	5.738	-11.380
18	ILE	HD11	-4.987	6.560	-11.884
18	ILE	HD12	-4.365	4.911	-12.110
18	ILE	HD13	-5.090	5.375	-10.555
19	GLU	N	-2.426	8.437	-6.718
19	GLU	CA	-2.209	9.220	-5.456
19	GLU	HN	-2.954	7.556	-6.669
19	GLU	HA	-2.898	10.084	-5.466
19	GLU	C	-0.786	9.777	-5.056
19	GLU	O	-0.692	10.794	-4.362
19	GLU	CB	-2.714	8.196	-4.390
19	GLU	CG	-2.806	8.605	-2.896
19	GLU	CD	-3.194	7.442	-1.992

19	GLU	OE1	-2.326	6.599	-1.686
19	GLU	OE2	-4.375	7.339	-1.613
19	GLU	HB1	-3.720	7.818	-4.667
19	GLU	HB2	-2.044	7.314	-4.436
19	GLU	HG1	-1.845	8.993	-2.521
19	GLU	HG2	-3.546	9.409	-2.747
20	MET	N	0.304	9.081	-5.411
20	MET	CA	1.613	9.205	-4.724
20	MET	HN	0.064	8.269	-5.989
20	MET	HA	1.499	9.758	-3.773
20	MET	C	2.703	9.961	-5.580
20	MET	O	3.391	9.307	-6.372
20	MET	CB	2.021	7.758	-4.320
20	MET	HB1	1.924	7.072	-5.187
20	MET	HB2	3.096	7.734	-4.080
20	MET	CG	1.245	7.190	-3.111
20	MET	SD	1.761	5.508	-2.777
20	MET	CE	0.862	5.232	-1.245
20	MET	HG1	1.366	7.818	-2.209
20	MET	HG2	0.155	7.174	-3.311
20	MET	HE1	0.982	4.201	-0.876
20	MET	HE2	1.153	5.949	-0.457
20	MET	HE3	-0.219	5.377	-1.430
21	PRO	N	2.965	11.301	-5.432
21	PRO	CA	4.032	12.006	-6.211
21	PRO	CD	2.094	12.217	-4.662
21	PRO	HA	3.958	11.712	-7.278
21	PRO	HD1	1.931	11.903	-3.614
21	PRO	HD2	1.100	12.301	-5.145
21	PRO	C	5.513	11.694	-5.772
21	PRO	O	5.777	10.728	-5.055
21	PRO	CB	3.558	13.475	-6.078
21	PRO	HB1	4.365	14.226	-6.161
21	PRO	HB2	2.843	13.707	-6.894
21	PRO	CG	2.833	13.550	-4.735
21	PRO	HG1	2.144	14.412	-4.664

21	PRO	HG2	3.555	13.637	-3.900
22	GLN	N	6.492	12.482	-6.259
22	GLN	CA	7.971	12.242	-6.117
22	GLN	HN	6.130	13.269	-6.807
22	GLN	HA	8.237	11.652	-7.014
22	GLN	C	8.571	11.380	-4.938
22	GLN	O	9.183	10.336	-5.185
22	GLN	CB	8.687	13.611	-6.328
22	GLN	HB1	9.776	13.432	-6.440
22	GLN	HB2	8.393	14.021	-7.315
22	GLN	CG	8.480	14.719	-5.249
22	GLN	HG1	7.400	14.880	-5.075
22	GLN	HG2	8.893	14.382	-4.280
22	GLN	CD	9.089	16.086	-5.575
22	GLN	OE1	9.447	16.412	-6.700
22	GLN	NE2	9.203	16.949	-4.600
22	GLN	HE21	8.880	16.664	-3.672
22	GLN	HE22	9.586	17.853	-4.892
23	GLN	N	8.363	11.795	-3.682
23	GLN	CA	8.769	11.029	-2.462
23	GLN	HN	7.850	12.681	-3.626
23	GLN	HA	9.766	10.583	-2.655
23	GLN	C	7.858	9.817	-2.049
23	GLN	O	8.366	8.773	-1.628
23	GLN	CB	8.984	12.075	-1.331
23	GLN	HB1	9.753	12.795	-1.680
23	GLN	HB2	9.473	11.581	-0.469
23	GLN	CG	7.730	12.848	-0.815
23	GLN	HG1	6.971	12.936	-1.613
23	GLN	HG2	7.219	12.273	-0.019
23	GLN	CD	8.018	14.281	-0.367
23	GLN	OE1	8.162	15.184	-1.181
23	GLN	NE2	8.113	14.540	0.911
23	GLN	HE21	7.995	13.761	1.562
23	GLN	HE22	8.301	15.524	1.123
24	ALA	N	6.527	9.922	-2.191

24	ALA	CA	5.598	8.770	-2.032
24	ALA	HN	6.246	10.756	-2.719
24	ALA	HA	5.810	8.295	-1.054
24	ALA	C	5.702	7.618	-3.104
24	ALA	O	5.540	6.445	-2.745
24	ALA	CB	4.202	9.401	-1.926
24	ALA	HB1	4.133	10.148	-1.112
24	ALA	HB2	3.901	9.909	-2.861
24	ALA	HB3	3.433	8.639	-1.708
25	ARG	N	6.020	7.917	-4.378
25	ARG	CA	6.491	6.901	-5.368
25	ARG	HN	5.937	8.921	-4.609
25	ARG	HA	5.870	6.003	-5.211
25	ARG	C	7.958	6.348	-5.212
25	ARG	O	8.226	5.246	-5.698
25	ARG	CB	6.139	7.358	-6.810
25	ARG	CG	6.910	8.577	-7.389
25	ARG	CD	7.630	8.344	-8.738
25	ARG	NE	8.675	7.276	-8.682
25	ARG	CZ	9.882	7.391	-8.144
25	ARG	NH1	10.343	8.483	-7.617
25	ARG	NH2	10.647	6.350	-8.127
25	ARG	HB1	5.050	7.561	-6.864
25	ARG	HB2	6.250	6.485	-7.481
25	ARG	HG1	6.185	9.408	-7.513
25	ARG	HG2	7.623	8.968	-6.640
25	ARG	HD1	6.870	8.070	-9.502
25	ARG	HD2	8.049	9.297	-9.123
25	ARG	HE	8.487	6.333	-9.036
25	ARG	HH12	9.678	9.253	-7.562
25	ARG	HH11	11.269	8.411	-7.176
25	ARG	HH21	10.262	5.474	-8.478
25	ARG	HH22	11.531	6.451	-7.608
26	GLN	N	8.883	7.013	-4.478
26	GLN	CA	10.024	6.300	-3.813
26	GLN	HN	8.547	7.923	-4.141

26 GLN HA	10.567	5.729	-4.593
26 GLN C	9.557	5.221	-2.773
26 GLN O	9.940	4.063	-2.908
26 GLN CB	11.056	7.278	-3.178
26 GLN HB1	10.541	7.954	-2.472
26 GLN HB2	11.746	6.698	-2.531
26 GLN CG	11.938	8.128	-4.132
26 GLN HG1	12.574	8.807	-3.533
26 GLN HG2	11.290	8.808	-4.715
26 GLN CD	12.851	7.379	-5.112
26 GLN OE1	12.666	7.434	-6.322
26 GLN NE2	13.859	6.683	-4.658
26 GLN HE21	13.951	6.566	-3.644
26 GLN HE22	14.393	6.190	-5.379
27 LYS N	8.661	5.530	-1.814
27 LYS CA	7.965	4.488	-0.985
27 LYS HN	8.437	6.532	-1.767
27 LYS HA	8.749	3.968	-0.397
27 LYS C	7.205	3.320	-1.738
27 LYS O	6.925	2.294	-1.118
27 LYS CB	7.084	5.278	0.032
27 LYS CG	6.375	4.464	1.151
27 LYS CD	4.824	4.447	1.123
27 LYS CE	4.146	3.508	0.100
27 LYS NZ	4.039	4.152	-1.240
27 LYS HB1	6.354	5.914	-0.500
27 LYS HB2	7.736	6.020	0.539
27 LYS HG1	6.775	3.431	1.209
27 LYS HG2	6.683	4.897	2.125
27 LYS HD1	4.499	4.110	2.129
27 LYS HD2	4.421	5.479	1.064
27 LYS HE1	4.692	2.536	0.045
27 LYS HE2	3.132	3.226	0.470
27 LYS HZ1	3.433	4.985	-1.252
27 LYS HZ2	4.943	4.472	-1.617
27 LYS HZ3	3.653	3.537	-1.972

28	LEU	N	6.852	3.447	-3.034
28	LEU	CA	6.417	2.288	-3.875
28	LEU	HN	7.273	4.279	-3.462
28	LEU	HA	5.700	1.669	-3.298
28	LEU	C	7.599	1.309	-4.230
28	LEU	O	7.644	0.200	-3.695
28	LEU	CB	5.656	2.809	-5.135
28	LEU	HB1	6.358	3.414	-5.737
28	LEU	HB2	5.429	1.941	-5.788
28	LEU	CG	4.345	3.618	-4.944
28	LEU	HG	4.521	4.455	-4.242
28	LEU	CD1	3.889	4.207	-6.289
28	LEU	HD11	3.626	3.417	-7.017
28	LEU	HD12	2.996	4.851	-6.178
28	LEU	HD13	4.664	4.825	-6.770
28	LEU	CD2	3.199	2.752	-4.415
28	LEU	HD21	2.261	3.324	-4.268
28	LEU	HD22	2.945	1.949	-5.132
28	LEU	HD23	3.435	2.251	-3.461
29	GLN	N	8.551	1.701	-5.102
29	GLN	CA	9.681	0.813	-5.525
29	GLN	HN	8.445	2.659	-5.444
29	GLN	HA	9.296	-0.228	-5.547
29	GLN	C	10.927	0.704	-4.581
29	GLN	O	11.555	-0.350	-4.563
29	GLN	CB	10.058	1.100	-7.008
29	GLN	HB1	10.824	0.361	-7.320
29	GLN	HB2	9.184	0.826	-7.631
29	GLN	CG	10.521	2.525	-7.440
29	GLN	HG1	9.707	3.243	-7.230
29	GLN	HG2	10.628	2.539	-8.541
29	GLN	CD	11.813	3.109	-6.855
29	GLN	OE1	11.817	4.184	-6.267
29	GLN	NE2	12.940	2.471	-7.031
29	GLN	HE21	12.865	1.517	-7.397
29	GLN	HE22	13.731	2.870	-6.518

30	ASN	N	11.300	1.729	-3.796
30	ASN	CA	12.455	1.663	-2.841
30	ASN	HN	10.673	2.543	-3.835
30	ASN	HA	13.328	1.287	-3.409
30	ASN	C	12.294	0.683	-1.616
30	ASN	O	13.296	0.164	-1.122
30	ASN	CB	12.777	3.128	-2.412
30	ASN	HB1	12.124	3.435	-1.575
30	ASN	HB2	12.518	3.827	-3.229
30	ASN	CG	14.217	3.499	-2.051
30	ASN	OD1	14.740	4.505	-2.512
30	ASN	ND2	14.897	2.774	-1.201
30	ASN	HD21	14.495	1.861	-0.955
30	ASN	HD22	15.872	3.070	-1.104
31	LEU	N	11.065	0.414	-1.141
31	LEU	CA	10.771	-0.779	-0.283
31	LEU	HN	10.324	0.878	-1.678
31	LEU	HA	11.547	-0.852	0.505
31	LEU	C	10.791	-2.187	-0.999
31	LEU	O	11.021	-3.200	-0.334
31	LEU	CB	9.400	-0.555	0.422
31	LEU	HB1	8.613	-0.511	-0.357
31	LEU	HB2	9.161	-1.468	1.000
31	LEU	CG	9.234	0.657	1.379
31	LEU	HG	9.418	1.589	0.808
31	LEU	CD1	7.793	0.696	1.913
31	LEU	HD11	7.540	-0.215	2.491
31	LEU	HD12	7.624	1.560	2.582
31	LEU	HD13	7.056	0.771	1.091
31	LEU	CD2	10.205	0.614	2.572
31	LEU	HD21	10.050	1.463	3.263
31	LEU	HD22	10.099	-0.315	3.165
31	LEU	HD23	11.260	0.669	2.244
32	PHE	N	10.538	-2.258	-2.316
32	PHE	CA	10.696	-3.495	-3.136
32	PHE	HN	10.482	-1.340	-2.768

32 PHE HA	10.395	-4.364	-2.515
32 PHE C	12.179	-3.811	-3.566
32 PHE O	12.658	-4.914	-3.301
32 PHE CB	9.693	-3.392	-4.333
32 PHE HB1	9.145	-2.429	-4.348
32 PHE HB2	10.258	-3.342	-5.286
32 PHE CG	8.648	-4.516	-4.425
32 PHE CD1	8.796	-5.536	-5.370
32 PHE HD1	9.665	-5.563	-6.012
32 PHE CD2	7.508	-4.495	-3.613
32 PHE HD2	7.370	-3.707	-2.887
32 PHE CE1	7.815	-6.513	-5.511
32 PHE HE1	7.935	-7.287	-6.256
32 PHE CE2	6.530	-5.480	-3.751
32 PHE HE2	5.644	-5.463	-3.137
32 PHE CZ	6.679	-6.481	-4.707
32 PHE HZ	5.903	-7.220	-4.840
33 ILE N	12.931	-2.860	-4.163
33 ILE CA	14.249	-3.145	-4.844
33 ILE HN	12.381	-2.034	-4.432
33 ILE HA	14.130	-4.126	-5.346
33 ILE C	15.529	-3.369	-3.934
33 ILE O	16.676	-3.233	-4.369
33 ILE CB	14.418	-2.106	-6.019
33 ILE HB	13.426	-2.035	-6.516
33 ILE CG1	15.384	-2.601	-7.135
33 ILE HG11	15.188	-3.677	-7.326
33 ILE HG12	16.434	-2.566	-6.789
33 ILE CG2	14.822	-0.685	-5.541
33 ILE HG21	14.801	0.051	-6.363
33 ILE HG22	14.142	-0.317	-4.756
33 ILE HG23	15.844	-0.676	-5.117
33 ILE CD1	15.254	-1.881	-8.489
33 ILE HD11	14.229	-1.989	-8.896
33 ILE HD12	15.491	-0.806	-8.425
33 ILE HD13	15.936	-2.326	-9.236

34	ASN	N	15.344	-3.823	-2.688
34	ASN	CA	16.279	-4.802	-2.047
34	ASN	HN	14.332	-3.912	-2.532
34	ASN	HA	17.316	-4.527	-2.325
34	ASN	C	16.140	-6.303	-2.523
34	ASN	O	17.115	-7.053	-2.449
34	ASN	CB	16.199	-4.624	-0.503
34	ASN	HB1	16.971	-5.266	-0.040
34	ASN	HB2	16.514	-3.598	-0.235
34	ASN	CG	14.875	-4.948	0.199
34	ASN	OD1	14.645	-6.042	0.695
34	ASN	ND2	13.967	-4.009	0.275
34	ASN	HD21	14.152	-3.184	-0.301
34	ASN	HD22	13.053	-4.355	0.578
35	PHE	N	14.955	-6.729	-2.996
35	PHE	CA	14.720	-8.055	-3.644
35	PHE	HN	14.230	-6.001	-3.022
35	PHE	HA	15.681	-8.604	-3.688
35	PHE	C	14.267	-7.997	-5.150
35	PHE	O	14.703	-8.857	-5.922
35	PHE	CB	13.790	-8.914	-2.732
35	PHE	HB1	14.297	-9.051	-1.757
35	PHE	HB2	13.757	-9.938	-3.149
35	PHE	CG	12.346	-8.419	-2.481
35	PHE	CD1	11.297	-8.823	-3.315
35	PHE	HD1	11.490	-9.483	-4.149
35	PHE	CD2	12.085	-7.518	-1.443
35	PHE	HD2	12.890	-7.171	-0.812
35	PHE	CE1	10.013	-8.316	-3.124
35	PHE	HE1	9.216	-8.591	-3.799
35	PHE	CE2	10.805	-7.002	-1.262
35	PHE	HE2	10.636	-6.252	-0.503
35	PHE	CZ	9.770	-7.402	-2.104
35	PHE	HZ	8.787	-6.965	-2.001
36	CYS	N	13.391	-7.059	-5.568
36	CYS	CA	12.937	-6.919	-6.979

36	CYS	C	12.642	-5.431	-7.337
36	CYS	O	13.077	-4.984	-8.423
36	CYS	CB	11.711	-7.838	-7.186
36	CYS	SG	11.181	-7.821	-8.935
36	CYS	OXT	11.882	-4.739	-6.619
36	CYS	HN	13.082	-6.376	-4.869
36	CYS	HA	13.741	-7.243	-7.669
36	CYS	HB1	11.954	-8.878	-6.906
36	CYS	HB2	10.872	-7.519	-6.542
36	CYS	HG	10.855	-6.530	-9.009
END					
1	CYS	N	8.859	-12.826	-0.866
1	CYS	CA	7.463	-12.830	-1.374
1	CYS	HN1	9.334	-13.726	-0.991
1	CYS	HN2	9.421	-12.087	-1.305
1	CYS	HN3	8.864	-12.628	0.142
1	CYS	HA	7.468	-13.235	-2.407
1	CYS	C	6.828	-11.396	-1.494
1	CYS	O	7.522	-10.392	-1.317
1	CYS	CB	6.712	-13.837	-0.472
1	CYS	SG	6.308	-13.188	1.176
1	CYS	HB1	5.744	-14.101	-0.939
1	CYS	HB2	7.235	-14.807	-0.360
2	TYR	N	5.529	-11.294	-1.812
2	TYR	CA	4.750	-10.029	-1.672
2	TYR	HN	5.009	-12.171	-1.934
2	TYR	HA	5.241	-9.395	-0.905
2	TYR	C	3.318	-10.348	-1.118
2	TYR	O	2.710	-11.362	-1.482
2	TYR	CB	4.792	-9.194	-2.987
2	TYR	HB1	4.452	-8.169	-2.757
2	TYR	HB2	5.851	-9.037	-3.272
2	TYR	CG	3.999	-9.693	-4.206
2	TYR	CD1	4.589	-10.559	-5.132
2	TYR	HD1	5.609	-10.885	-5.003
2	TYR	CD2	2.682	-9.266	-4.405

2	TYR	HD2	2.215	-8.590	-3.702
2	TYR	CE1	3.859	-11.011	-6.232
2	TYR	HE1	4.307	-11.690	-6.943
2	TYR	CE2	1.957	-9.716	-5.506
2	TYR	HE2	0.936	-9.388	-5.641
2	TYR	CZ	2.547	-10.590	-6.416
2	TYR	OH	1.833	-11.038	-7.494
2	TYR	HH	0.967	-10.629	-7.471
3	TRP	N	2.784	-9.498	-0.230
3	TRP	CA	1.456	-9.732	0.411
3	TRP	HN	3.400	-8.720	0.047
3	TRP	HA	1.393	-10.807	0.685
3	TRP	C	0.227	-9.448	-0.539
3	TRP	O	0.394	-9.065	-1.703
3	TRP	CB	1.498	-8.898	1.727
3	TRP	HB1	2.506	-8.943	2.193
3	TRP	HB2	1.353	-7.829	1.491
3	TRP	CG	0.519	-9.345	2.820
3	TRP	CD1	-0.639	-8.655	3.245
3	TRP	CD2	0.588	-10.478	3.609
3	TRP	NE1	-1.306	-9.343	4.282
3	TRP	CE2	-0.520	-10.467	4.493
3	TRP	HD1	-0.967	-7.716	2.824
3	TRP	HE1	-2.095	-9.033	4.857
3	TRP	CE3	1.538	-11.532	3.661
3	TRP	HE3	2.409	-11.541	3.020
3	TRP	CZ2	-0.682	-11.505	5.441
3	TRP	HZ2	-1.510	-11.494	6.133
3	TRP	CZ3	1.353	-12.549	4.598
3	TRP	HZ3	2.088	-13.342	4.654
3	TRP	CH2	0.260	-12.537	5.476
3	TRP	HH2	0.160	-13.332	6.200
4	GLU	N	-1.026	-9.624	-0.065
4	GLU	CA	-2.251	-9.398	-0.900
4	GLU	HN	-1.066	-9.985	0.896
4	GLU	HA	-2.059	-9.850	-1.895

4	GLU	C	-2.579	-7.874	-1.150
4	GLU	O	-3.531	-7.282	-0.629
4	GLU	CB	-3.423	-10.225	-0.289
4	GLU	CG	-4.548	-10.658	-1.279
4	GLU	CD	-5.428	-9.594	-1.902
4	GLU	OE1	-5.983	-8.751	-1.176
4	GLU	OE2	-5.630	-9.609	-3.130
4	GLU	HB1	-3.026	-11.161	0.155
4	GLU	HB2	-3.858	-9.678	0.569
4	GLU	HG1	-4.114	-11.254	-2.103
4	GLU	HG2	-5.235	-11.354	-0.770
5	LEU	N	-1.753	-7.242	-1.991
5	LEU	CA	-1.972	-5.882	-2.541
5	LEU	HN	-0.922	-7.815	-2.212
5	LEU	HA	-3.057	-5.734	-2.704
5	LEU	C	-1.333	-5.919	-3.973
5	LEU	O	-1.967	-6.436	-4.899
5	LEU	CB	-1.517	-4.805	-1.497
5	LEU	HB1	-0.421	-4.840	-1.373
5	LEU	HB2	-1.897	-5.131	-0.508
5	LEU	CG	-2.002	-3.346	-1.723
5	LEU	HG	-3.062	-3.370	-2.045
5	LEU	CD1	-1.930	-2.530	-0.421
5	LEU	HD11	-2.500	-2.998	0.402
5	LEU	HD12	-0.889	-2.404	-0.065
5	LEU	HD13	-2.344	-1.512	-0.553
5	LEU	CD2	-1.183	-2.584	-2.778
5	LEU	HD21	-1.272	-3.021	-3.788
5	LEU	HD22	-1.512	-1.532	-2.878
5	LEU	HD23	-0.102	-2.555	-2.533
6	GLU	N	-0.102	-5.418	-4.147
6	GLU	CA	0.670	-5.433	-5.427
6	GLU	HN	0.318	-5.068	-3.279
6	GLU	HA	0.760	-6.480	-5.776
6	GLU	C	2.125	-4.958	-5.064
6	GLU	O	3.021	-5.761	-4.797

6	GLU	CB	-0.062	-4.615	-6.547
6	GLU	CG	0.643	-4.580	-7.927
6	GLU	CD	-0.149	-3.863	-8.997
6	GLU	OE1	-0.877	-4.532	-9.753
6	GLU	OE2	-0.072	-2.625	-9.100
6	GLU	HB1	-1.073	-5.034	-6.699
6	GLU	HB2	-0.241	-3.577	-6.203
6	GLU	HG1	1.630	-4.089	-7.869
6	GLU	HG2	0.842	-5.603	-8.299
8	TRP	N	2.313	-3.638	-4.926
8	TRP	CA	3.537	-2.986	-4.364
8	TRP	HN	1.515	-3.090	-5.263
8	TRP	HA	4.424	-3.433	-4.856
8	TRP	C	3.848	-3.117	-2.821
8	TRP	O	4.653	-2.346	-2.288
8	TRP	CB	3.456	-1.496	-4.839
8	TRP	HB1	4.309	-0.929	-4.424
8	TRP	HB2	3.659	-1.485	-5.927
8	TRP	CG	2.153	-0.690	-4.582
8	TRP	CD1	1.178	-0.428	-5.575
8	TRP	CD2	1.662	-0.105	-3.421
8	TRP	NE1	0.101	0.325	-5.068
8	TRP	CE2	0.430	0.525	-3.742
8	TRP	HD1	1.240	-0.780	-6.598
8	TRP	HE1	-0.765	0.609	-5.546
8	TRP	CE3	2.173	-0.038	-2.098
8	TRP	HE3	3.108	-0.507	-1.834
8	TRP	CZ2	-0.283	1.234	-2.751
8	TRP	HZ2	-1.204	1.736	-2.998
8	TRP	CZ3	1.437	0.648	-1.130
8	TRP	HZ3	1.792	0.681	-0.112
8	TRP	CH2	0.230	1.282	-1.455
8	TRP	HH2	-0.324	1.816	-0.694
8	LEU	N	3.264	-4.088	-2.102
8	LEU	CA	3.536	-4.329	-0.654
8	LEU	HN	2.865	-4.819	-2.705

8	LEU	HA	3.941	-3.411	-0.189
8	LEU	C	4.558	-5.516	-0.479
8	LEU	O	4.209	-6.629	-0.884
8	LEU	CB	2.165	-4.593	0.042
8	LEU	HB1	1.408	-3.926	-0.417
8	LEU	HB2	1.824	-5.619	-0.207
8	LEU	CG	2.061	-4.358	1.574
8	LEU	HG	2.296	-3.294	1.781
8	LEU	CD1	3.002	-5.228	2.425
8	LEU	HD11	4.062	-4.953	2.285
8	LEU	HD12	2.805	-5.135	3.510
8	LEU	HD13	2.927	-6.303	2.177
8	LEU	CD2	0.619	-4.623	2.040
8	LEU	HD21	0.492	-4.415	3.118
8	LEU	HD22	-0.111	-3.989	1.507
8	LEU	HD23	0.316	-5.674	1.876
9	PRO	N	5.780	-5.358	0.119
9	PRO	CA	6.694	-6.502	0.430
9	PRO	CD	6.411	-4.035	0.314
9	PRO	HA	7.030	-6.917	-0.541
9	PRO	HD1	6.017	-3.549	1.227
9	PRO	HD2	6.254	-3.346	-0.539
9	PRO	C	6.165	-7.738	1.254
9	PRO	O	4.962	-7.953	1.399
9	PRO	CB	7.873	-5.753	1.096
9	PRO	HB1	8.834	-6.283	0.969
9	PRO	HB2	7.706	-5.659	2.189
9	PRO	CG	7.892	-4.373	0.455
9	PRO	HG1	8.381	-4.416	-0.539
9	PRO	HG2	8.450	-3.636	1.059
10	CYS	N	7.083	-8.610	1.703
10	CYS	CA	6.766	-10.017	2.059
10	CYS	HN	8.045	-8.317	1.519
10	CYS	HA	6.123	-10.428	1.255
10	CYS	C	5.908	-10.281	3.352
10	CYS	O	4.684	-10.146	3.295

10	CYS	CB	8.136	-10.743	1.930
10	CYS	SG	7.929	-12.525	2.158
10	CYS	HB1	8.849	-10.378	2.694
10	CYS	HB2	8.613	-10.553	0.953
11	ALA	N	6.523	-10.747	4.456
11	ALA	CA	5.941	-11.825	5.306
11	ALA	HN	7.531	-10.788	4.308
11	ALA	HA	6.701	-12.037	6.082
11	ALA	C	5.832	-13.184	4.541
11	ALA	O	6.858	-13.901	4.464
11	ALA	OXT	4.767	-13.516	3.972
11	ALA	CB	4.694	-11.381	6.092
11	ALA	HB1	3.843	-11.199	5.412
11	ALA	HB2	4.376	-12.169	6.797
11	ALA	HB3	4.873	-10.456	6.664

END

Table V

Residue	NH	$C_\alpha H$	$C_\beta H$	$C_\gamma H$	$C_\delta H$	Others
Met1		4.159	2.124	2.566		2.012
Glu2	8.803	4.572	1.967	2.510, 2.319		
Lys3	8.787	4.147	1.900	1.559, 1.431	1.729	2.969
Val4	8.314	3.889	2.132	1.026, 0..951		
Gln5	7.846	4.092	2.364, 2.252	2.369		7.431, 6.823
Tyr6	7.924	4.225	3.114		7.046	6.780
Leu7	8.536	4.013	1.831	1.586	0.915	
Thr8	7.975	3.955	4.247	1.222		
Arg9	8.156	3.518	1.845, 1.725	1.587	3.092	7.242
Ser10	7.991	4.082	3.936, 3.767			
Ala11	8.051	4.085	1.510			
Ile12	8.126	3.681	1.857	1.704, 1.014	0.769	0.860
Arg13	8.181	3.983	1.941, 1.735	1.606	3.162	7.189
Arg14	8.143	4.052	1.941, 1.733	1.725, 1.604	3.169	7.154
Ala15	8.422	4.114	1.500			
Ser16	8.110	4.275	4.029, 3.979			
Thr17	7.695	4.316	4.373	1.270		
Ile18	7.589	4.102	1.925	1.576, 1.216	0.851	0.912
Glu19	8.149	4.351	2.121, 2.011	2.468, 2.426		
Met20	7.958	4.702	2.088	2.544		2.027
Pro21		4.487	2.539, 2.483	2.082, 1.948	3.876, 3.591	
Gln22	8.766	4.008	2.173	2.438		7.433, 6.742
Gln23	8.954	4.079	2.084, 1945	2.464		7.457, 6.784
Ala24	7.455	4.155	1.474			
Arg25	7.858	3.944	1.876, 1712	1.604	3.246, 3.181	7.253
Gln26	8.143	4.019	2.136, 2.115	2.461, 2.374		7.371, 6.721
Lys27	7.647	4.069	1.954, 1.598	1.613, 1.465	1.682	2.937, 7.604
Leu28	8.099	4.063	1.773, 1.712	1.510	0.849, 0.818	
Gln29	8.212	3.985	2.198, 2.117	2.480, 2.367		7.172, 6.668
Asn30	7.908	4.482	2.884, 2.803		7.486, 6.821	
Leu31	7.878	4.154	1.718, 1.625	1.557	0.859, 0.797	
Phe32	8.162	4.430	3.238, 3.096		7.173	7.197
Ile33	7.974	3.986	1.930	1.611, 1.283	0.900	0.891
Asn34	7.801	4.570	2.588, 2.511		7.337, 6.759	
Phe35	8.006	4.694	3.272, 3.058		7.277	7.207
Cys36	7.727	4.452	2.890			

TABLE VI. NMR assignments of cP226 in water.

1H-chemical shifts of cP226 in 90% H_2O/10% D_2O, pH 6.50 at 10°C.

Values expressed in ppm.

res.	HN	HA	HB1*	HB2	HG*	HD1/ HD*	HD2/ HE*	HE3	HZ2
Cys 1		4.054	2.991	2.896					
Tyr 2	6.924	4.695	2.884			6.986	6.792		
Trp 3	8.094	4.599	3.199	3.087		7.106	10.024	7.427	7.465
Glu 4	8.313	3.907	1.909	1.785					
Leu 5	7.857	4.093	1.495	1.496	1.132	0.822			
Glu 6	8.227	4.123	2.032	1.982	2.195	7.074			
Trp 7	7.871	4.398	3.207			0.790	10.188	7.449	7.458
Leu 8	7.326	4.514	1.377		1.256				
Pro 9		4.179	2.214	1.820	1.974	3.617	3.505		
Cys 10	8.457	4.505	3.128	2.906					
Ala 11	8.062	4.115	1.330						

TABLE VII. Quality of the structure of cP226 obtained by noe data

RMSD values were calculated from a family od 12 structures without NOE restrain violation bigger than 0.3 Å. The local RMSD was calculated on 3 residues

res.	Global displacem.			local RMSD	Local displacem.			NOEs
	bb	heavy	heavysc	bb	bb	heavy	heavysc	(total)
Cys 1	1.80	1.99	1.77	0.00	0.00	0.00	0.00	2
Tyr 2	0.92	3.52	4.23	0.72	0.59	3.21	3.86	6
Trp 3	0.76	1.36	1.50	0.35	0.26	0.73	0.81	17
Glu4	0.83	2.22	2.86	0.29	0.23	1.77	2.33	12
Leu 5	0.63	1.38	1.78	0.26	0.20	1.04	1.44	23
Glu 6	0.73	2.34	3.00	0.26	0.24	1.73	2.23	9
Trp 7	0.65	2.06	2.39	0.27	0.25	1.67	1.96	16
Leu 8	0.53	1.55	2.11	0.18	0.16	1.58	2.22	27
Pro 9	0.60	0.83	1.04	0.17	0.12	0.18	0.21	15
Cys10	0.71	0.94	1.11	0.27	0.18	0.36	0.54	13
Ala11	1.20	1.67	1.73	0.00	0.00	0.00	0.00	6

Abbreviations

PLB, phospholamban; PLB[a.a.1-36], 36 a.a. N-terminal fragment of human phospholamban; SR, sarcoplasmic reticulum; SERCA, sarco/endoplasmic reticulum Ca^{2+}-ATPase; SERCA_2, cardiac isoform of the sarco/endoplasmic reticulum Ca^{2+}-ATPase; CD, circular dichroism; COSY, correlation spectroscopy; TOCSY, total correlation spectroscopy; NOESY, nuclear Overhauser-enhancement spectroscopy; d_3-TFE, perdeuterated trifluoroethanol; d_{10}-DTT, perdeuterated dithiotreitol.